DESIGN OF SOL-GEL METAL OXIDE THIN FILM CATALYST SUPPORT FOR CAPILLARY MICROREACTOR

BY

ABDULKADIR TANIMU

A Thesis Presented to the

DEANSHIP OF GRADUATE STUDIES

KING FAHD UNIVERSITY OF PETROLEUM & MINERALS

DHAHRAN, SAUDI ARABIA

In Partial Fulfillment of the
Requirements for the Degree of

MASTER OF SCIENCE

In

CHEMISTRY

MAY, 2015

KING FAHD UNIVERSITY OF PETROLEUM & MINERALS

DHAHRAN- 31261, SAUDI ARABIA

DEANSHIP OF GRADUATE STUDIES

This thesis, written by **ABDULKADIR TANIMU** under the direction his thesis advisor and approved by his thesis committee, has been presented and accepted by the Dean of Graduate Studies, in partial fulfillment of the requirements for the degree of **MASTER OF SCIENCE IN CHEMISTRY.**

Dr. Khalid R. Alhooshani
(Advisor)

Dr. Abdulaziz Alsaadi
Department Chairman

Dr. Nisar Ullah
(Member)

Dr. Salam A. Zummo
Dean of Graduate Studies

Dr. Oki Muraza
(Member)

24/5/15
Date

To the memory of my late sister Hauwa'u Tanimu, May her soul rest in eternal peace, Ameen.

ACKNOWLEDGEMENTS

All praise is to Allah lord of the world, the most beneficent, most merciful. May His peace and blessing continue to be on our noble prophet, Muhammad bin Abdullah (S.A.W), his household, companions, and those that follow his guided path till the day of resurrection.

I would like to express my appreciation to King Fahd University of Petroleum and Minerals for giving me the opportunity to move to the next level of my ambition, through a full M.S. Scholarship.

My profound gratitude goes to my advisor, Dr. Khalid Alhooshani for his expertise, guidance, caring and most importantly his patience with me throughout the research period. To my committee members, Dr. Nisar Ullah and Dr. Oki Muraza, I said a big thank you for your support and advices. Special thanks goes to the Chairman, Chemistry Department for providing me enabling environment for study and research and other faculty members, staff and students of chemistry departments.

To my research group members, you mean a family to me and your support and advices at the moments of difficulties were well appreciated.

This piece would remain incomplete without expressing my thanks to my parents, they are always loving, caring and understanding. Your prayers of course keep me going and to Tanimu's family, I am proud of you all and thank you.

TABLE OF CONTENTS

LIST OF TABLES

LIST OF FIGURES

LIST OF ABBREVIATIONS

TEOS	:	Tetraethoxysilane
S_N2	:	Nucleophilic substitution bimolecular
TEM	:	Transmission electron microscope
TGA	:	Thermogravimetric analysis
TTB	:	Titanium tetrabutoxide
ICP-MS	:	Inductive coupled plasma mass spectrometry
EP	:	Ellipsometric porosimetry
FESEM	:	Field emission scanning electron microscopy
***i*-PrOH**	:	Isopropanol
DME	:	Dimethoxyethane
$Ce(OPr^i)_4$	:	Cerium isopropoxide
acac-H	:	Acetylacetone
EtOH	:	Ethanol
DFT	:	Density functional theory
Pd/CeO_2	:	Cerium thin film immobilized with palladium nanoparticles
TOF	:	Turn over frequency

ABSTRACT

Full Name : Abdulkadir Tanimu

Thesis Title : Design of SOL-GEL Metal Oxide Thin Film Catalyst Support for Capillary Microreactor.

Major Field : Chemistry

Date of Degree: May, 2015

Ceria thin films as catalyst support for application in capillary microreactor was developed for the first time from freshly prepared cerium isopropoxide precursor using sol-gel approach. The thin film was characterized using powder XRD. FESEM image showed available pores within the dried film inside which palladium nanoparticles (Pd NPs) were immobilized. Film thickness was measured to be approximately 200 nm from the capillary SEM. Mean particle size and dispersion of Pd NPs was determined from the TEM images. FTIR and Raman spectroscopy were recorded and the results were comparable to DFT computational calculations and previously reported data. The Pd/CeO_2 immobilized capillary was tested for hydrogenation of phenylacetylene in a microreactor. Higher conversion and selectivity towards ethylbenzene were recorded at higher temperature, while selectivity towards styrene was favored at higher phenylacetylene concentration and hydrogen flow rate. Catalyst turn over frequency of 0.733 s^{-1} was obtained for 158 ppm phenylacetylene hydrogenation at 60 ^{o}C and 0.5 $ml.min^{-1}$ hydrogen flow rate. Catalyst activity evaluation showed continuous decrease in catalyst activity for the first 4 days of operation and was then stabilized for further 2 days. ICP-MS result confirmed decrease in activity to be due to leaching of Pd in the Pd/CeO_2 capillary.

ABSTRACT (ARABIC)

ملخص الرسالة

الاسم الكامل: عبدالقادر تانيمو

عنوان الرسالة: تصميم اوكسيد معدن سول-جل غشاء رقيق داعم حفاز لمفاعل دقيق انبوبي شعري

التخصص : كيمياء

تاريخ الدرجة العلمية: مايو,2015

للمرة الأولى تم تطوير غشاء السيريوم الرقيق كدعامة حفازه لتطبيقات في مفاعل دقيق شعري من مركب طليعي للايزوبروبو اوكسيد السيريوم المحضر حديثا باستخدام نهج السول-جل. تم تشخيص الغشاء باستخدام مطيافية الاشعة السينية للبودرة, ووافقت النتيجة ملف JCPDS لاوكسيد السيريوم. اظهرت صورت FESEM مساهات متوفرة داخل الغشاء الجاف, وتم وتم ادخال جسيمات البليديوم النانومية داخلها. تم قياس سمك الغشاء ووجد حوالي 200 نانومتر من SEM للانبوب الشعري. تم تحديد حجم جسيمات البليديوم النانوية و تشتتها باستخدام صورة TEM. تم تسجيل طيف الاشعة تحت الحمراء ورمان وكان مقارنا مع حسابات DFT وبيانات تم دراستها سابقا. تم تجريب البليديوم/اوكسيد السيريوم في هدرجة فينيل استلين في مفاعل دقيق. تم تسجيل انتاجية و انتقائية عالية لايثيل البنزين في درجة حرارة عالية , بينما الانتقائية نحو الاستايرين كانت مفضلة عند تراكيز عالية من فينيل استلين وتيار هيدروجين عالي. تم الحصول على جهد اعلى للحفاز للهدرجة 0.733 1/ثانية لتركيز 158 جزء من المليون من فينيل استلين عند 60 درجة مئوية و 0.5 مل/دقيقة لمعدل سريان الهيدروجين. اظهرت فعالية الحفاز نقصان مستمر في فعاليته في اول اربعة ايام بعد ذلك استقرار في الفعالية بعد 2 اخريين. نتائج ICP-MS اكدت نقصان الفعالية نتيجة الى رشح البليديوم خارج انبوب البليديوم / اوكسيد البليدوم الشعري.

CHAPTER 1

INTRODUCTION

Nanodevices, chips and capillary-based systems have grown significantly to become a very promising tools in the areas of chemistry, reaction engineering and biotechnology[1].

Compared to conventional batch reactors, capillary based-reactors have several advantages which include improved heat and mass transfer because of increased surface area to volume ratio[1-2], precise temperature control enabling suppression of by-product[3], efficient mixing[4], higher conversion and selectivity[5] and environmental friendly through a reduced usage of reagents and solvents[6]. A range of application of capillary reactors spans across diverse research areas such as catalysis[7], nanoparticle synthesis[8], sensors[9], electrochemistry[10] and polymerization[11].

Furthermore, capillary microreactors have been improved by using alternative energy transfer such as ultrasound[12] and microwave radiations[13]. Both radiations have been shown to be effective in increasing reaction rate, improving yields, shortening reaction time and recording high conversion[12b, 14]. In a microwave oven, the heat can be transferred to the aqueous species efficiently and in ultrasonic bath, mass transfer and chemical reactions are intensified. Combined microwave-assisted or ultrasound-assisted syntheses with capillary microreactors have found many applications in synthetic chemistry[15]. Chemical sectors including petrochemicals, fine chemicals and pharmaceuticals have invested in nanodevices and capillary reactors in order to develop green and sustainable continuous manufacturing with less waste[16]. Herein, focus is given

to the different immobilization methods, various characterization methods of immobilized capillary and the performance of immobilized capillary in some reactions.

1.1 Principle of Microreactor

Microreactor technology within the past two decades has evolved to become the key technology for process intensification. 'Lab-on-a-chip' as it is proudly called, microreactors have contributed to the minimization of reagents and energy wastage due to their small dimensions which in most cases do not exceed 1mm. Also the small volume of microreactors enables safe and easy handling of hazardous and highly exothermic reactions while facilitating fast and easy parameter screening. Efficient heat and mass transfer in microreactors also significantly increases the productivity when compared to classical batch reactors.

The ability to increase effectively the productivity through running a series of continuous reactors concomitantly is another interesting feature of microreactor technology. Some reactions studied successfully using microreactor technology include Suzuki-Miyaura coupling reactions, wittig reactions, hydroformylation reactions, hydrogenation reactions, Diels-Alder reaction etcetera.

1.2 Characteristics of Microreactor

Apart from size, there are some other properties of microreactor that made it better in performance and handling to conventional batch reactors. Some of these properties are efficient mixing ability coupled with generation of extended phase interface, safety in

handling toxic and explosive reactions, effective and easy temperature, pressure, time and flow velocity adjustment while maintaining efficient heat transfer.

1.2.1 Efficient Mixing Ability

Mixing regime constitute the integral part of microreactor and the laminar flow regime of the fluids made microreactors different from classical continuous flow reactors. This regime is define by the Reynolds number *Re*, a dimensionless number which is a function of velocity *u*, travelled length *L*, density ρ, and viscosity η of the fluid.

$$R_e = u\rho L/\eta$$

The Reynolds number ranges from 10 – 500 for laminar flow regime in microreactors which is due to fast lateral diffusion, resulting in intensive mass transfer which occurred between layers and the consequence is residence time convergence[17]. Lamina flow has the advantages of restraining gradient formation in concentration, temperature, pressure, volume and time. Generally the channel diameter of microreactors lie between the range of 1mm - 100μm for chemicals production resulting in diffusion timescale of <1s for gases and even less for smaller channel diameters. However the diffusion timescale for liquids is in the range of seconds to minutes thus giving possibility of lateral diffusion as limiting factor for fast reactions. In order to reduce the diffusive barrier, preliminary lamellar micromixing is connected for intensification of mass transfer. The result is decrease in the time of response and increased space-time yield. Effective mixing with controlled molar ratio of reactants give rise to high yield and selectivity, hence suppressing side reactions.

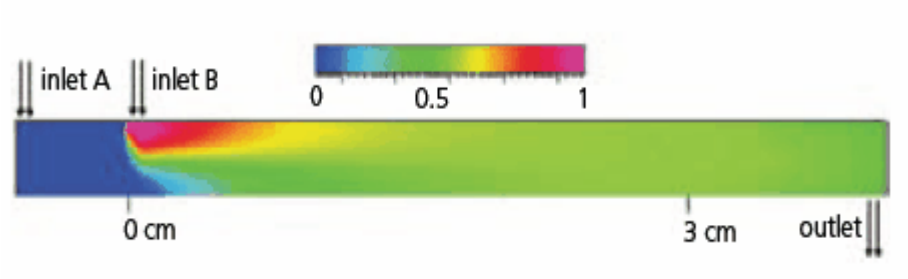

Figure 1.1 Efficient mixing in a microreactor: The green color indicates the perfect 1:1 mixture of reactants from inlet A and inlet B.

1.2.2 Heat Exchange/Temperature Control

The study of reaction kinetics and product characterization is known to be well influenced by temperature of the system and therefore controlling the temperature is paramount to achieving the desired selectivity in any chemical process while minimizing the reaction time. Heat exchange in microreactor is so efficient that it warrant immediate correction of temperature changes, unlike in large-scale reactors where temperature changes require some time to make effect on the system. This affords suppression of undesired by-product in microreactor. Since lamina flow regime is obtained with microfluidic devices, molecular diffusion theory could be used to determine the approximate time taken for thermal mixing across a microchannel and the heat transfer to lamina flow of fluids is described using the Nusselt number *Nu* which relates to the convective heat transfer coefficient α, characteristic length *L*, and thermal conductivity of fluid λ by the equation:[18]

$$Nu = \alpha L/\lambda \quad \text{(dimensionless)}$$

The Nusselt number could also be described as temperature gradient on a surface.

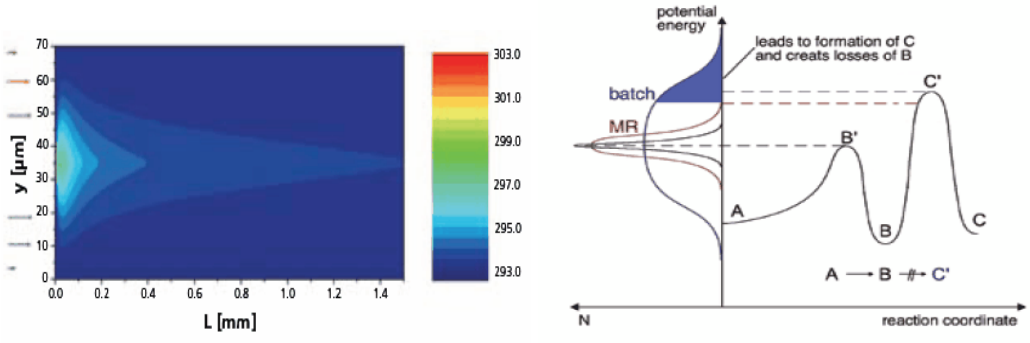

Figure 1.2 a) Heat distribution in microreactor b) By-product suppression due to temperature control

1.2.3 Surface Area to Volume Ratio

The small inner volume of a microreactor coupled with strong heat exchange ability result in high surface area-to-volume ratio, which enables rapid dissipation of heat generated during exothermic reactions. The heat transfer in terms of thermal diffusivity coefficient a, is related to the heat timescale t_w and the travelled length of the fluid L by the equation:

$$t_w = L^2/a$$

More recently, the advent of heat exchanger in microreactors now allows fast heat exchange to and from the reactor making it possible to study even explosives reactions under isothermal conditions.

1.2.4 Pressure Control

For gaseous reactant(s) flowing through capillary microreactor, very high pressure could be attained due to the microsize of the reactor. But interestingly, reactions have been

carried out safely under high pressures and up to above 400 ^{o}C in microreactors which is not the case in conventional batch reactors. Hence microreactors stand out to be the ideal reactors for studying reactions under supercritical conditions[19].

In summary, microreactors technology offers the following advantages:

1. Scale-independent synthesis
2. High yield and selectivity
3. Accelerated process development
4. Enhanced safety
5. Product profile improvement

Catalysts immobilization for heterogeneous catalysis in microreactors have been successfully studied with the catalysts forming thin films coatings or as monolith.

a) Thin films open tubular

Thin film is a layer of nanometer fractions to several micrometers in thickness, prepared from concentrated solutions. It is two dimensional and can be formed in the inside or outside of capillary microreactor by coating. Coating is done at room temperature while calcination and densification are performed at elevated temperature. Drying in air is usually fast and crack free due to the thin diameter of the films, thus forming adherent and continuous complete surface coverage. In the course of drying, thin films undergo shrinkage of the type anisotropic shrinkage.

b) Monolith formation

Formed from dilute solution of its precursors, a monolith is microporous preform that is nearly net shaped. Two types of solutions can be used to form monolith; alkoxides gel (with pore size < 10nm) and colloidal gel (with pore size > 10nm). Because of the three dimensional geometry and isotropic shrinkage pattern, crack free drying of monolith pose a big challenge. Both thin films and monolith coating can be performed on multi-channeled microreactor containing many silica capillaries held together using adhesives.

1.3 Silica Capillary

Silica could be considered as an interlinking SiO_4 polymer from silicic acid with the structure terminating at the surface either in a siloxane group (≡Si–O–Si≡, oxygen on the surface) or silanol group (≡Si-OH)[20]. This nature of silica surface enables silica capillary to partake in chemical reactions with various organic and inorganic compounds, warranting immobilization of different functionalization in either the outer or inner surface of the capillary according to the individual desire. Most prominent of these reactions are with chlorosilanes,[21] silanes[22] and siloxanes[23]. The silica capillary upon immobilization with a functionalized group directly or via a support can have many applications in chromatography,[24] catalysis[25] and biomaterials/biotechnology[26]. Fused silica capillaries with external protective polyimide coating and of various diameters are available commercially.

Silica

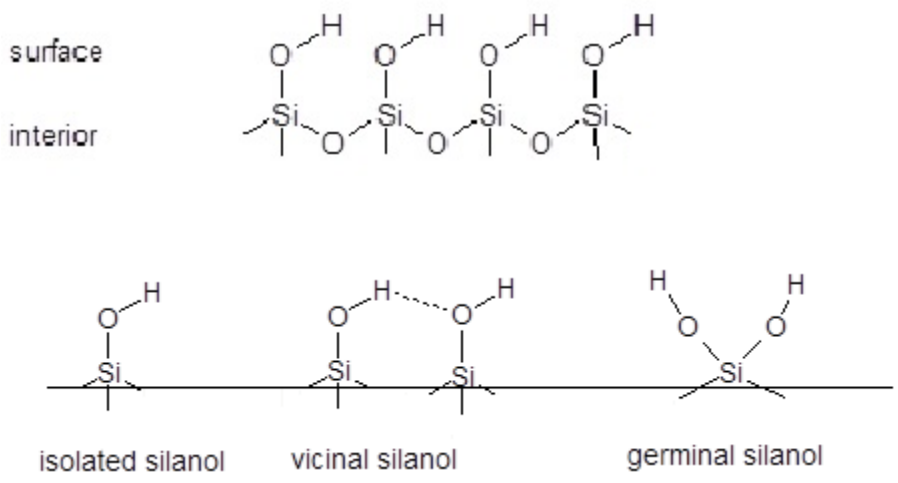

Scheme 1

1.4 Sol-Gel Process

A process where solution or sol undergoes a sol-gel transition, thus becoming rigid and porous mass[27]. Recently the technique is conveniently applied in immobilization of various organic, inorganic and biomolecule frameworks[28]. Prominently used example of sol-gel process is system of tetraethoxysilane (TEOS) and water mixed in a mutual solvent like ethanol[29]. Two steps are involved: formation of sol (dispersions of colloidal particles in liquid), then gelation of the sol to wet gel, which later dries.

1.4.1 Formation of Sol

When TEOS is mixed with appropriate amount of water in a mutual solvent (since TEOS is immiscible with water), the hydrolysis process initiates along with condensation. The product of complete hydrolysis is silicic acid ($Si(OH)_4$), but the hydrolysis does not get to completion before condensation starts, usually between two silanols or a silanol and

ethoxy group to form a siloxane group, resulting in elimination of water or ethanol. Both processes can be promoted under acidic or basic S_N2 conditions.

Hydrolysis

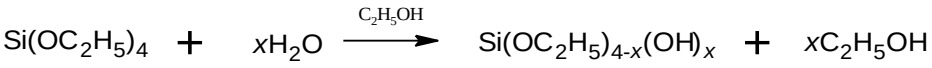

Condensation

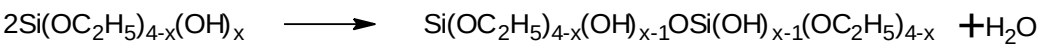

Scheme 2

1.4.1.1 Acid Catalyzed Hydrolysis

Hydrochloric acid is mostly used for catalysis of the hydrolysis process, although acetic acid, nitric acid and sulfuric acid have also been reported. The proposed mechanism is preceded by rapid protonation of –OR or –OH substituent bonded to Si, causing shifting of electron cloud away from Si, hence susceptible to attack by water molecule to form the transition state and subsequently ethanol or water will be eliminated.

1.4.1.2 Base Catalyzed Hydrolysis

Ammonia solution is generally used in base catalyzed sol-gel hydrolysis process. It hydroxyl ion being highly nucleophilic initiate the reaction by attacking Si which has the largest positive charge in TEOS.

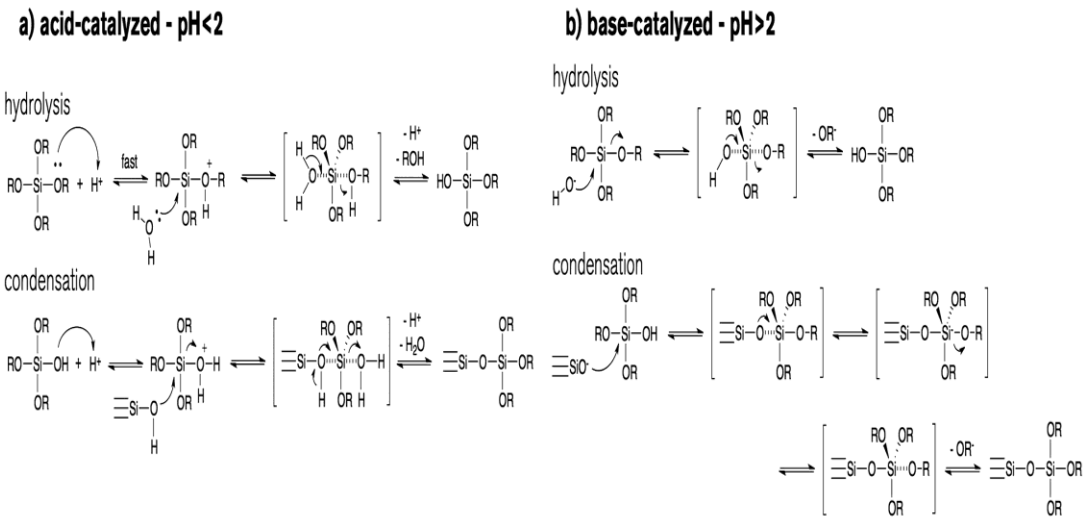

Scheme 3

1.4.2 Polycondensation

In acidic medium, due to slow hydrolysis, linear molecules that are occasionally cross-linked are formed as condensation continues and these chains entangle and form branches which result in gelation. However, in basic medium, where hydrolysis is fast highly branched clusters are formed that gelled by linking of the clusters. Studies conducted to compare the properties of gel formed from acid and base catalyzed hydrolysis showed TEM of acid catalyzed to exhibit a very fine microstructure and with very small pores that appear quite uniform throughout the material while TEM images of base catalysed showed resolved silica particles of larger pore size[30]. The surface of acid catalysed also showed more available silanols as further confirmed by the TGA results.

1.4.3 Gelation

When sufficient interconnected siloxane bonds are formed, colloidal particles or sol resulted which linked together with silica species after some time to form 3D network. As

gelation is being approached, sharp increase in viscosity occurred and instantly the sol lost its fluidity, forming an alcogel. Based on the method of solvent removal from the alcogel during drying, three kinds of gels are identified; xerogel, anbigels and aerogel.

1.4.4 Aging

Polycondensation reaction is allowed to continue in order to have more bonds formation and thus additional crosslinking. This makes the structure and properties such as strength of the gel to change as it aged.

1.4.5 Drying

At the last stage of gelation, solvent and water evaporate from the interconnected pore network resulting in gradual volume shrinkage of the solid alcogel. In order to prevent cracking while drying of the wet gel, controlled and monitored conditions must be put in place especially in large monoliths. When drying is achieved using thermal evaporation, xerogel of moderately low surface area and porosity results. Drying under supercritical conditions forms aerogel with large pores structure while drying at ambient temperature after changing the pore fluid with nonpolar and low surface tension organic solvent results in ambigel with 80-90% porosity of aerogel.

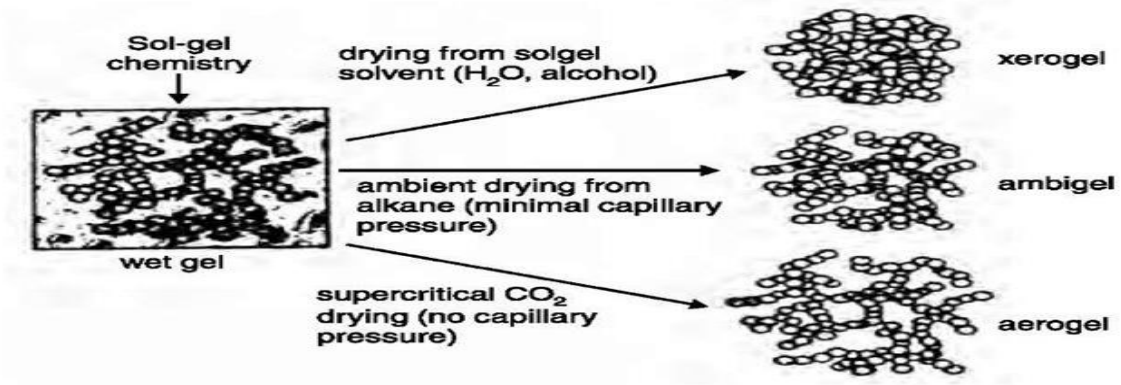

Figure 1.3 The sol gel process

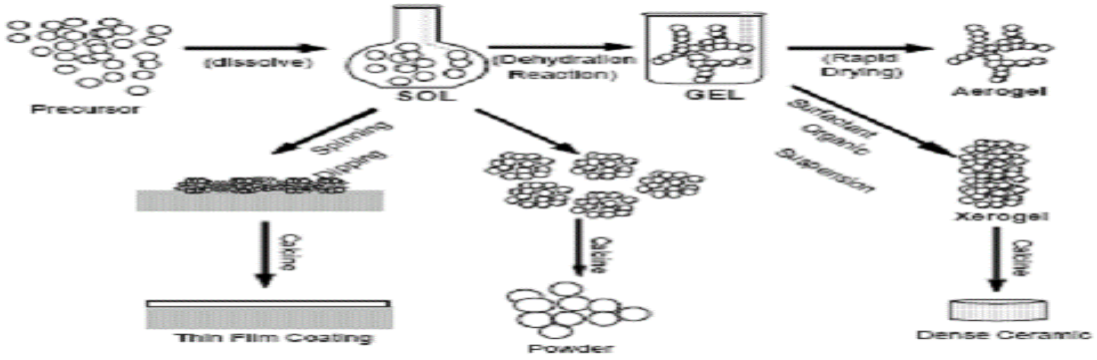

Figure 1.4 Applications of Sol Gel process

1.5 Statement of Research Problem

Most of the heterogeneous catalyses previously studied were based on γ – alumina, silica and titania supports. γ – alumina is used as catalyst support because of its surface area, pore size, pore volume and amphoteric character, although it suffers lack of chemical and hydrothermal stability[31]. This was later addressed by using mixed oxide films. Silica and titania thin films are frequently used due to their easy access, chemical and thermal stability, porosity and readiness to bond with different types of organic groups. Successes recorded in the use of these films has limited further research into novel metal oxide thin films which could offer better properties.

1.6. Objectives of Research

1. To develop new (cerium oxide) catalyst support in capillary microreactor.
2. Characterize the developed thin film.
3. Immobilize metal catalysts nanoparticles in the thin films.
4. Test run the developed capillary in some catalytic conversions.

1.6 Significance of the Study

The study targets development of novel thin film support for capillary microreactors which could be used as catalysts support for many catalytic conversions, one of the important research area defined in the “Strategic Priorities for Nanotechnology Program” of the Kingdom of Saudi Arabia.

CHAPTER 2

LITERATURE REVIEW

2.1 Catalyst Support

Since catalyst activity depends on the surface atoms, then anything that can maximize the surface area of the catalyst and enhanced the catalyst adhesion to the substrate is considered a catalyst support. The support may also affect the dispersion and shape of the catalysts particles[32]. Typical catalysts support are silica[33], alumina[34] and titania[7a].

2.1.1 Silica Support

Most of the heterogeneous catalysis studied are based on silica support due to its easy access, chemical and thermal stability, porosity and readiness to bond with different types of organic groups. For example in order to introduce –COOH functionality on a thin film, Brinker and co-workers fabricated –CN terminated silica thin films by an evaporation induced self-assembly (EISA) method using Brij56 nonionic surfactant which acted as a directing agent[35]. Nakamara et al. reported the surface modification of capillary by injecting silica suspension into a capillary of 60 cm length via Teflon tube connected to syringe while ensuring absence of bubbles and placed it horizontally in an oven at 60-120 ^{o}C[36]. After several hours of drying, the Teflon tube was removed from the capillary and further allowed to dry for 12 h at 90 ^{o}C. The modification can be furthered by flushing of octadecyltrimethoxysilane solution in toluene into the dried capillary, followed by heating at 100 ^{o}C for 30 min in order to activate the inner surface. By heating a mixture of $Pd(PPh_3)_4$, tetra(ethylene glycol), and $Si(OMe)_4$ and the resulting black suspension

treated with water, a silica gel containing trapped Pd nanoparticle was prepared and after washing and drying of the gel, it was used for the catalysis of Heck reaction[37]. Sonogashira cross-coupling has also been studied using silica-supported palladium complexes[38]. Stille coupling reactions were also reported to be catalysed using Pd catalyst supported on amorphous silica (SiO_2/TEG/Pd) prepared from $Pd(PPh_3)_4$ in tetra(ethylene glycol) and $Si(OMe)_4$ via the sol-gel method[37]. Other reactions studied using silica-supported catalysts are Suzuki-Miyaura coupling[39], carbonylation of aryl halides[40], cyanation of aryl halides[41], allylic alkylation[42] and Buchwald–Hartwig reactions[43].

2.1.2 Alumina Support

γ – alumina among other known alumina is more often used as catalyst or catalyst support and this is not unconnected to its surface area, pore size, pore volume and amphoteric character. Although the oxide has this favourable combinations, there is still something critical for it catalytic application that is practically lacking which is chemical and hydrothermal stability[31]. This has limit it application in catalytic support, however some researchers have tried to improve the properties when using it as support. For example Bravo et al.[5b], Lim et al.[44] and Park et al.[45] reported independently the use of alumina/zirconia support prior to coating with the catalyst. CeO_2 and La_2O_3 promoted α-alumina support was used for hydrogen production in microreactor and CeO_2 additive was observed to contribute more to the surface area increase than La_2O_3[46]. Kawamura and co-worker formed a thin Al_2O_3 boehmite layer on a microchannel using Al_2O_3-sol prepared by hydrolysis of aluminium isopropoxide[47] while Hwang et al. pre-coated the inner surface of microreactor with alumina[48]. In another research conducted by Zapf et

al.[49], alumina binder formed from γ-alumina, water, PVA and acetic acid was used as the catalyst support, although Haas-Santo reported that the calcined surface layer formed from this method used to be non-uniform[50]. Kundu et al. compared the stability and performance of alumina, zirconia and 1:1 mixture of both, as catalyst support for the study of steam reforming of methanol[51].

2.1.3 Titania Support

By atomic layer deposition, TiO_2 catalyst support formed from titanium tetrachloride and water was deposited on a borosilicate glass substrate for microstructured reactors[52]. Li Xiaohong used TiO_2 coated on SBA-15 as catalyst support for liquid-phase hydrogenation of benzaldehyde and found it effective [53], while Bian et al. studied the effect of experimental conditions on mesoporous TiO_2 thin films for platinum catalyst support by varying substrate type, aging conditions and films post-treatment method[54]. In other selective hydrogenation reactions in a capillary micro reactor, colloidal solution of metal or polymetallic nanoparticles was first mixed with titania precursor, surfactant and solvent then coated in the capillary after ageing[55]. However, the coating of mesoporous titania thin films without metal incorporation was also reported[7a], in which case the films acted as both catalyst and catalyst support.

Some researchers used porous polymer monolith synthesized *in situ* as support for catalysts[56]. GMA-*co*-EDMA was used as monolith support for the anchoring of palladium complex catalyst in a study conducted by Bolton et al.[57]. The monolith was synthesized *in situ* following a method reported by Preinerstorfer et al.[58] after treatment of the inner surface of capillary. Poly(chloromethylstyrene-co-divinyl benzene) was also

used as a polymeric monolith pre-catalyst support and was synthesized in situ using a mixture of 60% porogens, 24% monovinyl monomer and 16% crosslinking monomer[56], a 6:4 porogen/monomer ratio[59].

Several metal oxide supports have been reported for gold nanoparticles catalyst in selective hydrogenation of unsaturated aldehydes and ketones. Okumura et al. for example used Al_2O_3, SiO_2 and TiO_2 in their research[60], Mohr et al. used titania and zirconia[61] while Milone et al. used goethite, maghemite, hematite and iron oxy-hydroxide[62]. SiO_2-supported Au/TiO_2 and $Pt\text{-}Sn/TiO_2$ were also used to study the kinetics of liquid-phase hydrogenation of citral[55b] and SiO_2 was as well used for niobium and titanium catalysts support prepared via solventless organometallic precursor dry impregnation (OM-DI) and liquid-phase grafting post synthesis methods[63]. Ceria was reported to have large application in electric and electronics due to high electric and ionic conductivity and catalytic applications[64], however little was reported about it application as thin films and no report for thin film capillary application. Therefore in this research, ceria thin film was developed from cerium isopropoxide via the sol gel process and coated in capillary.

2.2 Catalyst Immobilization

In general, both heterogeneous and homogeneous catalysts can be applied in capillary microreactor. In heterogeneous system, the major challenges are the packing and retention of the supported catalyst inside the microreactor coupled with the high back pressure over the capillary tubes[65]. Contrastingly, in homogeneous system, the main challenge is the need for steady and constant plug flow behavior[66]. In developing a

capillary microreactor for heterogeneous catalytic reactions, the main task is how to deposit the catalyst in the capillary microreactor so as to have very stable and uniform immobilized surface.

Several studies reported different ways of achieving excellent catalyst deposition in microreactor beginning with preparation of the capillary wall in order to gain better catalyst adhesion, a process known as pretreatment, to calcination of the post coated capillary.

2.2.1 Pre-treatment

Surface pre-treatment has to do with preparing of a pre-coated surface towards increased surface adherence in order to achieve full potential for immobilization of catalyst. Free electrons, ions, radicals, metastables and UV radiation can hit substrate surface with high energies resulting in breakage of molecular bonds on the surface. Free reactive radicals are generated from the surface which can react rapidly with the incorporating groups to form cross-link and other functionalities. Several methods have been used that result in excellent pre-treatment some of which include:

2.2.1.1 Plasma Oxidative Treatment

Involves combustion of hydrocarbon fuel to generate flame plasma which is used to modify the substrate surface without affecting its bulk properties. This method had been used for silica[67] and stainless steel substrate[68] pre-treatment. Plasma oxidation is most effective within 5-10nm of the substrate surface and it offers great deal of wettability and aging stability to the surface. Three factors can affect nature of the oxidation: the flame chemistry, substrate distance from plasma and dwell time.

2.2.1.2 Anodic Oxidation

An electrochemical method of producing oxide film on the surface of a substrate by oxidation of the anode electrode dipped into acid solution. The method find application in surfaces and properties modification of titanium and aluminium[69] due to corrosion resistance and biocompatible resultant mechanical properties. In Pt electrodeposition on boron-doped diamond, anodic oxidation pre-treatment plays dual role: at short-term anodic pre-treatment, Pt deposition was increased and at longer pre-treatment time, the deposition was inhibited which was explained based on the wettability and stability of the surface.

2.2.1.3 Thermal Oxidation

Through high temperature heating in the range of 800 – 1200 ^{o}C inside furnace, oxide can be formed on the surface of substrate due to fast oxidation with environment water vapour or oxygen. This techniques has been reported in the pre-treatment of silica[70] and gold surface was also thermally activated to such a level that it undergoes oxidation at a lower potential than a copper surface[71].

2.2.1.4 UV Radiation

High energy UV radiation can cause the excitation of valence electron or even break chemical bonds. When this occurs on substrate, atoms, ions and radicals formed can react with atmospheric oxygen or other functionalities. This treatment was used by Bolton and co-workers[57] in an attempt to develop a palladium complex anchored solid macroporous monolith for catalysis in capillary microreactor following a procedure described by Rohr[72] and Greenway[73]. In the method, inner surface of capillary is activated by the

excitation of photoactive species such as benzophenone using UV light resulting in hydrogen abstraction and formation of free radical on the polymer substrate which accord quick and effective binding with many other functionalities[74]. In the studies of selectivity control in hydrogenation reactions[75], UV irradiation on TiO_2 layer deposited by atomic layer deposition[76] was done to render it super hydrophilic[77] after which the metal or polymetallic nanoparticles got impregnated on the layer.

2.2.1.5 Chemical Oxidation

Surface oxidation through chemical reaction as pre-treatment method is highly pronounced and most adopted by researchers. Studies conducted on prevention of inertial effects during the process of coating by the use of multi-channeled structures involved cleaning of the microchannel with pirancha etch, then water, then ethanol and dried it in an oven at 80 ^{o}C before coating with the catalyst[78]. While comparing the enzyme reactivity of SiO_2 supported capillary with non SiO_2 supported capillary, the latter was treated with piranha solution for 12 h at 25 ^{o}C and then rinsed with pure water[36]. Pre-treatment with sulphuric acid solution or seeding with silicalite seeds was used in the coating of zeolite films on the channels of stainless steel reactor[79]. Three step treatment was employed in the optimization of coating parameters of microchannel reactor using 99+% acetone, 99+% acetic acid, 1.0M ammonium hydroxide, 85 wt.% phosphoric acid and 29-32% hydrogen peroxide[80]. In methanol steam reforming using microchannel reactor, the pre-treatment was done by dipping a micro-channeled stainless steel into concentrated nitric acid for 45 min followed by washing with demineralized water[51]. Anisotropic wet etching with 30 wt.% KOH solution was applied on micro-channels as pre-treatment strategy in the investigations of preassembled methods of microreactors

coating[48]. Pre-treatment of inner surface of capillaries in the investigation of the applicability of poly(chloromethylstyrene-*co*-divinyl benzene) catalyst supported-polymer as monolith in capillary microreactor for Suzuki-Miyaura and Sonogashira reactions[56] was done by rinsing the capillaries with acetone followed by 0.2 M NaOH at rate of 2.0 µl.min^{-1} for 2 h. After rinsing with water and 0.2 M HCl under the same condition, the capillaries were further rinsed with water, followed by ethanol at 2.0 µl.min^{-1} for 30 min and lastly 20 wt.% solution of 3-(trimethoxysilyl)propyl methacrylate in ethanol at pH 5 was flushed through the capillaries at 0.25 µl.min^{-1} for 1 h, as surface modifying agent, then washed with acetone and dried with air for 24 h[58]. Adhesion properties of the inner surface capillary was enhanced in a research conducted by Rebrov and co-workers[7a, 55a] by treating the capillary with continuous flow of 1 M NaOH at rate of 0.03 ml.min^{-1} for 15 min, followed by flushing with demineralized water, after which the capillary was dried and calcined in an oven at 300 ^{o}C and 16 mbar. Protasova et al., apply similar pre-treatment procedure by passing 1 M NaOH solution through the capillary at 70 ^{o}C for 2 h, then washed the capillary with water and ethanol at 25 ^{o}C[55b] while Zeng et al., used 1 M NaOH solution for 1 h, then washed with deionized water followed by 0.1 M HCl solution and deionized water again[81]. The inner surface of a glass capillary, in study done by Ng et al., was filled with 2-aminopropyl trimethoxysilane solution in methanol and left for 15 h at 25 ^{o}C after washing of the capillary with 1 M NaOH, water and ethanol in order to enhance covalent bonding with the catalyst[82]. Similar procedure was also used by Kobayashi research team in developing a microfluidic device for conducting multiphase hydrogenation reactions[7b].

2.2.2 Sol Solution

Excellent design of a sol solution is pre-requisite to successful catalyst deposition in a capillary microreactor. Basic properties that need to be monitored in sol solution preparation are viscosity, surface tension and time-to-gel with the last property being particularly more important because film formation, drying and creation of pore must be rapid. Some or all of the following are what constitute the sol solution: catalyst precursor, support precursor, surfactant, deactivating agent, acidic/basic/fluoride catalyst and solvent(s). Different methodologies were reported in preparation of a sol solution for the coating process based on the research needs. For synthesis of –COOH terminated highly ordered mesoporous thin films , cyanoethyltriethoxysilane used as cyanide precursor was mixed with TEOS, Brij56, hydrochloric acid, ethanol and water, which upon deposition resulted in the cyano-functionalized mesoporous film and on hydrolysis with sulphuric acid yield the corresponding –COOH derivatized mesoporous thin films[35]. The sol solution of silica coated microcapillary was prepared by addition of silica nanosphere to a mixture of water and ethanol, then injected into the pretreated capillary with a syringe pump[36]. Another study utilised only Pd acetate as catalyst precursor and dimethylformamide as solvent in preparation of sol solution which was filled into borosilicate capillaries[13]. In preparing the sol solution of $CuO/ZnO/Al_2O_3$ catalyst, the mixed oxides were crushed and sieved to <24 μm diameter, then added to a mixed solution of boehmite, deionized water and nitric acid, and ball milled overnight[78]. Studies on kinetics of methanol synthesis over $CuO/ZnO/Al_2O_3/V_2O_3$ catalyst used 10 wt.% suspension of the ball milled and sieved form of the catalyst in 2-propanol for coating after sonication[83]. Phan et al. used 1 wt.% of polyvinyl alcohol instead of 2-propanol in

preparing sol solution for ball milled $CuO/ZnO/Al_2O_3$ precursor[84]. Aluminium secondary butoxide and zirconium (IV) propoxide were used as precursors for preparing sol solutions of alumina, zirconia and 1:1 mixture of both using the method described by Zeng[85]. Hydrolysis of alkoxide was protected during the sol preparation by addition of acetylacetone in 1:1 ratio with alkoxide[51]. Hwang and co-worker used two different solvents to prepare $Cu\text{-}Zn\text{-}Al_2O_3$ catalyst slurry after ball milling; alumina sol and deionized water which were coated on alumina pre-coated microchannel[48]. While attempting two different ways of anchoring metal/bimetallic nanoparticles on films and capillaries, Muraza et al. used two different approaches; first, thin films were prepared separately and then nanoparticles were anchored on the films and secondly, one-spot synthesis was done containing the films as well as the nanoparticles[75, 86]. Appropriate amounts of pluronic F127, titanium tetrabutoxide (TTB), ethanol, H_2O and nitric acid were used in preparing sol solution for mesoporous titania thin film coating[7a]. Titanium tetrabutoxide (TTB) was substituted by $Ti(O\text{-}2Pr)_4$, and then Au nanoparticles were added in preparation of sol solution for Au/TiO_2 deposition in a one-spot synthesis procedure[55b]. Many thin films parameters could be successfully varied through altering of sol solution components or changing their percentage. Tetraethoxysilane (TOES) was reported to be an excellent sol-gel precursor due to its structure which enables fast drying thus preventing cracking[87]. Lu et al. in their research varied the metallic ratio in a nanoparticle by changing initial concentration of the metal precursor[88] while by changing the amount of protecting agent, Alberius successfully changed the nanoparticle size[89]. The porosity of films was also reported to be changed by increasing the percentage volume of surfactant or changing the surfactant[90].

2.2.3 Coating and Post Coating

In order to flow the sol solution through capillaries for coating, two methods are commonly employed. They are injection method and gas-fluid displacement method. Both used pressure to overcome the sol solution viscous drag[91]. In injecting catalyst suspension into a capillary, Nakamura et al. connected a Teflon tube to the microcapillary and used a syringe to inject silica suspension into the microcapillary[36]. Chen and co-worker adopted similar approach in filling Pt/Al_2O_3 catalyst sol solution into closed microchannels[92]. Hayes and Malik used capillary filling/purging device in the gas-fluid displacement method, by inserting one capillary end into the pressurization chamber until it moves into a solution vial positioned inside the chamber, then airtight the capillary filling system before discharging inert gas[93]. Bravo et al. also used the gas-fluid displacement method in coating $CuO/ZnO/Al_2O_3$ catalyst in inner surface of capillary[5b]. The sol solution could be kept for some time in the capillary before is finally expelled (flow coating) or allowed to slowly dry and then calcined (fill-and-dry)[48, 94]. In the case of monolith formation, the sol solution is left undisturbed in capillary until gelation is complete, then pressure is slowly released through the capillary[95].

After coating, a post coating treatment is applied by subjecting the capillary to thermal conditioning in the form of slow temperature programming with continuous flow of inert gas in order to complete bond formation between the silica capillary and the immobilized system and at the same time increase the strength of the bonding hence decrease leaching possibility of the catalyst. For example after drying for 12 h at 90 ^oC, octadecyltrimethoxysilane in toluene was further flushed through an already treated capillary and heated at 100 ^oC in an oven for 30 min[36]. Kunde et al. conditioned their

microchannel, after coating it and allowing it to dry at room temperature, by first heating at 80 ^{o}C in an oven for 5 h and then calcined at 500 ^{o}C for 2 h in order to decompose the carbon species present in the sol solution, thus increasing the surface area[51]. Rebrov subjected the capillary to 300 ^{o}C heating at 15 mbar in an oven after drying it[7a] and Protasova used the same 300 ^{o}C heating but under a 10 mbar pressure in the post treatment[55b].

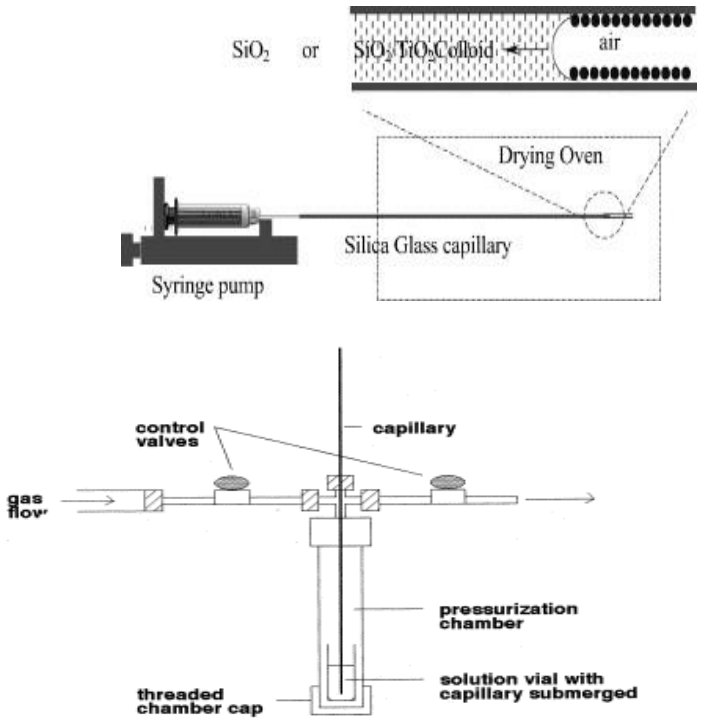

Figure 2.1 a) Injection method with syringe b) Capillary filling/purging device

2.3 Characterization of Immobilized Capillary

Many techniques have been used for studies of properties such as surface morphology and chemical composition of coated surfaces. Most of the techniques were chosen based on research demand, instrument availability and expertise in operation, and ability to interpret result. For inner surfaces of capillaries, characterization can be done by

removing catalyst film on the inner surface and use it for the analysis. However, this is only possible if the capillary diameter is large enough as in the case of 1150 µm capillary used by Shore et al in their research[13]. When the capillary diameter is quite small, a similar coating is done on a flat surface and used for the characterization[7a, 55b].

2.3.1 Inductive Coupled Plasma

Metal loading in coated capillary is determined by using inductive coupled plasma (ICP). For example Gomann et al determined palladium content in the polymer-supported capillary microreactor using ICP-MS[56], while Ng et al quantified Pd loading in Palladium coated capillary using ICP-AES[82].

2.3.2 Thermogravimetric Analysis

Variation in physical or chemical properties of coated surfaces as a function of increasing temperature can be determined using thermogravimetric analysis (TGA). For example TGA of –COOH derivatized mesoporous thin films in argon to temperature of 800 ^{o}C showed *ca.* 14% weight loss between 200-450 ^{o}C which was thought to be result of decomposition of $–CH_2CH_2COOH$ groups[35]. Porous system of styrene divinylbenzene resin used as platinum catalyst support was found resistant to heating up to 160 ^{o}C with 4.4% surface area lost in its TGA result[96].

2.3.3 Adsorption-Desorption Isotherm

Adsorption-desorption isotherm provide information on the size and shape of pores based on the type of hysteresis loop formed[97]. A type IV isotherm typical of mesoporous materials was reported in the N_2 adsorption-desorption isotherm performed by Liu et al[35]

and Rebrov et al[7a] also reported similar result. Ethanol adsorption-desorption isotherm recorded with ellipsometric porosimetry (EP) was also reported[52, 55b].

2.3.4 Electron Microscopy

Crystal structural information, direct surface imaging, elemental distribution and composition are routinely determined using electron microscopy such as transmission electron microscopy (TEM), high resolution electron microscopy (HREM) and scanning electron microscopy (SEM). In order to confirm complete filling of capillary with monolith, Bolton and co-worker used SEM and observed the resulting images[57]. Sample imaging was also carried out for Pd coated capillary and the SEM results showed highly porous and nanometer sized crystallites[13]. Field emission scanning electron microscopy (FESEM) was used to determine the cross-sectional morphologies and thicknesses of catalysts layers coated onto micro-channels[48]. Rebrov et al. used transmission electron microscopy (TEM) and field emission gun scanning electron microscopy (FEG-SEM) to determine the morphology and cross sectional thickness of coated fused silica capillary respectively[7a].

2.3.5 X-ray and Neutron Diffraction

Complete structure description could be achieved using X-ray diffraction (XRD) and neutron diffraction. XRD was used to determine the phase composition of Pt-Ru surface coated microstructured reactor[52] and the crystalline state of mesoporous titania thin films[54].

2.3.6 NMR

Information concerning the nuclei environment is obtained using NMR such as ^{1}H NMR, ^{13}C NMR, and ^{29}Si MAS NMR. ^{13}C, ^{29}Si and ^{31}P cross polarization magic angle spinning (CP/MAS) NMR were used in characterization of surface rhodium siloxide complexes[98].

2.3.7 EPR and Mossbauer Speectroscopy

Electron spin resonance (ESR) or electron paramagnetic resonance (EPR) could give access to number and location of unpaired electrons while oxidation state of some metals and coordination number in complexes can be determined using Mossbauer spectroscopy. Wang for example studied the chemical state of Manganese in Mn/SiO_2, $Rh\text{-}Mn/SiO_2$ and $Rh\text{-}Mn\text{-}Li/SiO_2$ catalysts by EPR, since Mn^{2+} is paramagnetic, with in situ reduction treatment[99]. ^{197}Au Mossbauer absorption spectroscopy (MAS), X-ray photoelectron emission (XPS) and TEM were used by Zwijnenburg et al in characterization of gold catalysts supported on TiO_2 and TiO_2/SiO_2[100].

2.3.8 IR and FTIR

Vibrational spectroscopy techniques like IR and FTIR are relevant in the study of the behaviour of precursor compounds during catalyst preparation. For example in order to confirm the conversion of –CN to –COOH on thin films pore surface, FTIR was performed on the thin film and the spectrum showed complete disappearance of –CN stretching vibration along with appearance of –COOH stretching vibration[35] and in another studies, FTIR was used to characterize SBA-15-based chiral rhodium catalysts and the results showed that the catalysts exhibited the general characteristics bands of pure SBA-15[101].

2.4 Applications of Coated Capillaries in Reactions

Studying reactions in capillaries required the use of some analytical tools such as ICP, HPLC, GC-MS, NMR, etcetera. These techniques are used to analyse the reaction product and in the long run conclude on the performance of the coated capillary. Some of the reactions studied include:

2.4.1 Enzymatic Reactions

Nakaruma et al. studied enzymatic reactions in a SiO_2 coated capillary microreactor by immobilizing the enzyme on the inner wall of the reactor. The hydrolysis product of the enzyme reaction, unbelliferone, was obtained at high yield in 10 min[36]. Photocatalytic reaction of methylene blue solution was also carried out by same group in microcapillaries coated with TiO_2 and SiO_2/TiO_2 in which case, the latter showed complete reduction of methylene blue in 40-50 s. In both cases, reactions were monitored using UV – visible spectroscopy.

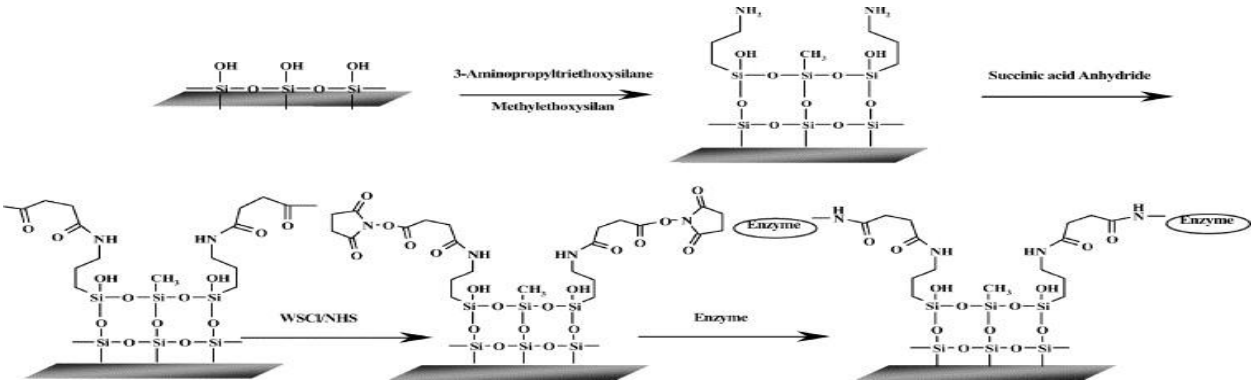

Figure 2.2 Enzyme immobilization on the inner surface of capillary.

2.4.2 Suzuki-Miyaura

Suzuki-Miyaura reaction of iodobenzene and *p*-tolyboronic acid was studied in a continuous flow capillary coated with palladium complex anchored on macroporous monolith supports[57]. GC-MS analysis of the reaction products (Scheme 4) showed 68% yield of 4-methylbiphenyl and the yield remained constant for 4 days of continuous capillary flow, which demonstrates the application of the method for sustainable continuous flow processes. A Pd leaching of 15-20% after 4 days of operation was calculated from ICP-MS results.

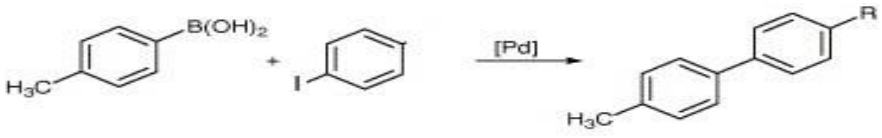

Scheme 4

Gomann et al. used different monolith support in a capillary microreactor to study the Suzuki-Miyaura reaction of aryl halides and *p*-tolyboronic acid[56] whose products were analyzed using GC-MS and GC-FID. The results showed low activity for the less reactive halides, however the selectivity was very high with small amount of by-product detected for bromobenzene coupling. The researchers also studied Sonogashira coupling reactions of iodobenzene with phenylacetylene (Scheme 5) and high catalytic activity with nearly complete conversion was recorded. After 8 days of continuous operation, leaching of Pd in the capillary was determined to be only 4% loading using ICP-MS.

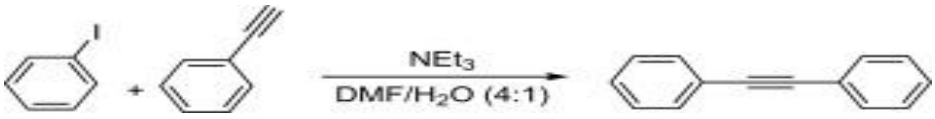

Scheme 5

Suzuki-Miyaura coupling of aryl boronic acids with bromides were also studied in Pd-coated capillaries and the products analyzed by ^{1}H NMR[13]. Good to excellent conversions for both electron-rich and electron-poor aryl halides with electron-poor boronic acids were recorded. It was further observed that with the capillaries inside microwave, yield was increased, while in batch reactor, no yield was recorded. ICP-AES analysis showed no leaching of Pd catalyst for up to 2 ppm detection limit. Heck coupling of aryl iodides with acrolein derivatives was also tested and very good conversions were obtained.

2.4.3 Steam Reforming of Methanol

Steam reforming of methanol was studied in a non-porous multi-channeled microreactors coated with $CuO/ZnO/Al_2O_3$ catalyst and the product analyzed by GC[78]. Both the methanol conversion and CO_2 selectivity were calculated from the analysis of gaseous CO_2, CO and CH_3OH along with a carbon balance, and 50% methanol conversion was recorded and more than 97% CO_2 selectivity.

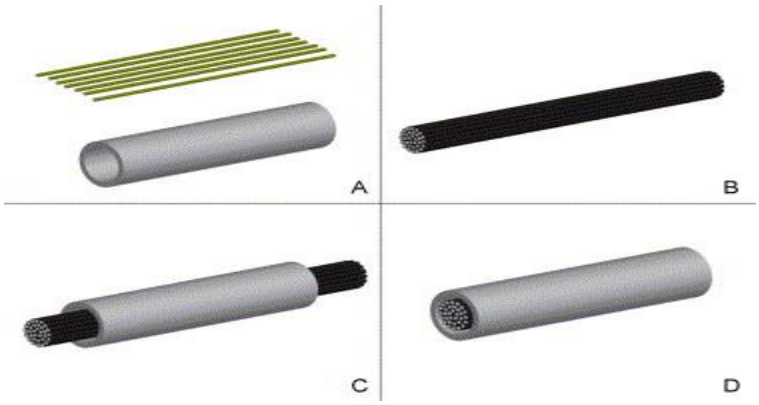

Figure 2.3 Fused-silica capillaries combined to form multichanneled capillary

Steam reforming of methanol in alumina, zirconia and 1:1 alumina-zirconia catalysts coated micro-channel reactor was also studied by Kundu et al.[51] and an overwhelming result was obtained with alumina-zirconia mixed catalyst with 99.3% methanol conversion at 290 ^{o}C and 0.01 ml.min^{-1} feed rate.

In another study, steam reforming of methanol was carried out in Cu-Zn-Al_2O_3 catalyst coated microreactor of four different types: based on slurry type; alumina sol-based and DI water based and based on coating method; flow coating and fill-and-dry coating[48]. Analysis of the micro-Gas Chromatograms showed maximum gas production of 118 cm^3, of which 85 cm^3 was H_2 at 300 ^{o}C and methanol feed rate of 9 ml.h^{-1}.

2.4.4 Hydrogenation

Continuous capillary microreactor with mesoporous titania thin films of Pd or $Pd_{25}Zn_{75}$ nanoparticles was reported to be used in selective hydrogenation of 2-methyl-3-butyn-2-ol[55a]. GC-MS results showed the major reaction products to be 2-methyl-3-buten-2-ol and 2-methyl-3-butan-2-ol. However, at low hydrogen partial pressure, significant amount of 2,7-dimethyl-3,5-octadiyne-2,7-diol (C_{10}-dimer) was produced. Selective hydrogenation

of phenylacetylene in similar capillary microreactor was also studied under different flow and temperature control[7a]. The results showed that conversion of phenylacetylene to styrene increased with temperature while selectivity decreased and on the contrary, as liquid flow rate increased, the conversion significantly decreased while selectivity to styrene formation increased. It was observed that the capillary microreactor maintained both activity and selectivity after one month of continuous application.

In the investigation into the kinetics of liquid phase hydrogenation of citral on Au/TiO_2 and $Pt\text{-}Sn/TiO_2$ thin films capillary, it was observed that $Pt\text{-}Sn/TiO_2$ thin film at 343K, liquid residence time of 30 min and a hydrogen partial pressure of 1 gave the highest yield of 79% unsaturated alcohol[55b]. The reaction orders were found to be 1 for hydrogen over $Pt\text{-}Sn/TiO_2$ and nearly zero for citral over Au/TiO_2 and $Pt\text{-}Sn/TiO_2$ catalysts respectively.

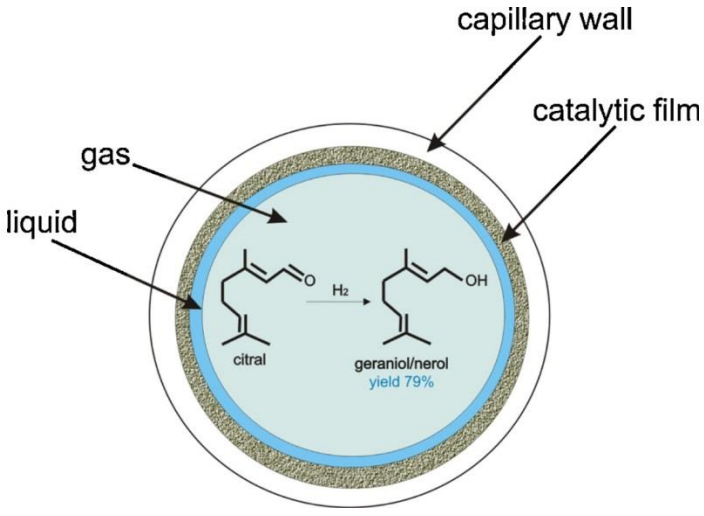

Figure 2.4 Hydrogenation of citral on Au/TiO_2 and $Pt\text{-}Sn/TiO_2$ thin films.

2.4.5 Hydrogen Peroxide and Hydrogen Gas Production

Hydrogen peroxide formation via a capillary microreactor immobilized with palladium was reported by Ng et al[82]. Hydrogen and oxygen flow were controlled separately at flow rates of 2 and 4 ml/min respectively, and were mixed at T-coupling. Then liquid phase was added to the gas stream and the effluent was analyzed using colorimetry while the Pd leaching was measured with ICP-AES. The highest yield of H_2O_2 was obtained with MeOH/HCl/KBr/ as liquid phase solution among the different liquid phase solutions used.

Hydrogen production from ethylene glycol reforming using Rh catalysts supported on CeO_2 and La_2O_3 promoted α-Al_2O_3 was reported[46]. The activity tests were carried out in a lab scale set up and in all the experiments, a steam to carbon mixture (S/C) of 4.0 was used. Complete conversion and selectivity close to the equilibrium were recorded for all tested catalysts, with very low concentration of CH_4 and CH_3CHO by-products. Long-time stability test on the capillaries showed C_2H_4 and C_2H_6 by-products detected in minor amounts.

CHAPTER 3

EXPERIMENTAL

3.1 Chemicals and Materials

Ceric ammonium nitrate, ACS reagent grade was purchased from Riedel-de Haen AG, USA. Phenylacetylene, 65% nitric acid and palladium (ii) nitrate hydrate were purchased from Sigma – Aldrich, USA, while acetylacetone, hexane, ethanol, dimethoxyethane, isopropanol, sodium hydride and sodium borohydride were purchased from Fluka Chemie AG, Buchs, Switzerland. Fused silica capillary, 250 µm diameter was purchased from Polymicro technologies, USA.

3.2 Synthesis of Cerium Isopropoxide

Cerium isopropoxide was synthesized following the procedure described by Vaartstra et al. 1990[102]. The experiments were performed using the Schlenk line techniques under continuous nitrogen flow in order to prevent partial hydrolysis by atmospheric moisture. Ceric ammonium nitrate [$(NH_4)_2Ce(NO_3)_6$] was dried in an oven at 110 ^oC for 1 h before being used. Sodium hydride (NaH), anhydrous isopropanol (*i*-PrOH) and dimethoxyethane (DME) were used without further treatment. 22 ml of *i*-PrOH and 14 ml of DME were added to 2.4 g of NaH at 50 ^oC and stirred gently. After all the NaH had reacted, 10 ml of DME was added at room temperature, then followed by 9.138 g of $(NH_4)_2Ce(NO_3)_6$ dissolved in a mixture of 14 ml DME and 12 ml *i*-PrOH. The mixture was stirred overnight, then sodium nitrate formed was filtered off, leaving yellow solution of cerium isopropoxide in DME and excess *i*-PrOH. The solvents were removed

from the cerium isopropoxide by rotary evaporation at 50 ^{o}C and yellowish cerium isopropoxide was characterized by NMR.

3.3 Synthesis of Palladium Nanoparticles (Pd NPs)

Chemical reduction method of synthesizing nanoparticles reported by Rocio et al.[103] was adopted because it result in smaller size nanoparticles (2.5 nm). 10^{-3} M solution of palladium (ii) nitrate hydrate ($Pd(NO_3)_2.XH_2O$ was prepared by dissolving 23.04 mg of the salt in 100 ml of ethanol solution. In order to avoid agglomeration of nanoparticles, the solution was diluted to 4 x 10^{-4} M by dissolving 2.5 ml of the stock in 25 ml absolute ethanol.

Freshly prepared 10^{-3} M $NaBH_4$ solution in ethanol was added dropwise to the palladium salt solution while stirring at moderate rate at room temperature for 1 h.

Complete Palladium ions reduction was investigated using UV-Vis spectrophotometer and the formed nanoparticles were allowed to settle down, then washed in ethanol in order to remove excess $NaBH_4$.

3.4 Surface Pretreatment of Capillary

This was done by continuously flowing 1M NaOH into the capillary for 30 min, followed by flushing with demineralized water, after which the capillary was dried and calcined in an oven at 250 ^{o}C for 10 h. Surface pretreatment result in the activation of surface silanol of the silica capillary as shown below.

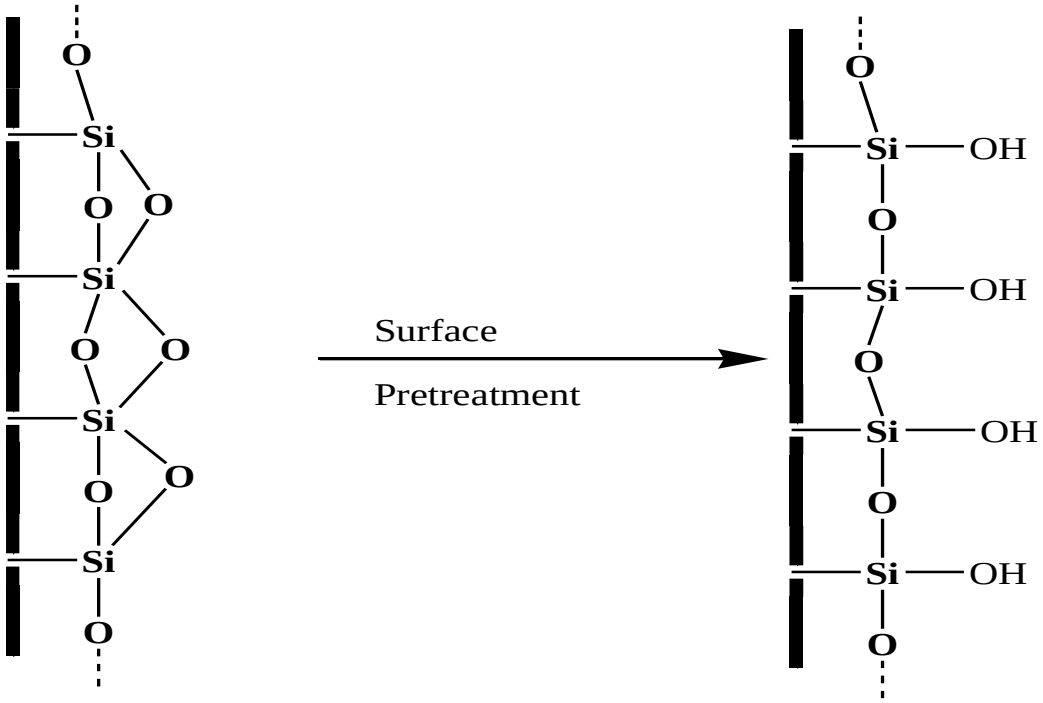

Figure 3.1 Surface pretreatment of fused silica capillary

3.5 Preparation of Sol Solution

Cerium isopropoxide ($Ce(OPr^i)_4$) was chosen among other ceria precursors due to its ease of hydrolysis and condensation, thus can be employed to form thin films. The as-synthesized cerium isopropoxide was dissolved in 33.4 ml isopropanol in order to have 0.5 M solution of the precursor. 98.1µl of acetylacetone (acac-H) was added to 4 ml of the precursor solution in order to prevent precipitation of cerium oxide through chelation of the acetylacetonato groups to cerium[104]. The mixture turned yellowish red after 15 min of swirling.

126 mg of Pluronic F127 was dissolved in 1.17 ml of ethanol at 50 ^oC and was added to 0.36 ml water and 0.161 ml trioxonitrate (V) acid (65 wt.%). To this solution, the acetylacetone-modified precursor solution was added gradually while stirring at 800 rpm at room temperature. The stirring was continued for 24 h at room temperature after which the solution in the form of sol-gel was flowed through a 250 µm diameter capillary for coating. The combining ratio was in the form: 1 $Ce(OPr^i)_4$: 0.5 acac-H: 25 *i*-PrOH: 10 EtOH: 10 H_2O: 1 HNO_3: 0.005 Pluronic F127.

In order to incorporate Pd nanoparticles in the sol-gel, 7.454 mg of as-synthesized nanoparticles were dispersed in the 1.17 ml absolute ethanol and added to the mixture, giving 1 wt.% loading.

The coated capillary was allowed to dry at room temperature under continuous flow of helium gas for 24 h before it was calcined under temperature programming of 25 – 330 ^oC at ramping of 1 ^oC/min, hold at 330 ^oC for 5 h. It was then flushed with absolute

ethanol for 15 min and reconditioned at 40 – 330 ^{o}C at ramping of 5 ^{o}C/min, hold at 330 ^{o}C for 1 h.

Synthesis of $Ce(OPr^{i})_4$

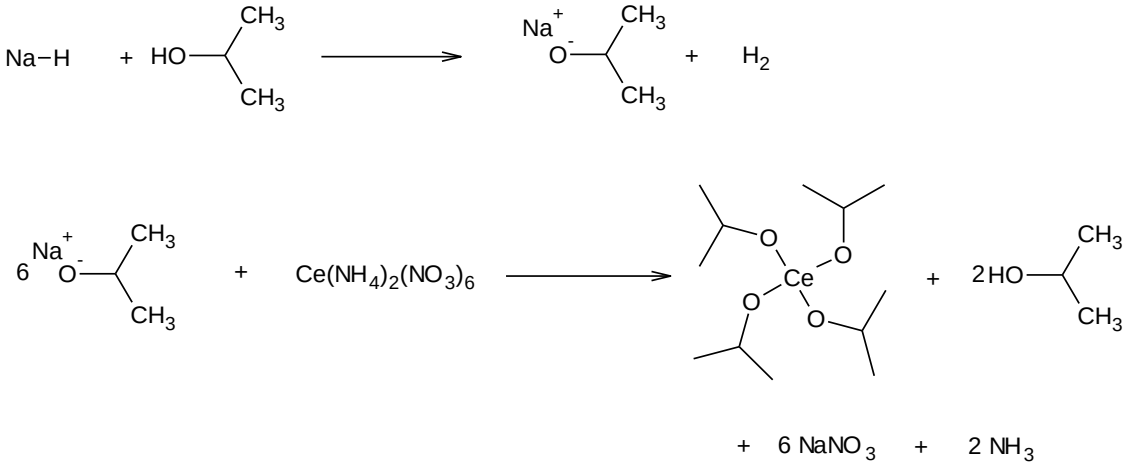

The hydrolysis and condensation of $Ce(OPr^{i})_4$ in the capillary can be shown as:

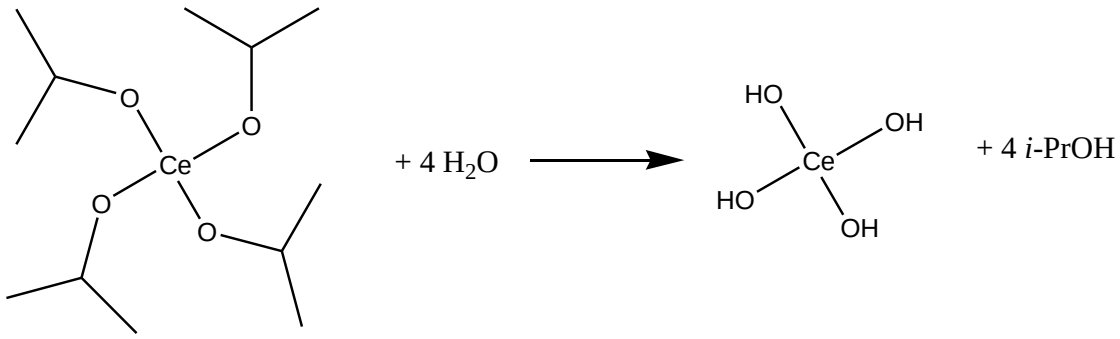

Scheme 6

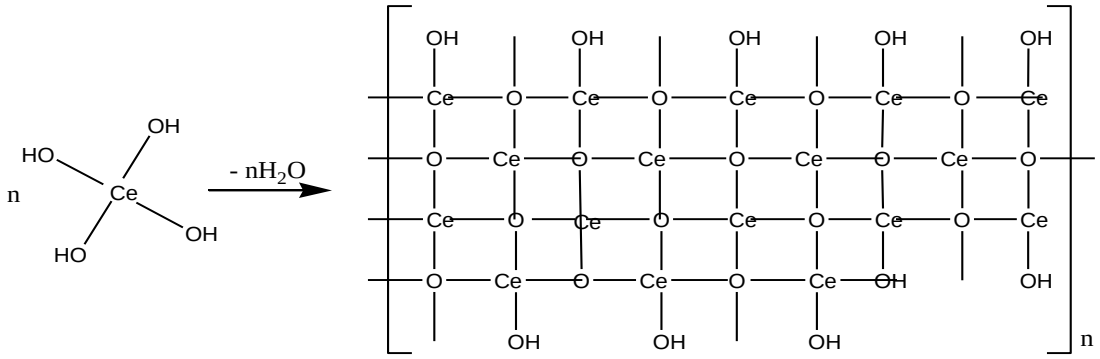

scheme 7

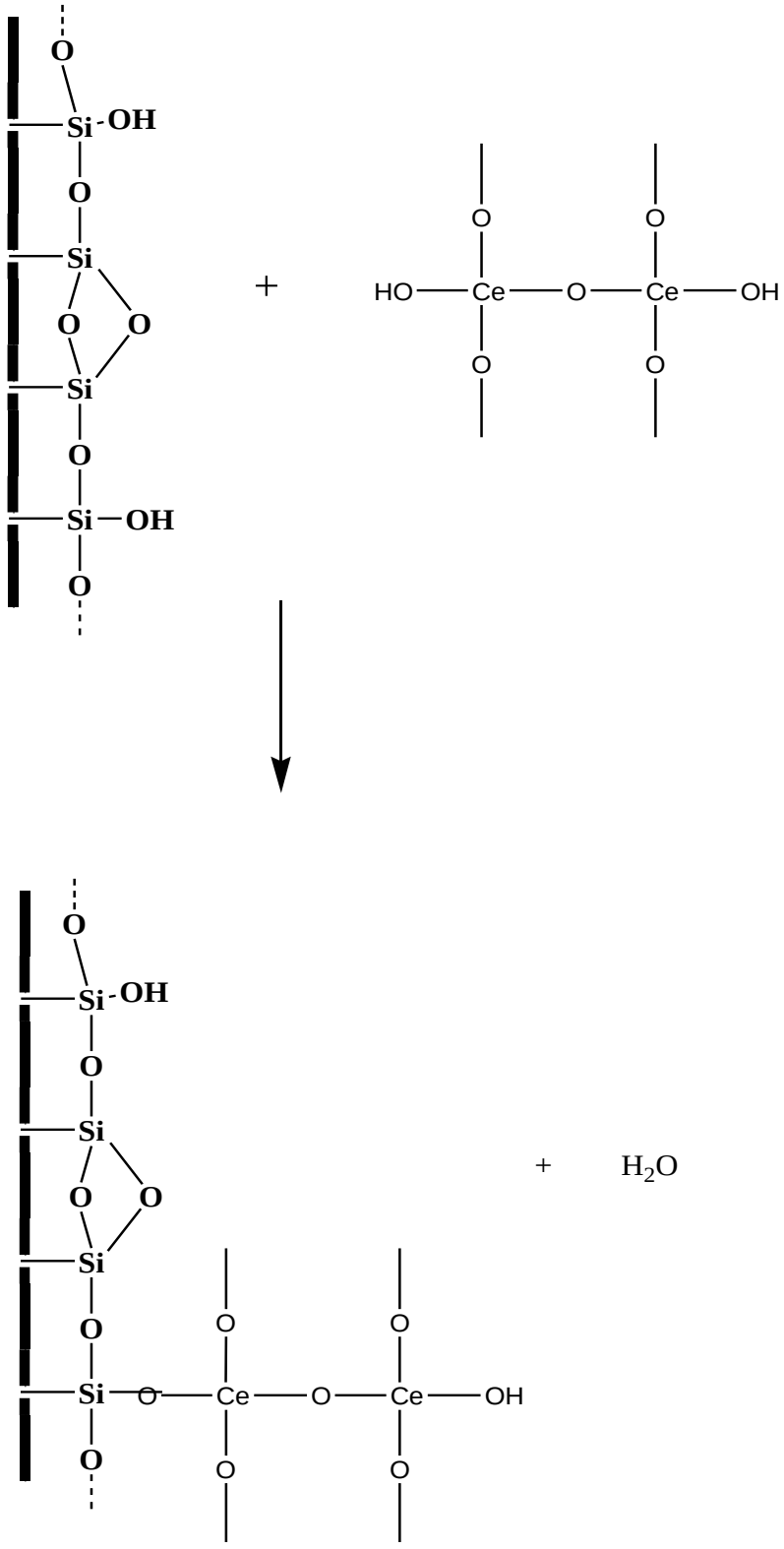

Figure 3.2 Fused silica capillary coated with ceria thin film

3.6 Characterization of Thin Film

Powder X-ray diffraction pattern (XRD) of the dried thin film was recorded on Rigaku miniflex II X-ray diffractometer in step scan mode between 20 and 90^0 2θ (scan rate 0.02^0 $2\theta s^{-1}$) using CuKα radiation (λ = 1.5414Å). Morphology of thin film on flat glass substrate and inside capillary were obtained using LYRA 3 dual beam field emission scanning electron microscopy (FESEM) at 15.0kV by making a gold coating in a nitrogen plasma coating unit. Palladium mean particle size was determined from the transmission electron microscope (TEM) image recorded on a Joel-JEM-2100 operated at 200 kV. The scratched thin film were grounded, dispersed in methanol and sonicated for 10 min. One drop of the suspension was dropped on a Cu grid coated with thin layer of carbon. The mean particle diameter was calculated using the relation: $d_m(nm) = {}^{1}/_{100} \sum_{i=1}^{100} n_i d_i$, for n_i number of particles with diameter d_i obtained from the TEM image. Palladium nanoparticle dispersion, $\%D$ was determined using the formula: $\%D = {}^{107}/_{d_m(nm)}$ [105].FT-IR was carried out on the sol gel using Nicolet 6700 FT-IR spectrometer containing the smart orbit accessory and on the dried thin film, KBr pellet containing 1% of the film was prepared and used for the analysis. Raman spectra was recorded at room temperature, using NXR FT-Raman module spectrograph equipped with InGaAs detector. Data from both FT-IR and XRD were analyzed using Microsoft excel.

3.7 Application of Pd/CeO_2 Capillary in controlled synthesis of styrene and ethylbenzene.

Hydrogenation of phenylacetylene in the Pd/CeO_2 coated capillary microreactor was studied in the range of 30 – 60 ^oC by flowing hydrogen gas through the 250 µm diameter

coated capillary at an angle of 90^0 with respect to the liquid flow. Phenylacetylene in hexane was flowed at constant rate of 0.01 $ml.min^{-1}$. The coated capillary was placed in a temperature controlled oven with both inlet and outlet tubes. The inlet tube was connected to the microreactor while the outlet was connected to 10 ml vial for product collection. Effects of capillary length, temperature, concentration and gas flow rate on the conversion and selectivity were investigated. The reaction product was collected and analyzed using GC-MS. Metal leaching due to flow of reactants through the capillary was investigated using ICP-MS by evaporating the collected reaction product(s) under reduced pressure and treating the empty vial with 1.5 ml aqua regia and 8.5 ml ultrapure water. The experimental flow diagram for preparation of immobilized Pd NPs capillary is shown below.

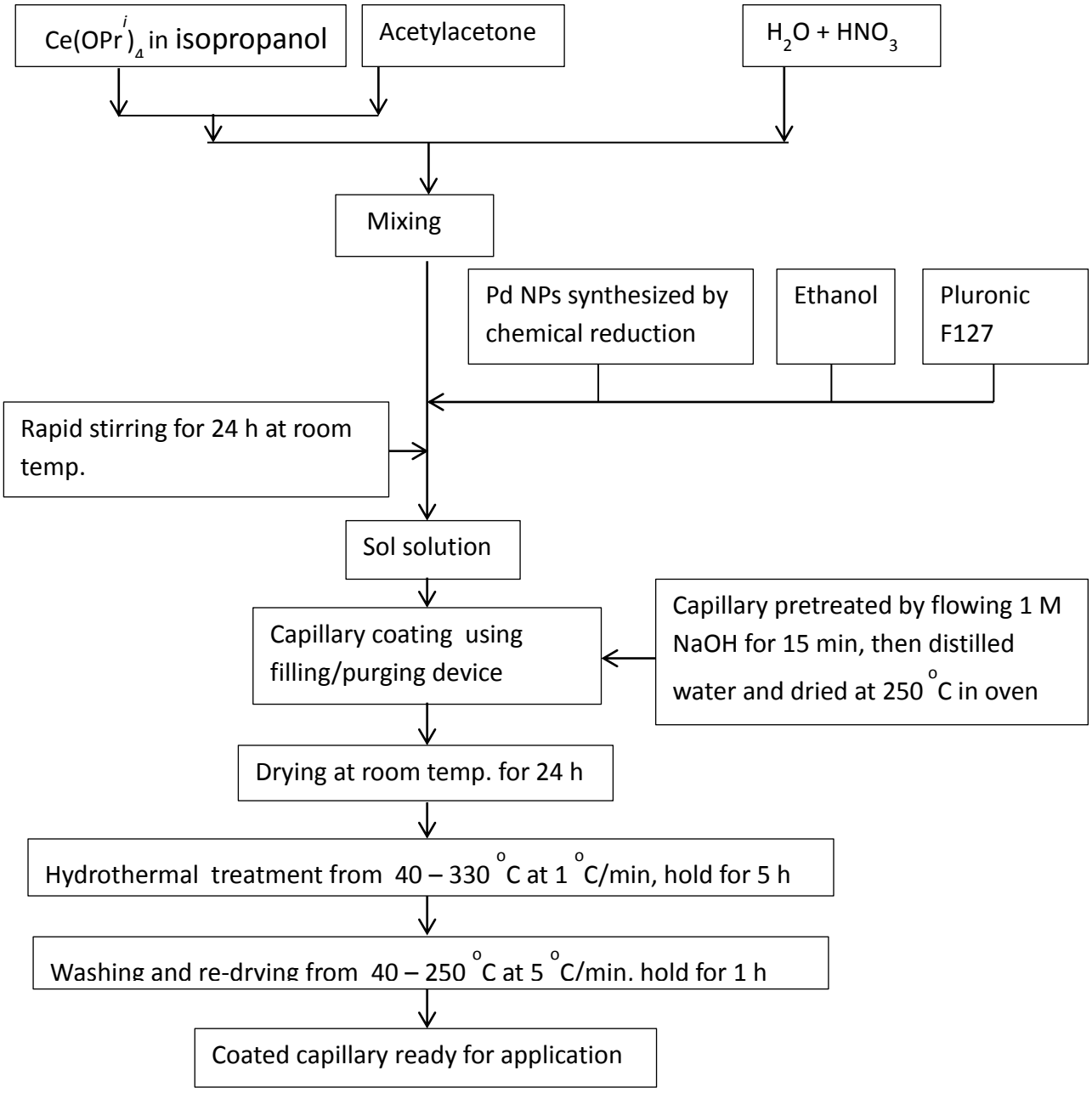
Ce(OPr^{i})$_4$ in isopropanol
Acetylacetone
$H_2O + HNO_3$
Mixing
Pd NPs synthesized by chemical reduction
Ethanol
Pluronic F127
Rapid stirring for 24 h at room temp.
Sol solution
Capillary coating using filling/purging device
Capillary pretreated by flowing 1 M NaOH for 15 min, then distilled water and dried at 250 °C in oven
Drying at room temp. for 24 h
Hydrothermal treatment from 40 – 330 °C at 1 °C/min, hold for 5 h
Washing and re-drying from 40 – 250 °C at 5 °C/min. hold for 1 h
Coated capillary ready for application

Scheme 8.

CHAPTER FOUR

RESULTS AND DISCUSSION

4.1 NMR of $Ce(OPr^i)_4$

^1H and $^{13}C\{^1H\}$ NMR spectra of $Ce(OPr^i)_4$ in $CDCl_3$ were recorded on Oxford NMR 500 at 300 MHz at 25 ^oC. From Fig. 4.1, it can be seen that the ^1H NMR showed two chemical shifts (δ): doublet at 1.2 ppm which was attributed to the hydrogen attached to carbon atom carrying the two methyl groups and a septet, enlarged in Fig. 4.2, for the two equivalent methyl protons. The $^{13}C\{^1H\}$ NMR showed also two chemical shifts (δ)as shown in Fig. 4.3: one at 25 ppm corresponding to the two equivalent methyl carbon and the other at 65 ppm which was assigned to the carbon carrying the Ce – O bond. Both ^1H and ^{13}C NMR showed only one environment for all the *i*-PrO – groups in the molecule[102].

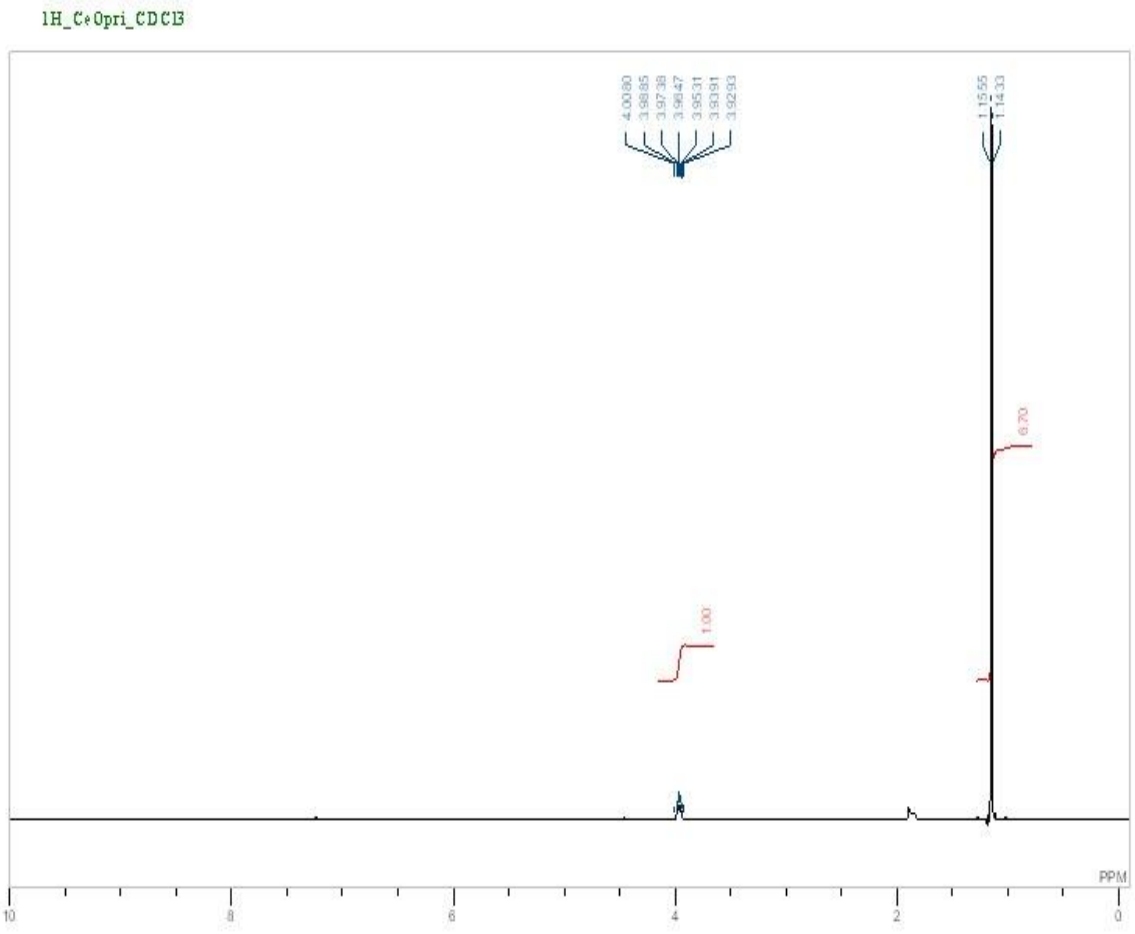

Figure 4.1 ^{1}H NMR spectrum of Ce(OPr^{i})$_4$ in CDCl$_3$ at 25 ^{o}C

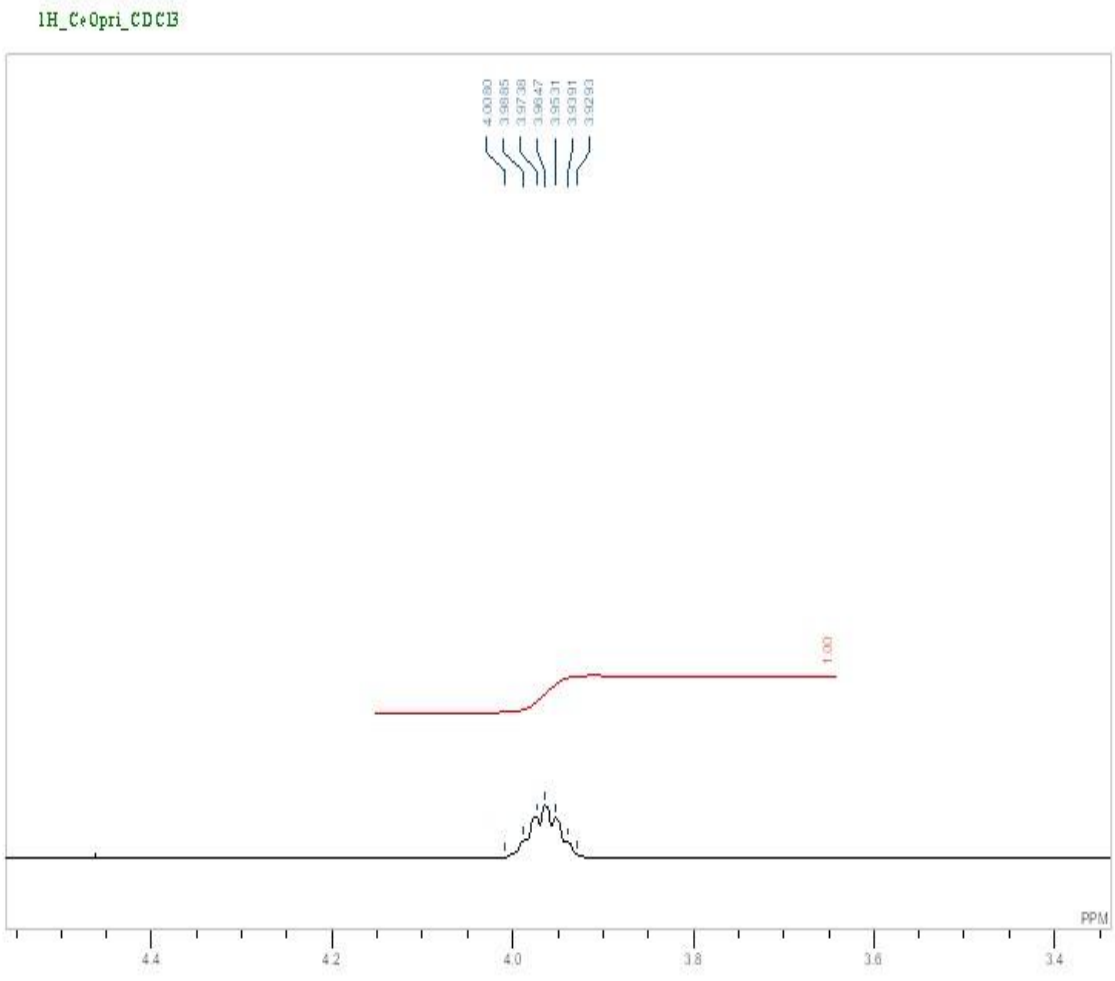

Figure 4.2 ^{1}H NMR spectrum showing the septet splitting of the 2 equivalent methyl protons.

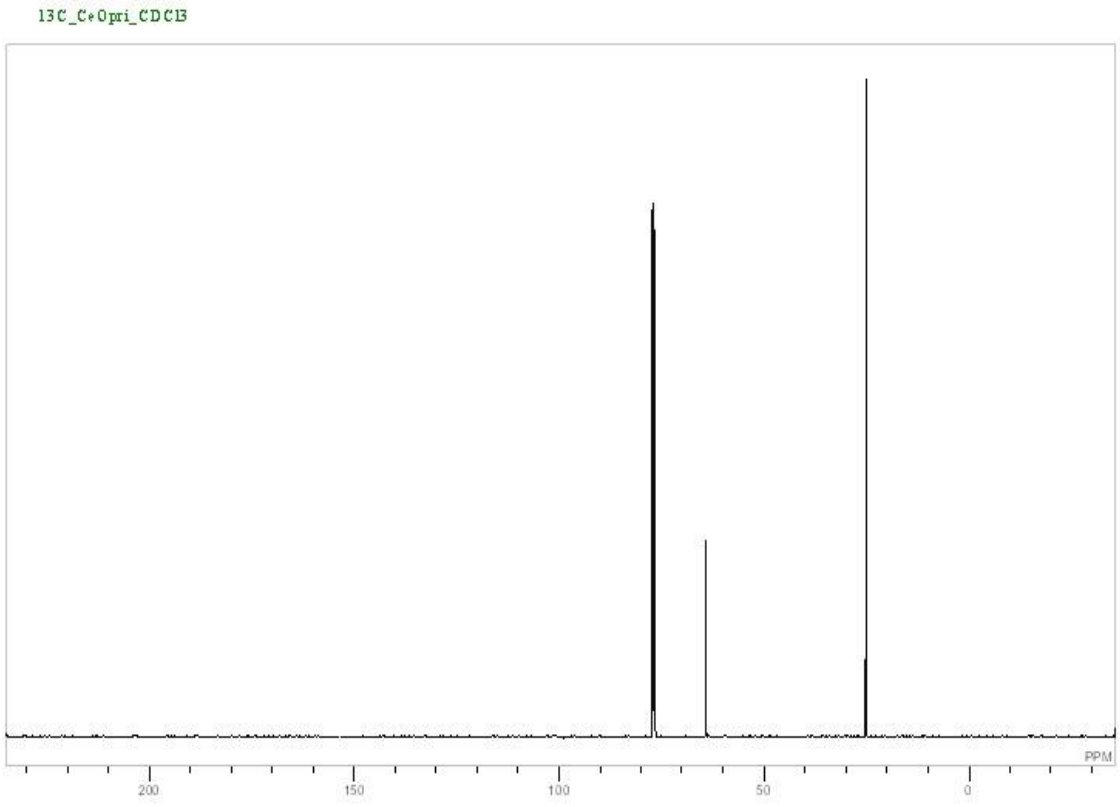

Figure 4.3 $^{13}C\{^{1}H\}$ NMR of $Ce(OPr^{i})_4$ in $CDCl_3$ at 25 ^{o}C

4.2 UV-Vis spectra of Pd NPs

UV-Vis spectrum was reported to be an effective method to investigate whether metal ions are completely reduced or not[106]. The UV-Vis spectrum of palladium (ii) nitrate hydrate solution was measured before reduction and absorption peaks characteristics of the solution were observed at 289 nm and 396 nm as was reported in literature[107]. However after addition of $NaBH_4$, the measured UV-Vis spectra showed no absorption peak, an indication of complete reduction of palladium ions. Fig. 4.4 shows the two UV-Vis spectra for Pd^{2+} and the reduced Pd.

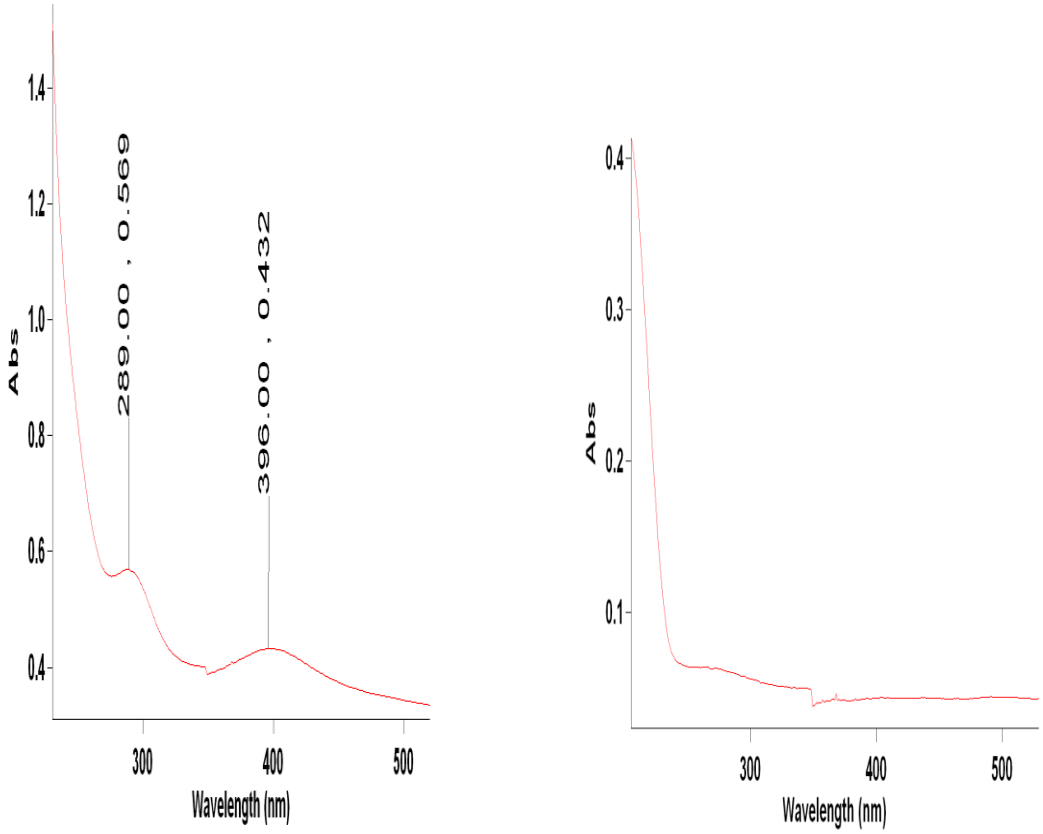

Figure 4.4 UV-Vis spectra of palladium (ii) nitrate hydrate solution and palladium nanoparticles showing peak disappearance.

4.3 Scanning electron microscope of Pd NPs

The SEM of palladium nanoparticles (Fig. 4.5) showed the particles distributed evenly in a form of a chain. According to Yang et al., the proposed mechanism for the formation of this short range ordered linear Pd NP chains is the scaffolding method, with the solvent used as scaffold for the adsorption of Pd(II).

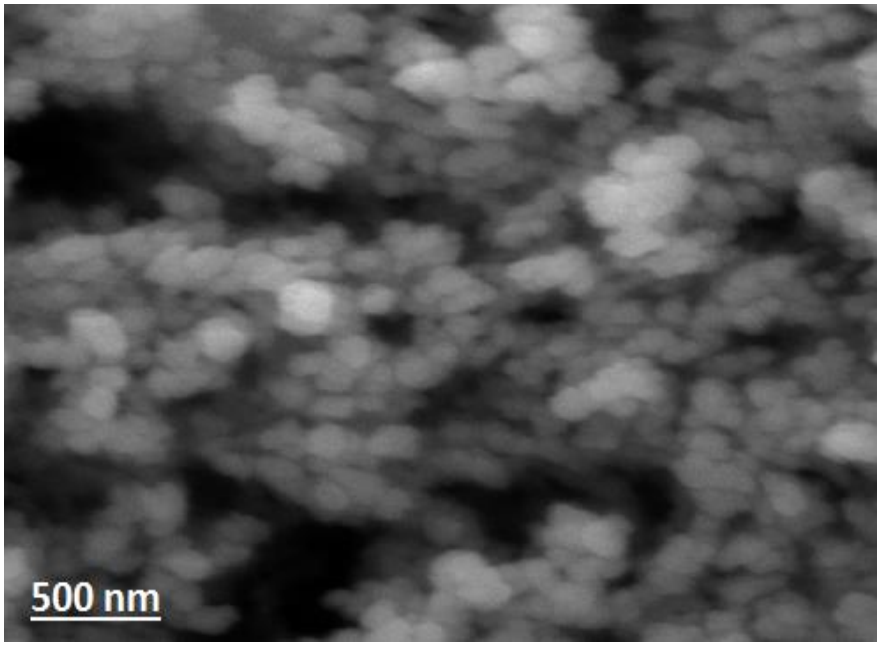

Figure 4.5 FESEM of Pd NPs

4.4 XRD

Powdered XRD pattern (Fig. 4.6) showed Bragg peaks with Miller indices (111), (200), (220), (311) and (222) which were associated with cubic phase fluorite structure of CeO_2 and are in good agreement with the JCPDS file for CeO_2 (JCPDS No. 34-0394). The sharpness of the peaks indicates the high crystallinity of the dried thin film, however upon immobilization of Pd NPs, the intensity got decreased. Similar result was obtained when Pd was supported on carbon-nitrogen composites for hydrogenation of phenol[108]. The presence of an unaccounted peak showed the presence of impurity in the thin film which was attributed to the substrate on which the film was coated and dried, then later scratched for the XRD analysis.

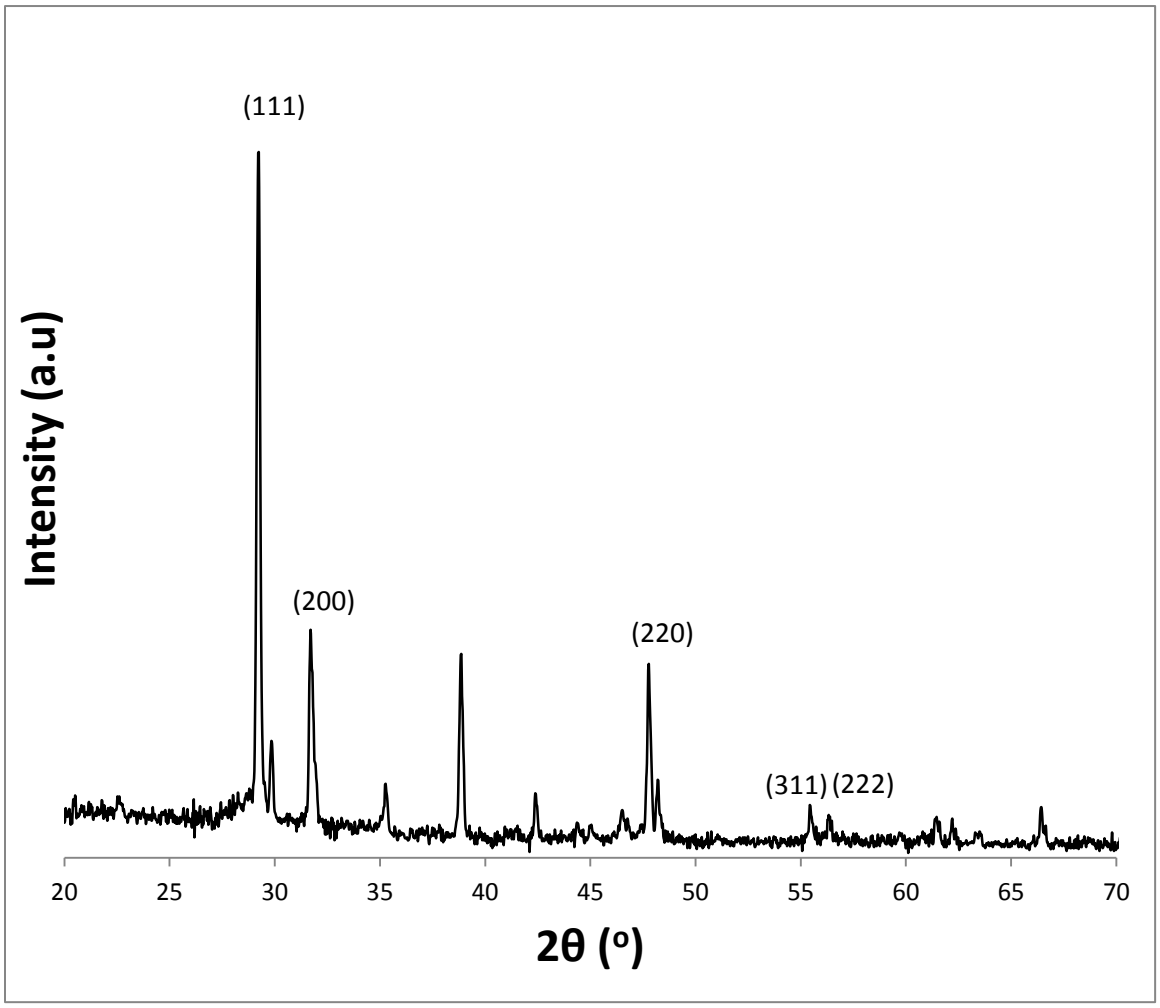

Figure 4.6 XRD pattern of CeO_2 thin film dried at 330 °C for 5 h.

4.5 FESEM and TEM

Field emission scanning electron microscope image of Pd/CeO_2 thin film on a glass substrate (Figs. 4.7 and 4.8) showed the thin film is crack free and has a random worm-like network of the mesopore. The nanoparticles are also homogeneous and well dispersed within the pores of ceria thin film. The dispersion of Pd NPs was due to their confinement within the mesopores of ceria. It was also observed that the nanoparticles retained their sizes throughout the process of thermal treatment. Scanning electron microscope of the coated capillary (Fig. 4.9) also showed the homogeneity of the thin film and the thickness of the film was approximately measured to be 200 nm. From Fig. 4.10, TEM image showed Pd NPs well dispersed on the support surface and Pd particles size was determined to be approximately 4.2 nm and its lattice fringes was measured to be 0.22 nm. The corresponding selective area electron diffraction (SAED) pattern shown in Fig. 4.11 confirmed the nanocrystalline nature of Pd/CeO_2 thin film and the d-spacings tabulated in table 4.1 also ascertained the presence of nanocrystalline Pd and CeO_2.

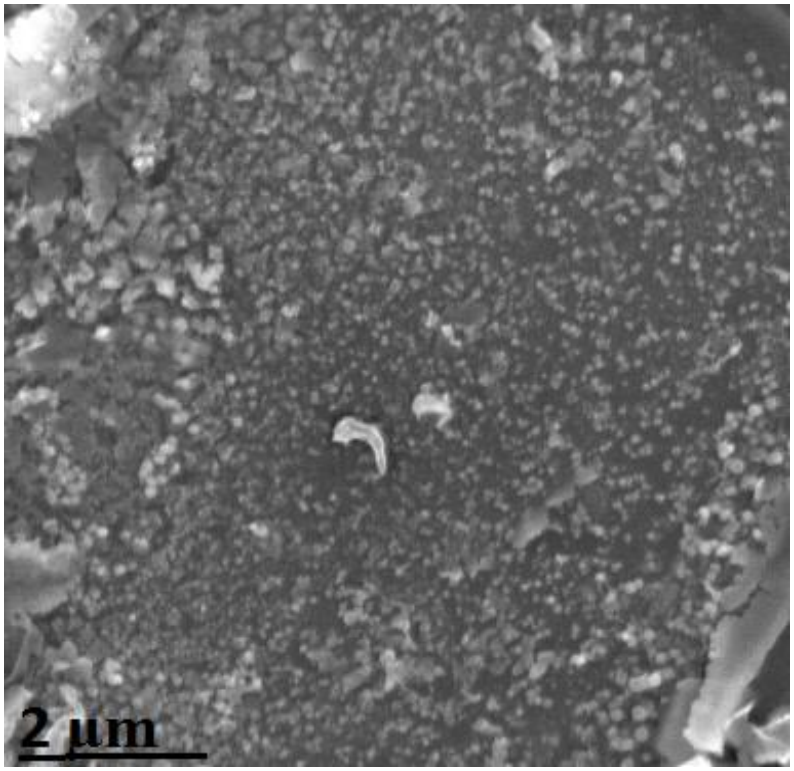

Figure 4.7 SEM Image of CeO_2 thin film deposited on glass substrate dried at 60 ^oC.

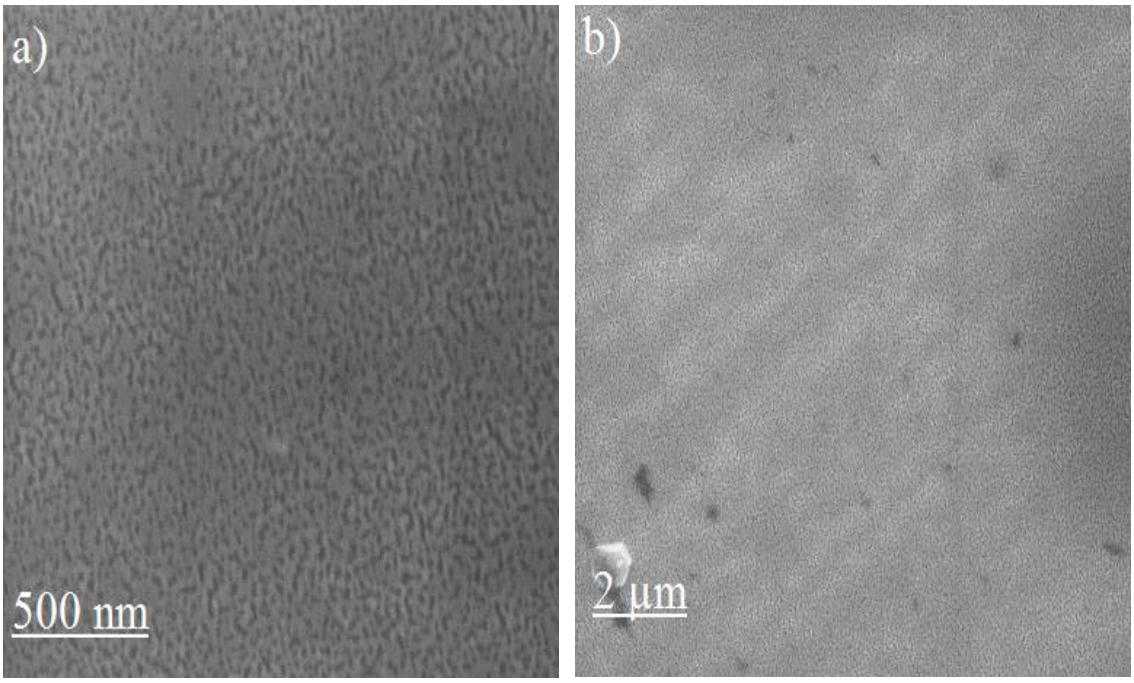

Figure 4.8 SEM Image of CeO_2 thin film containing 1 wt.% Pd NPs deposited on glass substrate dried at 330 ^{o}C.

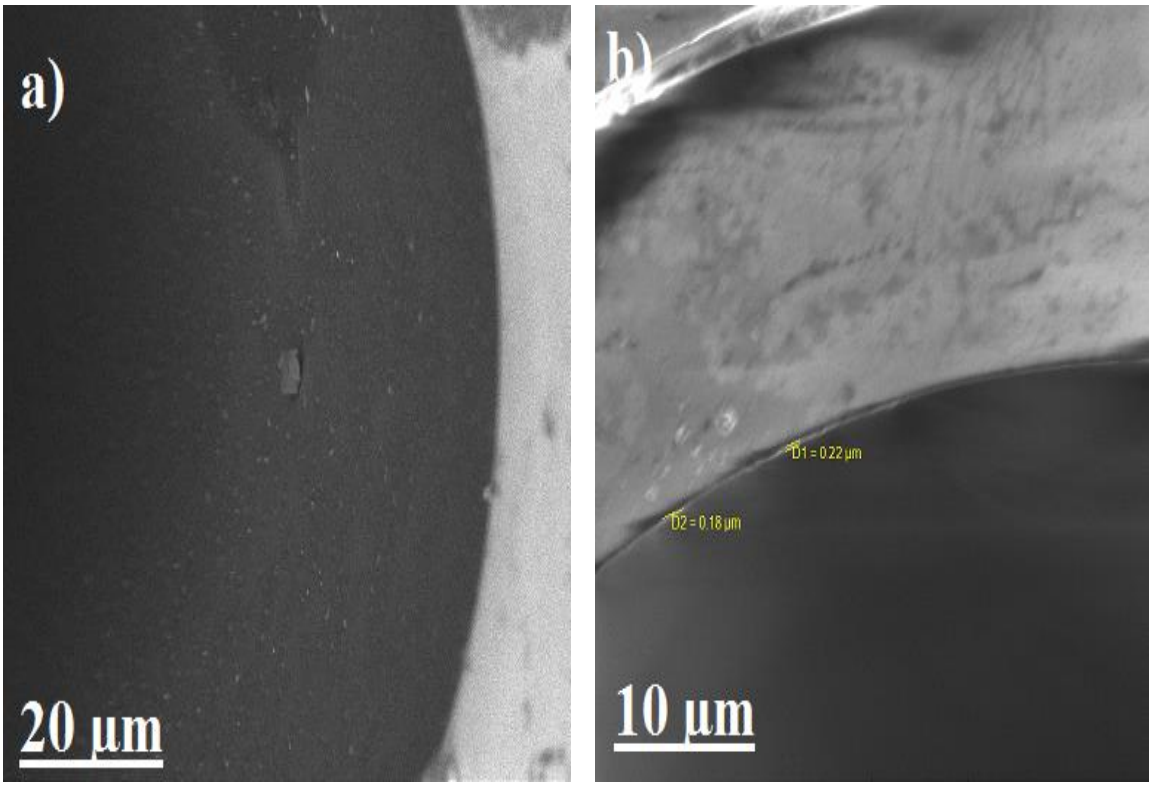

Figure 4.9 SEM Image of capillary immobilized with Pd NPs on CeO_2 thin films at different magnifications.

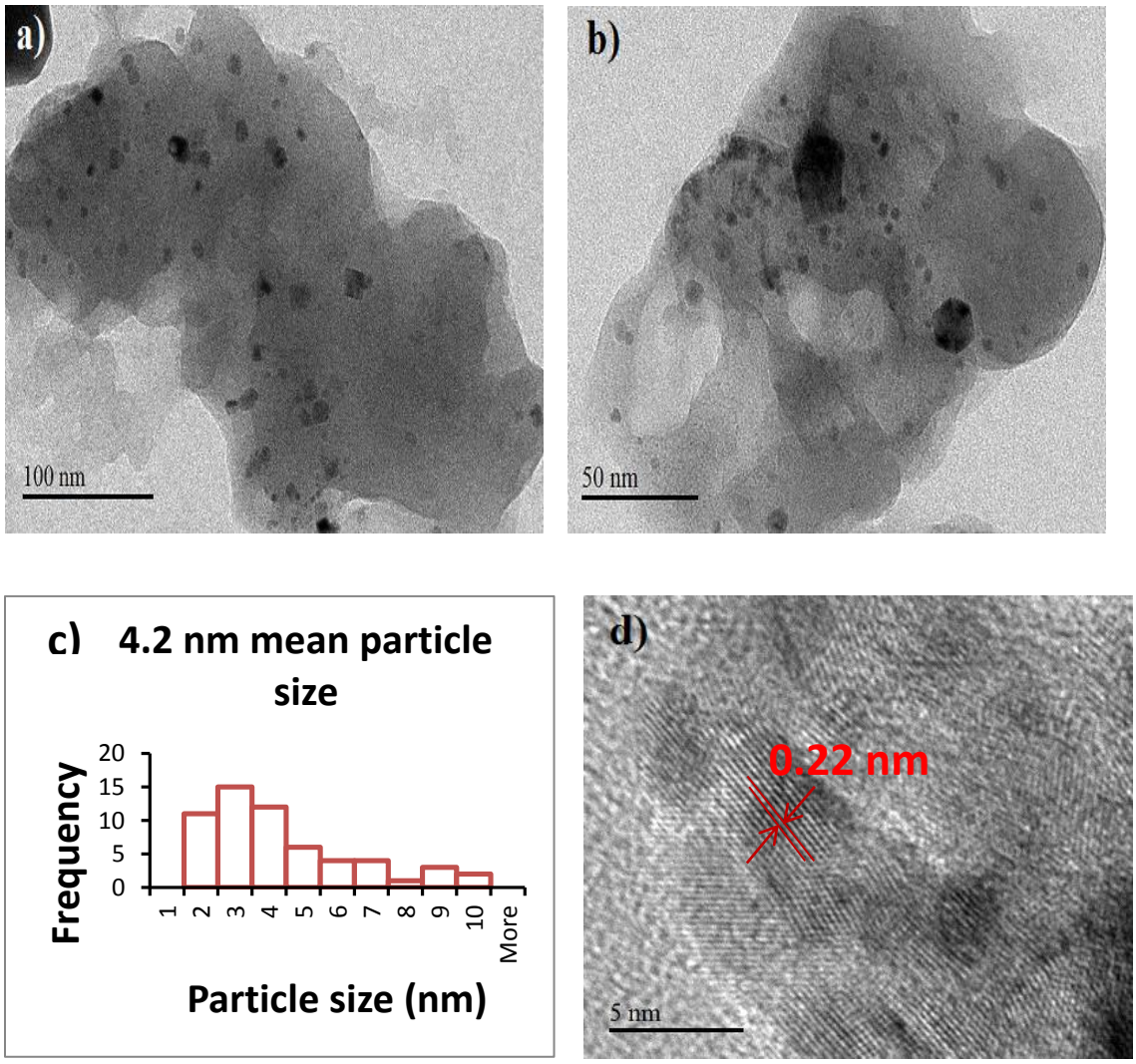

Figure 4.10 TEM images of a) and b) Pd in CeO_2 support at different magnification, c) the histogram for Pd mean size and d) showing Pd nanocrystal d-spacing.

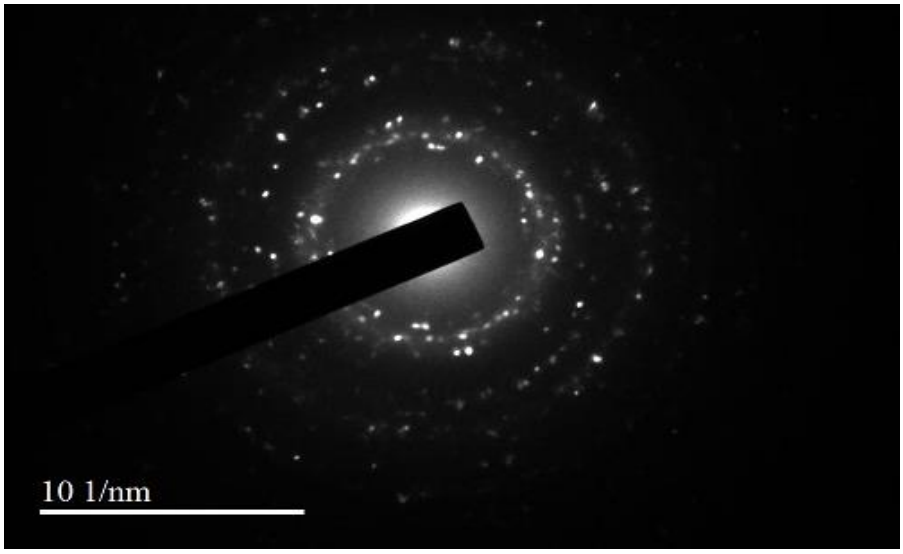

Figure 4.11 Corresponding SAED pattern of Pd/CeO_2.

Table 4.1 Showing d-spacing of different spot in SAED

Spot	d-Spacing (nm)	Rec. Pos. (1/nm)	Degrees to spot 1	Degrees to x-axis	Amplitude
1	0.2367	4.225	0	-48.47	1155
2	0.2003	4.993	54.2	5.73	1352.22
3	0.2389	4.185	107.72	59.25	544.24
4	0.2367	4.225	180	131.53	1274.65
5	0.2013	4.968	124.75	-173.23	1156.42
6	0.2301	4.347	72.25	-120.72	695.45
7	0.146	6.851	166.73	118.26	1517.91
8	0.1415	7.066	158.72	152.81	3364.83

4.6 FTIR

FTIR of the sol gel (Fig. 4.12a) showed broad absorption bands at around 3400 cm^{-1} and 2900 cm^{-1} which were attributed to -OH of the solvents and water and C-H stretching vibrations respectively. Vibration bands at around 1650 cm^{-1} showed the characteristic of acetylacetonato group bounded to cerium atom[109], while bands around 1350 cm^{-1} and 700 cm^{-1} were assigned to Ce-OH and Ce-O-Ce stretching vibrations as reported in literature[110]. IR spectra of thin film dried at 60 ^{o}C and 330 ^{o}C (Figs. 4.12b and c) showed the gradual collapse of OH, C-H and acetylacetonato absorption bands, however, absorption bands characteristics of CeO_2 thin film were still observed. Raman spectra of CeO_2 thin film (Fig. 4.14) showed a Raman mode at 461 cm^{-1} and was attributed to the symmetrical stretching mode of Ce-8O vibrational unit[111]. The observed broadening and increased asymmetry of the Raman line, due to the reduction of phonon lifetime in the nanocrystalline regime, explained the microstructure nature of CeO_2 thin film[112]. Density functional theory (DFT) calculations of CeO_2 using Guassian 09 revision D. 01 program at DFT-B3LYP/gen with 6-31G* basis set for oxygen atom and SDD basis for cerium, was found to be comparable to the experimental results of CeO_2 thin films as shown in Figs. 4.13 and 4.15.

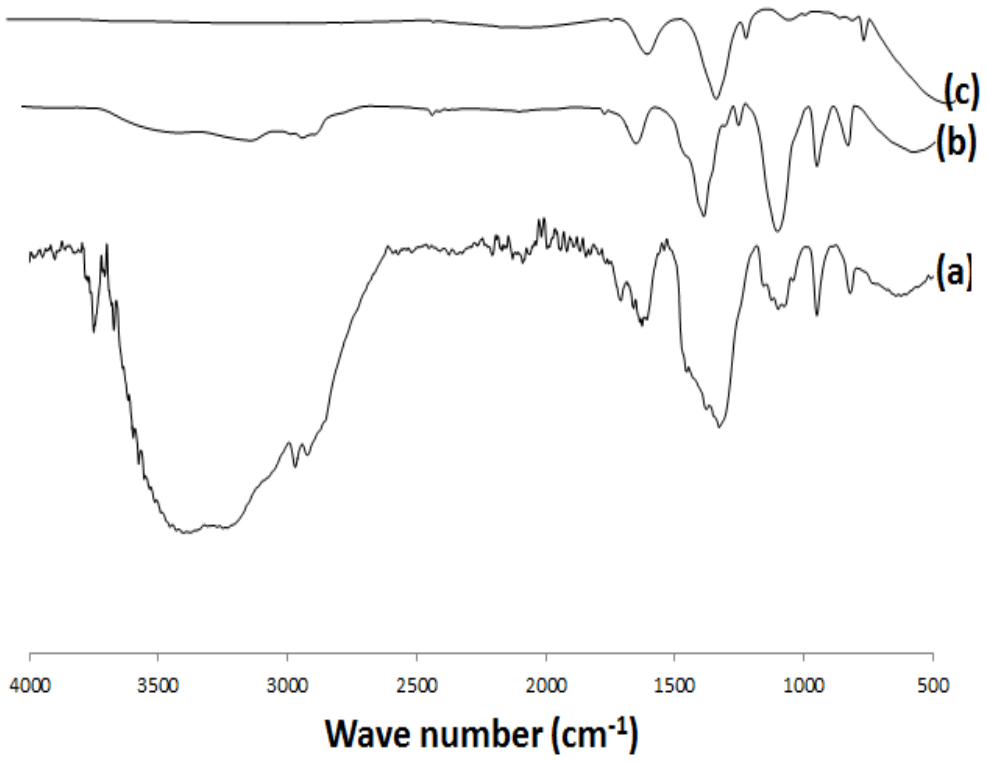

Figure 4.12 FTIR of (a) CeO_2 sol gel (b) CeO_2 thin film dried at 60 ^oC (c) CeO_2 thin film dried at 330 ^oC.

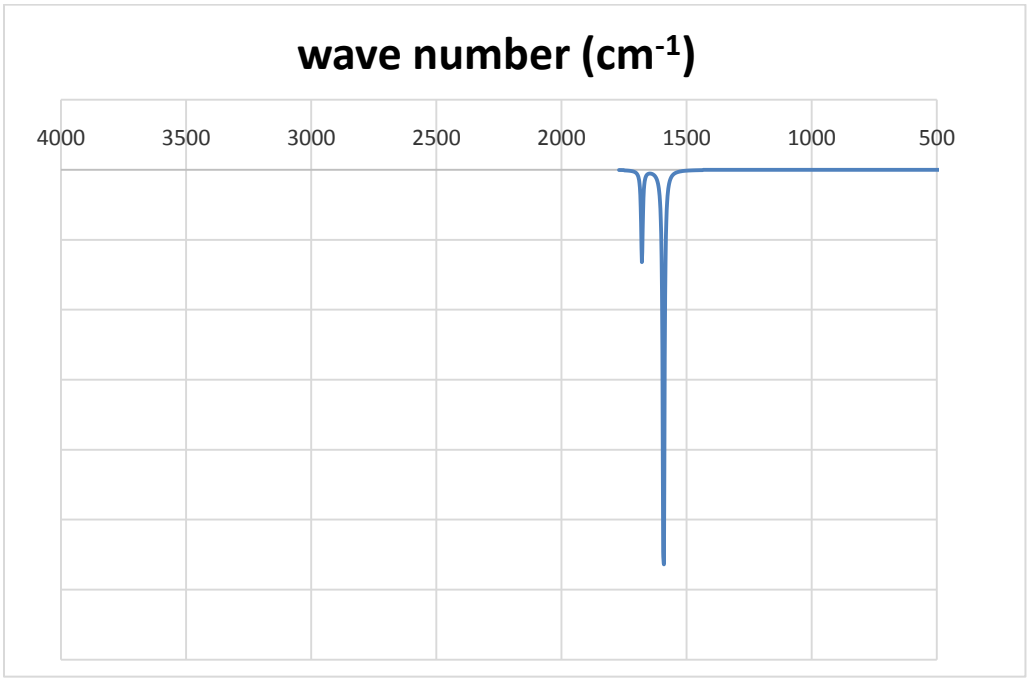

Figure 4.13 IR spectra of CeO_2 obtained from DFT using Guassian 09 revision D. 01 program at DFT-B3LYP/gen with 6-31G* basis set for oxygen atom and SDD basis for cerium.

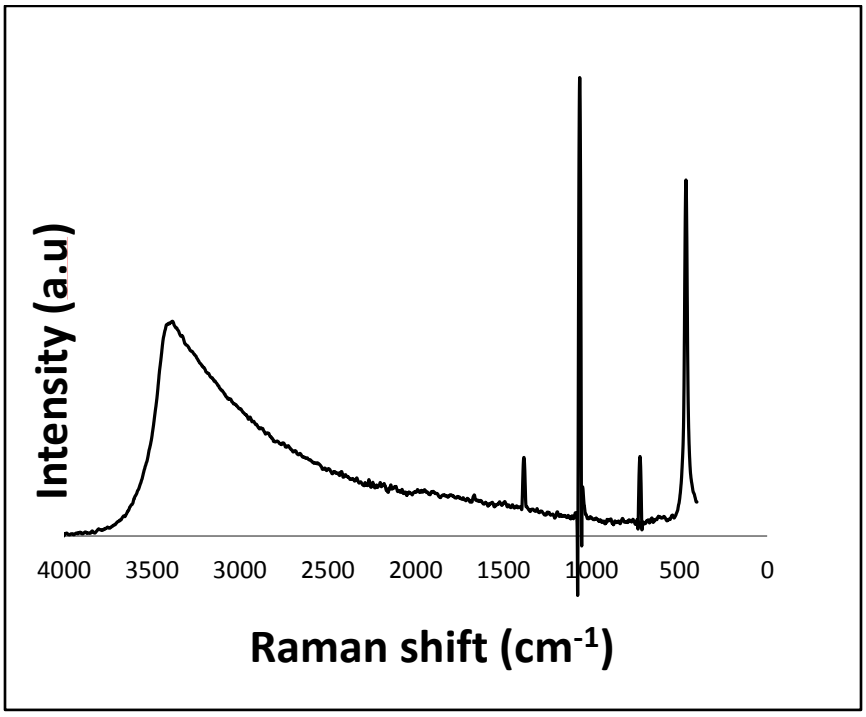

Figure 4.14 Raman spectra of CeO_2 thin film dried at 330 ^oC.

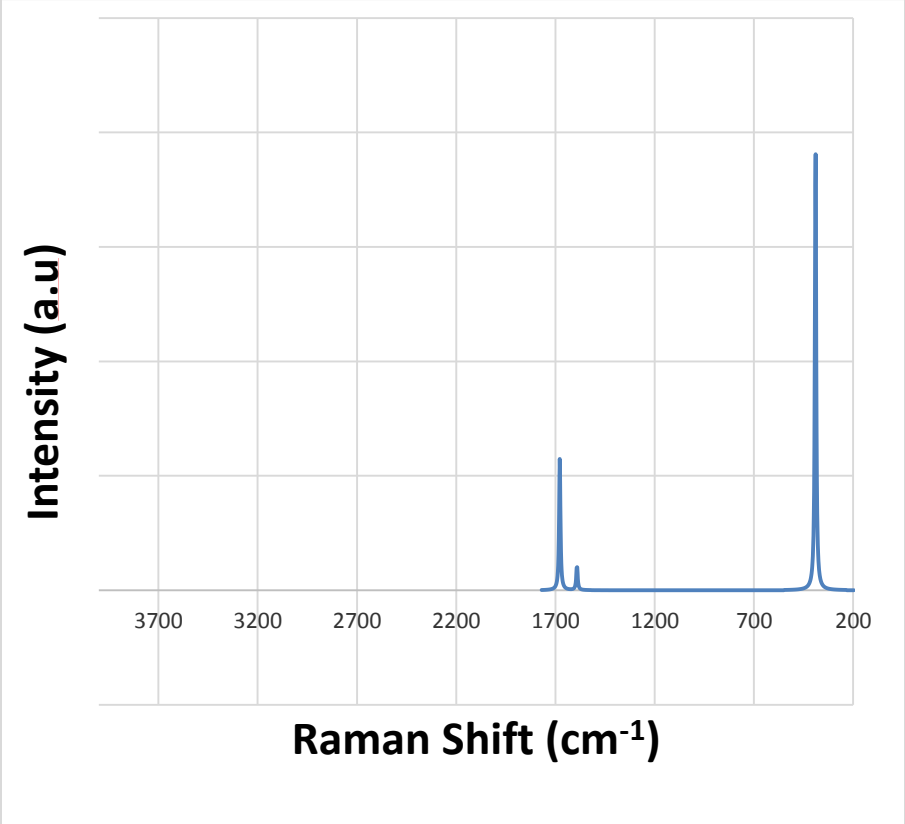

Figure 4.15 CeO_2 obtained from DFT using Guassian 09 revision D. 01 program at DFT-B3LYP/gen with 6-31G* basis set for oxygen atom and SDD basis for cerium.

4.7 Controlled synthesis of styrene and ethylbenzene in Pd/CeO_2 capillary microreactor

Hydrogenation of phenylacetylene in hexane was studied and the products quantified by an external calibration curve. Solution of phenylacetylene as blank, was flowed through the capillary microreactor containing uncoated capillary under the same reaction conditions with the sample under study. Percentage conversion and selectivity were calculated using the formulae:

- %conversion (X)
  X = $100.\frac{n}{n_0}$
- Selectivity (S)
  S = $100.\frac{n_i}{n}$, where n = amount of reactant converted to product(s), n_0= initial amount of reactant and n_i = amount of product formed.

Turn over frequency, TOF (s^{-1}) of the Pd/CeO_2 were calculated using the relation:

$$TOF = \frac{reaction\ rate}{catalyst\ active\ sites}$$

Catalyst active sites = $\%D.n$, where $\%D$ is the Pd NPs dispersion and n is the actual Pd NPs loading in a capillary, determined by flowing aqua regia solution into a freshly coated capillary, then ultrapure water and the collected solution analyzed by ICP-MS[56, 82].

4.7.1 Effect of capillary length

By coating 5 – 20 m capillary length with Pd/CeO_2 for capillary microreaction at 0.01 $ml.min^{-1}$ phenyacetylene flow rate, 0.5 $ml.min^{-1}$ H_2 flow rate and temperature of 40 ^oC, gradual increase in phenylacetylene conversion was observed (Fig. 4.16) and became only slightly for 20 m capillary. The increase in conversion was due to increase in the

capillary length which consequently increased phenylacetylene residence time in the microreactor. However slight increase noticed when 20 m capillary was used might be due to decreased uniformity in coating and cracking which usually occur when coating and drying time is long.

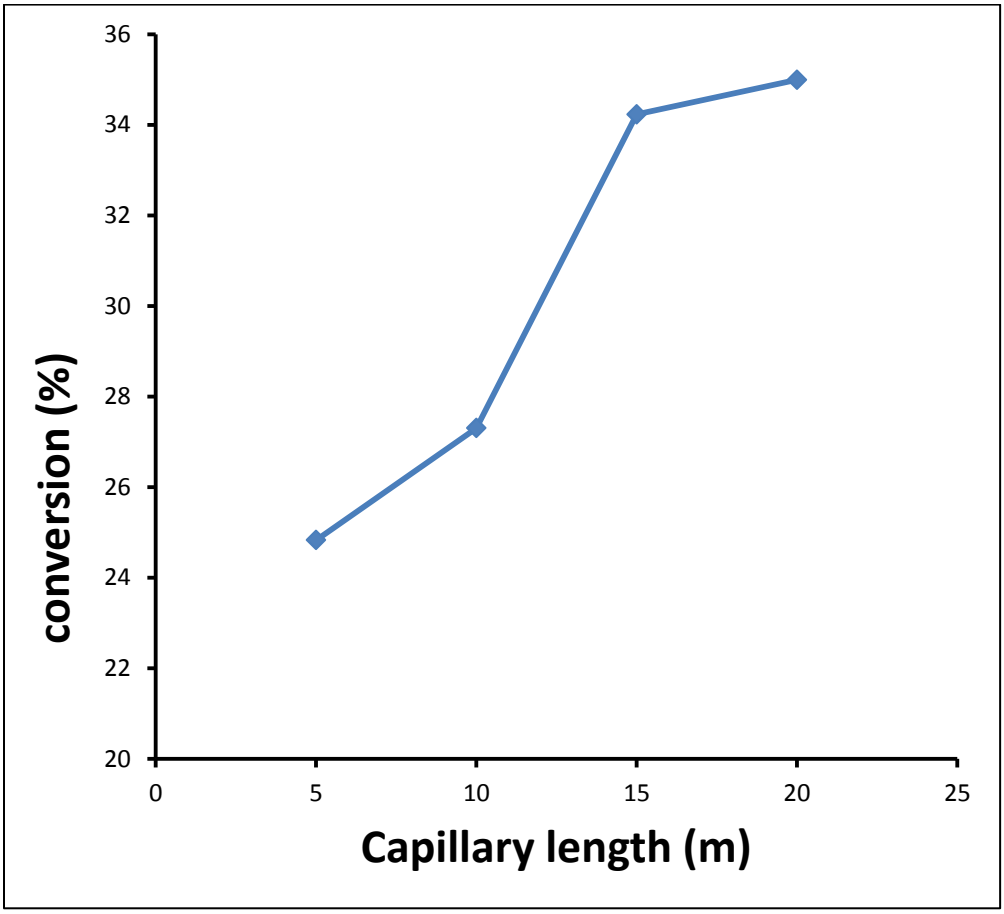

Figure 4.16 Effect of capillary length at 0.01 ml.min^{-1} phenyacetylene flow rate and 0.5 ml.min^{-1} H_2 flow rate at 40 ^{o}C.

4.7.2 Effect of temperature

Phenylacetylene hydrogenation over 15 m Pd/CeO_2 capillary was studied in the temperature range 30 – 60 ^oC, while maintaining a constant H_2 flow rate of 0.05 $ml.min^{-1}$. From Fig. 4.17, it can be seen that 95% phenylacetylene conversion was recorded at 60 ^oC, implying that higher conversion was reached at higher temperature. The activation energy from Arrhenius plot (Fig. 4.19) was calculated as 41.36 $KJ.mol^{-1}$ and was in correlation with those previously reported[113]. Increased selectivity towards ethylbenzene from 9.4% at 30 ^oC to 81.1% at 60 ^oC was also observed, which is in agreement with previously reported data indicating that product selectivity depends on the reaction temperature[7a, 55b]. Reverse was the case with styrene, which at 30 ^oC showed 90.8% selectivity at 21.1% conversion. The turn over frequency (TOF) (Fig. 4.18) also increased from 0.021 s^{-1} at 30 ^oC to 0.185 s^{-1} at 60 ^oC and this could be accounted on the basis of reaction kinetics where reaction rate increases with temperature increase.

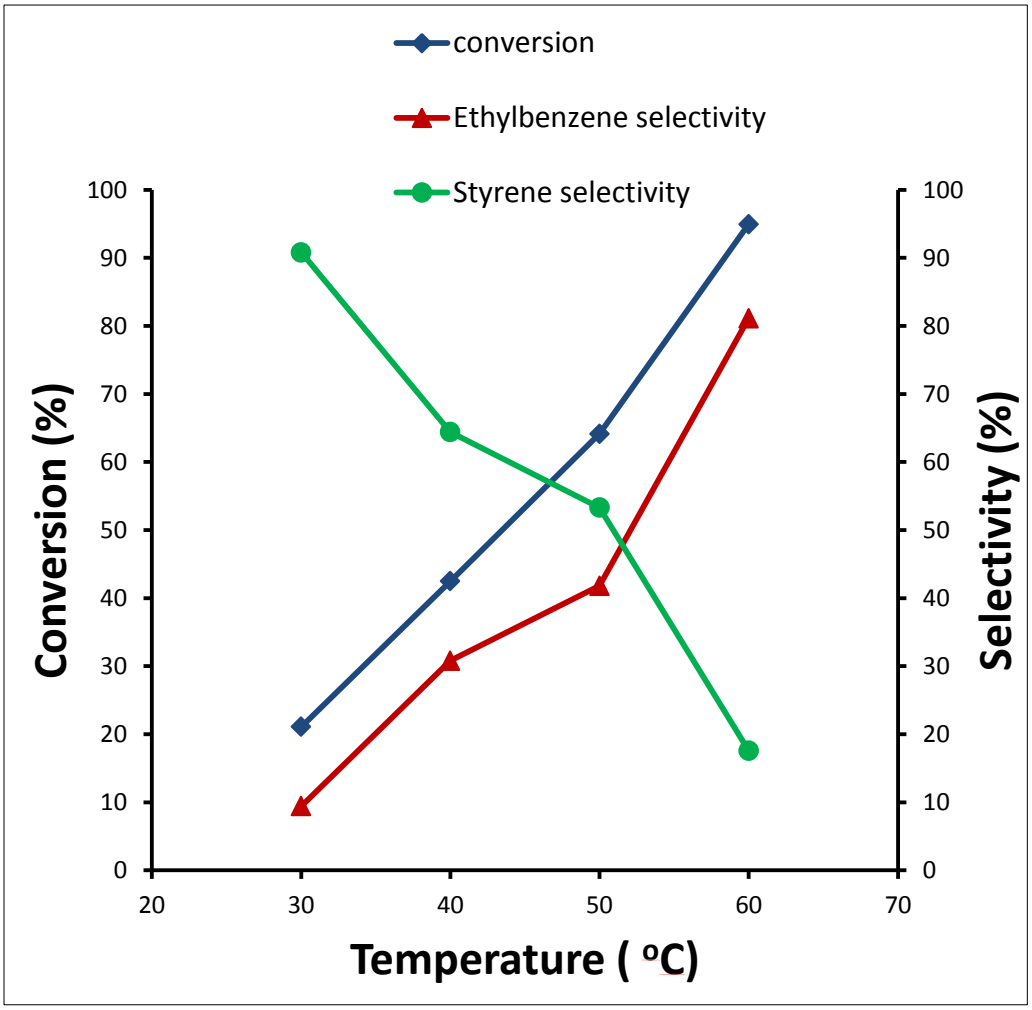

Figure 4.17 Effect of temperature with 15 m Pd/CeO_2 capillary in the range of 30 to 60°C at 0.01 ml.min^{-1} phenyacetylene flow rate and 0.5 ml.min^{-1} H_2 flow rate.

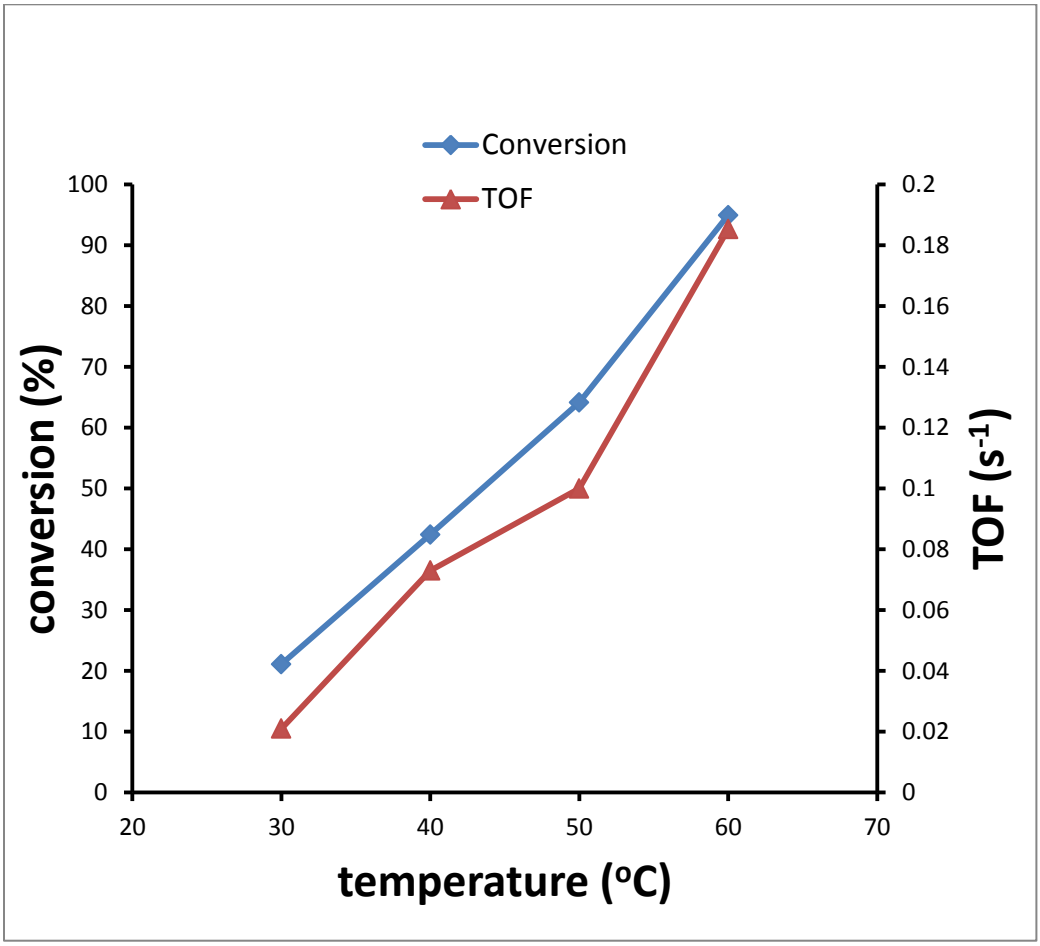

Figure 4.18 Conversion and TOF variation with temperature at liquid flow rate of 0.01 ml.min^{-1} and H_2 flow rate of 0.5 ml.min^{-1}.

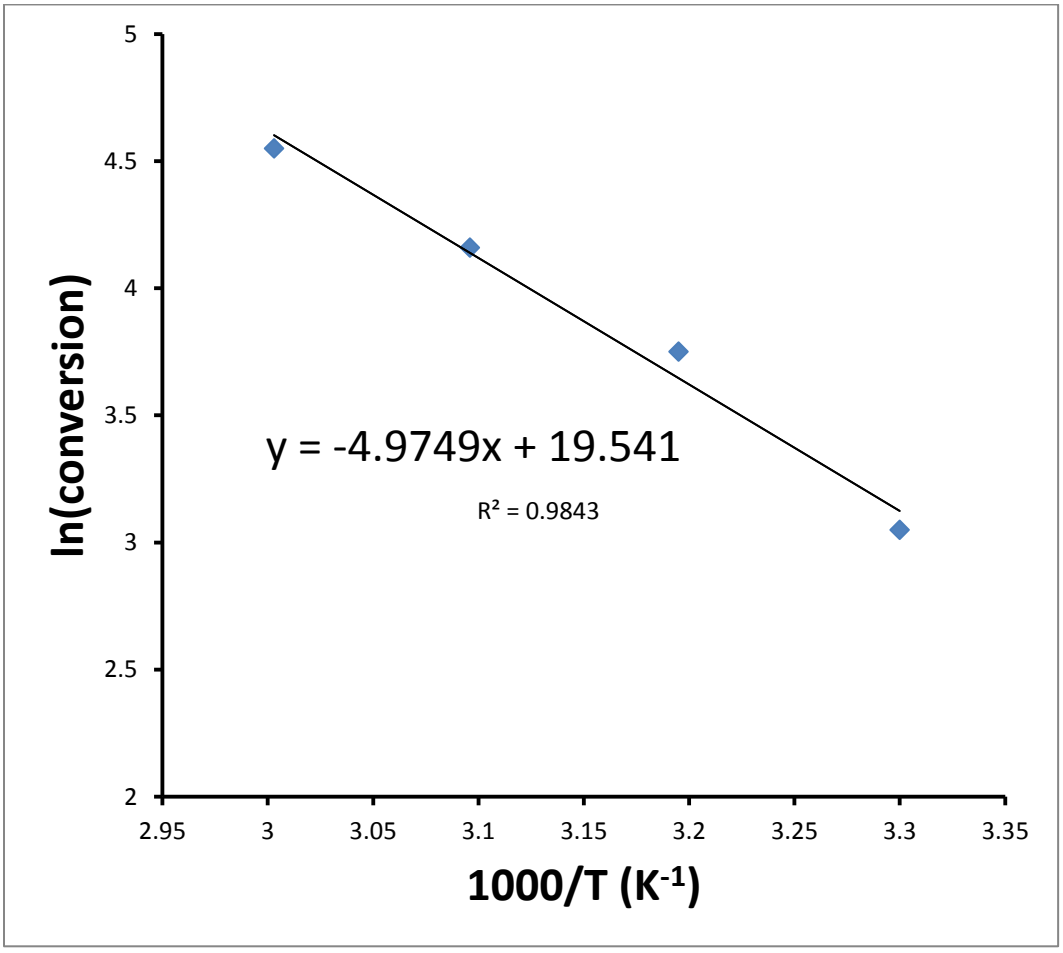

Figure 4.19 Arrhenius plot of phenylacetylene hydrogenation, E_a = 41.36 kJ.mol^{-1}.

4.7.3 Hydrogen gas flow rate

H_2 gas flow rate was varied between 0.25 – 1.5 ml.min^{-1} over 15 m Pd/CeO_2 capillary at temperature of 60 ^{o}C and both conversion and selectivity were found to be effectively changed by the change in flow rate. Maximum conversion and ethylbenzene selectivity was achieved at flow rate of 0.5 ml.min^{-1} (Fig. 4.20) and as the flow rate increases, both conversion and ethylbenzene selectivity got decreased, but styrene selectivity increased to 86.3% at 1.5 ml.min^{-1} flow rate. This could be explained on the basis of H_2 adsorption on the Pd active site and the phenylacetylene fluid phase behavior, which below 0.5 ml.min^{-1} were both not enough for the reaction, but when the flow rate got to 0.5 ml.min^{-1}, the reaction occurred in all domains at comparable level. Above 0.5 ml.min^{-1}, more hydrogen were bubbled into phenylacetylene which reduced the effective reaction volume of the capillary and the mean residence time, hence the observed decrease[66].

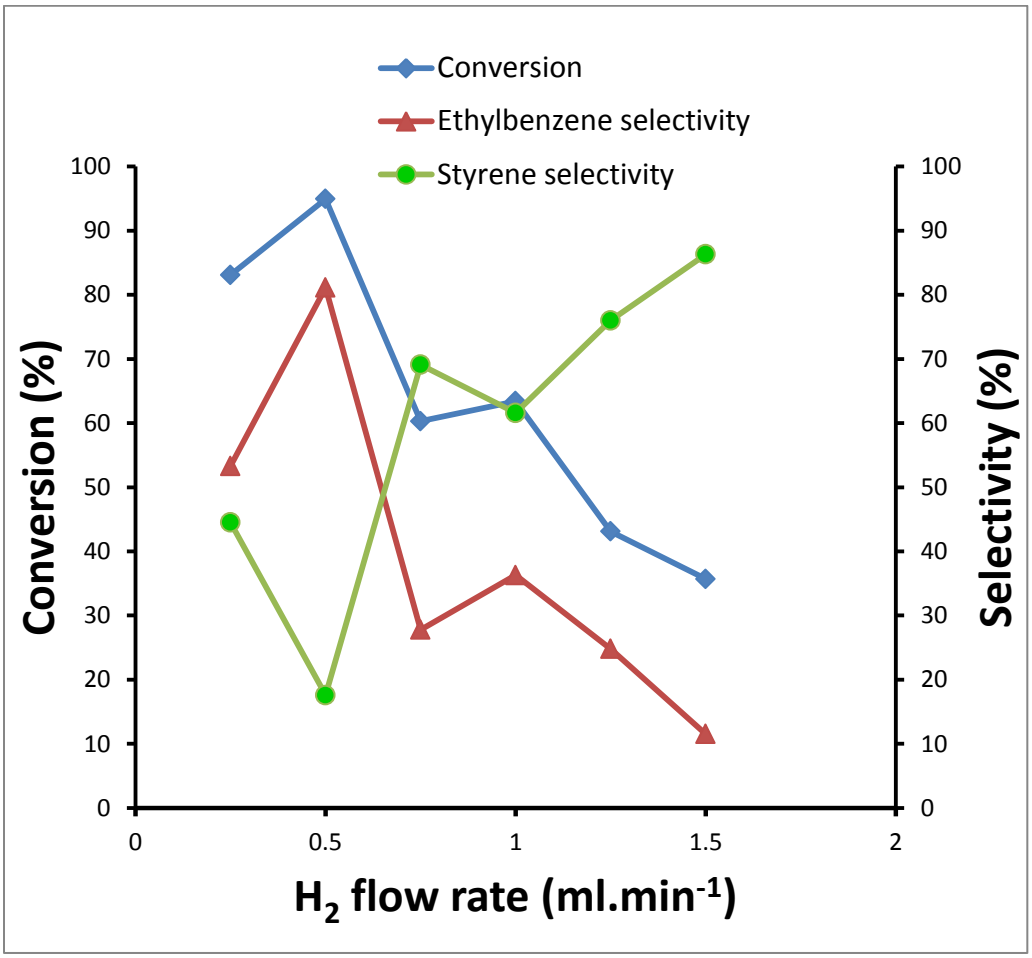

Figure 4.20 Conversion and selectivity response to change in flow rate

4.7.4 Effect of concentration

Phenylacetylene concentration was varied between 10 – 158 ppm over 15 m Pd/CeO_2 capillary at 60 ^{o}C, and from Fig. 4.21, it was observed that within the concentration range studied, more than 40% conversion was achieved in all cases, except 10 ppm in which 95% conversion was recorded. However, reaction turn over frequency was observed to increase as the concentration of phenylacetylene increases and this could be accounted for on the basis of reaction kinetics where reaction rate increases with increase in concentration for first and second order kinetics. It was also observed that concentration of phenylacetylene plays a role in the product selectivity. From Fig. 4.22, it can be seen that increasing the concentration favored the formation of styrene as against ethylbenzene, because at 158 ppm, selectivity to ethylbenzene was brought to less than 10%.

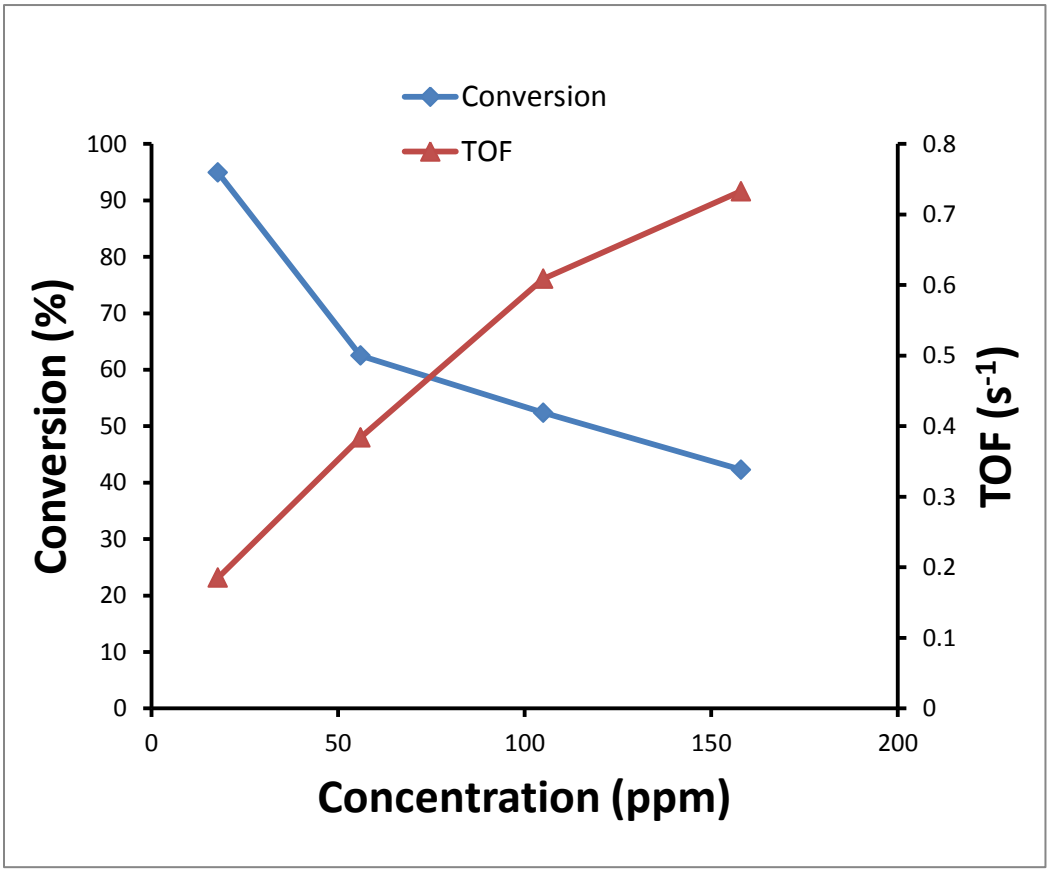

Figure 4.21 Effect of phenylacetylene concentration on conversion and TOF

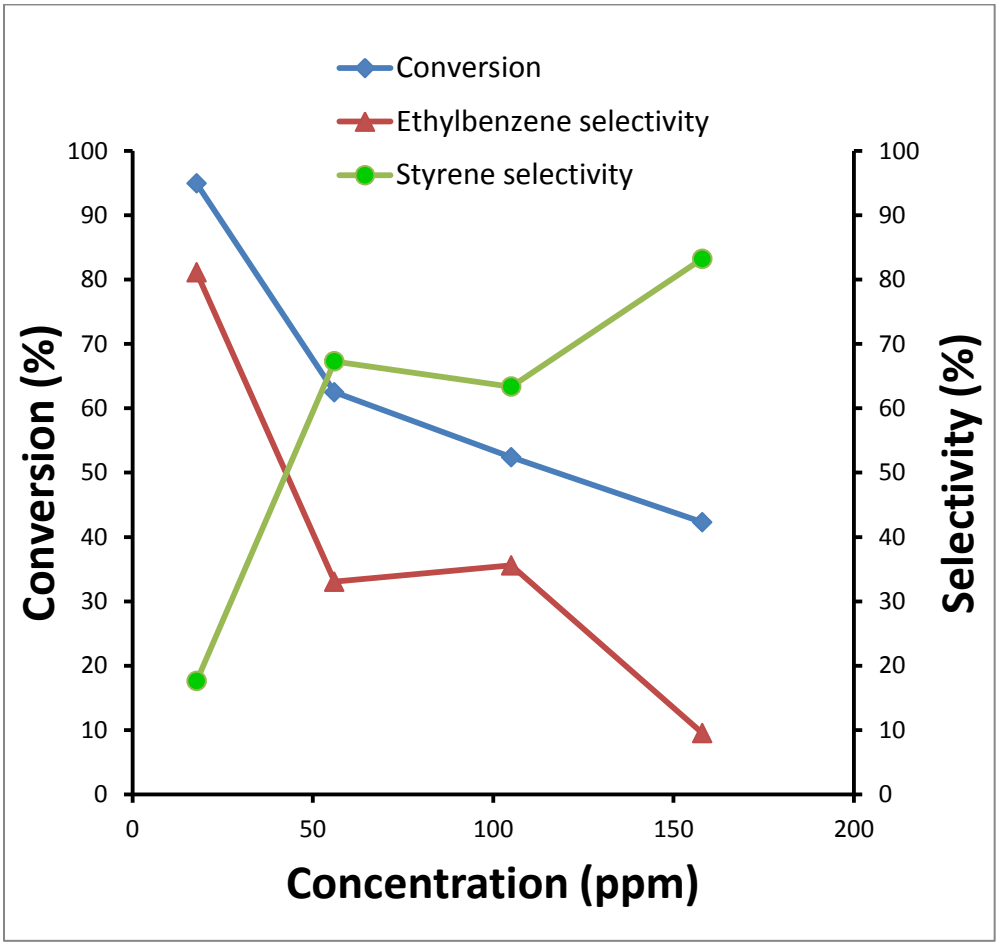

Figure 4.22 Effect of phenylacetylene concentration on conversion and selectivity

4.7.5 Catalyst lifetime

The reusability of the Pd/CeO_2 capillary microreactor for continuous production of the reaction products was evaluated by continuously running the microreactor for 6 days. The operation was stopped however, when more reactant is to be fed into the microreactor. The observed trend showed decrease in phenylacetylene conversion for the first 4 days and was later stabilized until the 6th day of operation. The observed decrease (Fig. 4.23) was attributed to loss of Pd NPs which were not tightly bound to CeO_2 thin film in the Pd/CeO_2 capillary microreactor. ICP-MS analysis of the reaction products collected for the six days of operation showed 38.4% of Pd leaching. This was considered partly due to the friction factor that result from the fast flow rate of phenylacetylene and the lack of capping agent in the immobilized Pd NPs capillary.

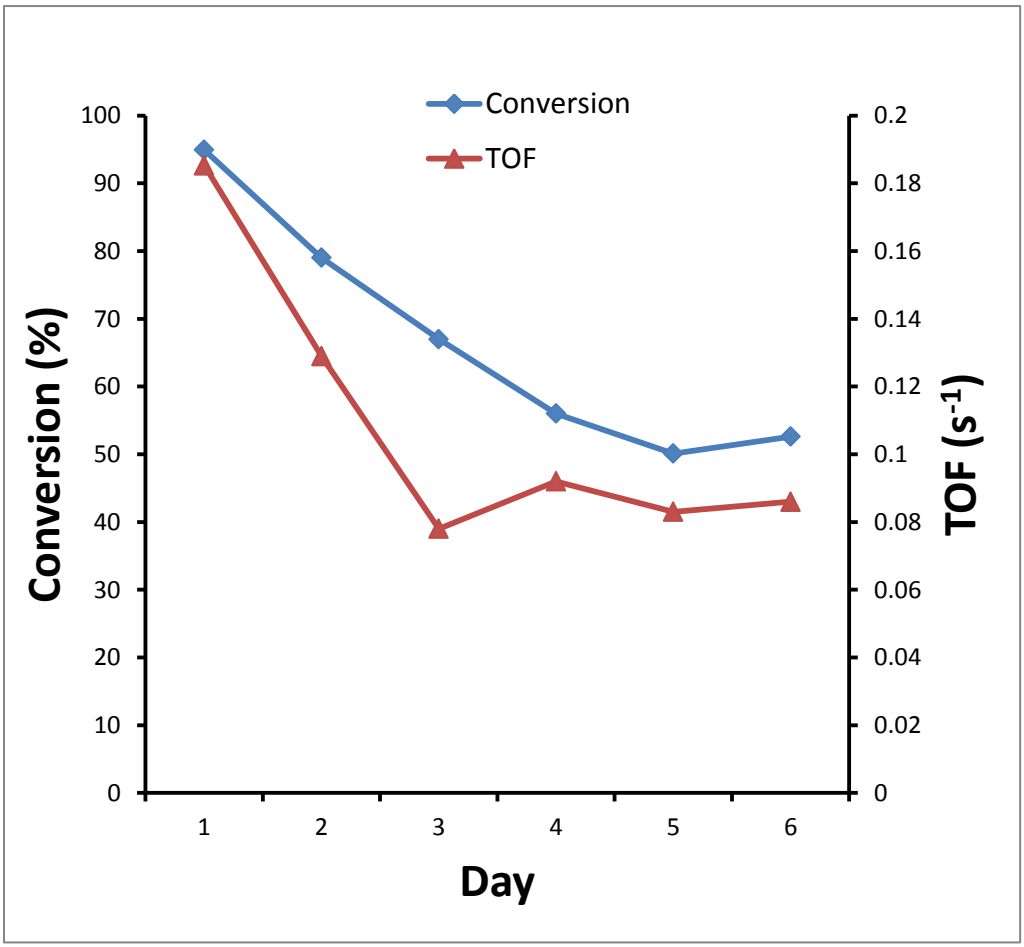

Figure 4.23 Phenylacetylene conversion as a function of time

CHAPTER 5

CONCLUSION

Palladium-doped CeO_2 thin film in capillary microreactor was developed for the first time using sol-gel approach. The film precursor was successfully synthesized and characterized following previously reported methodology. The film was characterized using PXRD, FESEM, TEM, FTIR and Raman spectroscopy. The film with thickness of approximately 200 nm was crack free and has a random worm-like network of mesopores. The Pd/CeO_2 capillary was used to study hydrogenation of phenylacetylene in a microreactor at different capillary length, temperature, H_2 flow rate and phenylacetylene concentration. Higher conversion and selectivity towards ethylbenzene was recorded at higher temperature, while selectivity towards styrene was favored at higher phenylacetylene concentration and hydrogen flow rate. Catalyst turn over frequency of 0.733 s^{-1} was obtained for 158 ppm phenylacetylene hydrogenation at 60 ^oC and 0.5 $ml.min^{-1}$ hydrogen flow rate. Catalyst reusability result showed continuous decrease in catalyst activity for first 4 days of operation and then was stabilized for further 2 days. This was as a result of Pd leaching in the Pd/CeO_2 capillary from the ICP-MS analysis of the collected product samples.

RECOMMENDATION

Ellipsometric porosimetry analysis of the thin films should be done in order to determine the pore size and pore volume of the film in the capillary.

Minimization of nanoparticle leaching after flowing of reactants, e.g by adding capping agent such as polyvinylpyrrolidine, should be studied.

The potential of the CeO_2 support in studying other forms of heterogeneous catalysis in microreactor should be harnessed.

APPENDIX

6.1 The retention time of the corresponding peaks

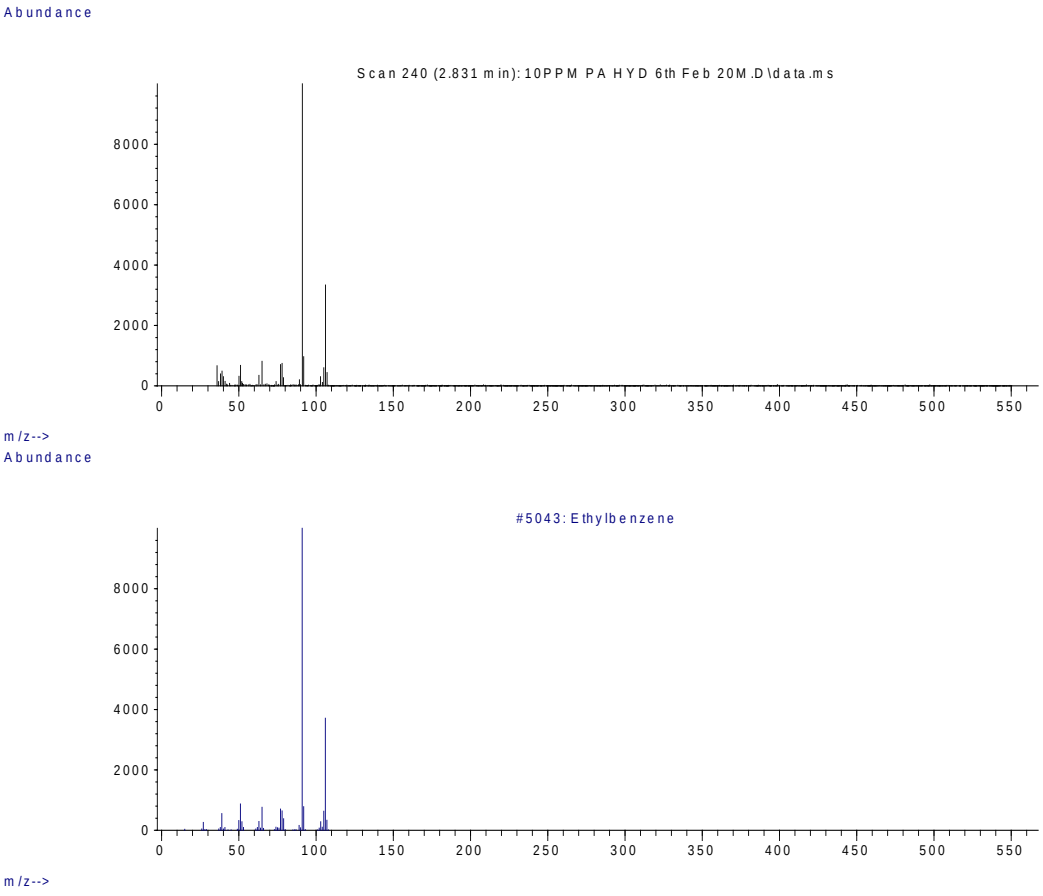

Figure 6.1 Mass spectra of ethylbenzene

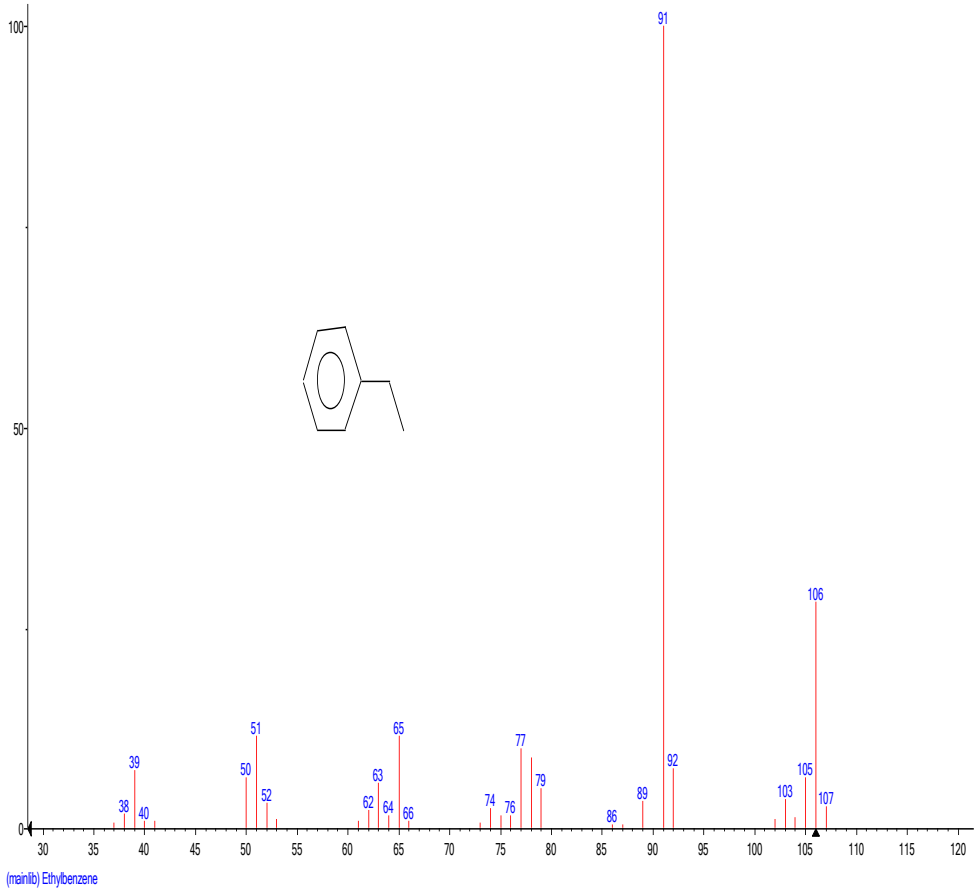

Figure 6.2 NIST mass spectrum of ethylbenzene

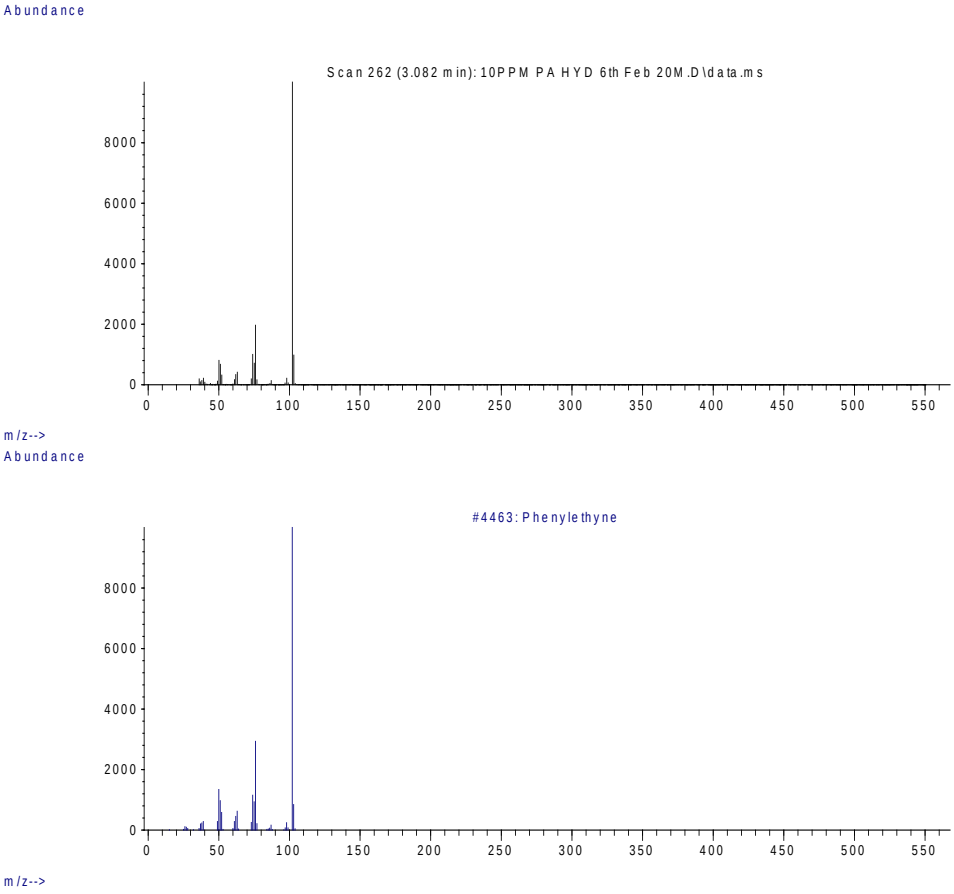

Figure 6.3 Mass spectra of phenylacetylene

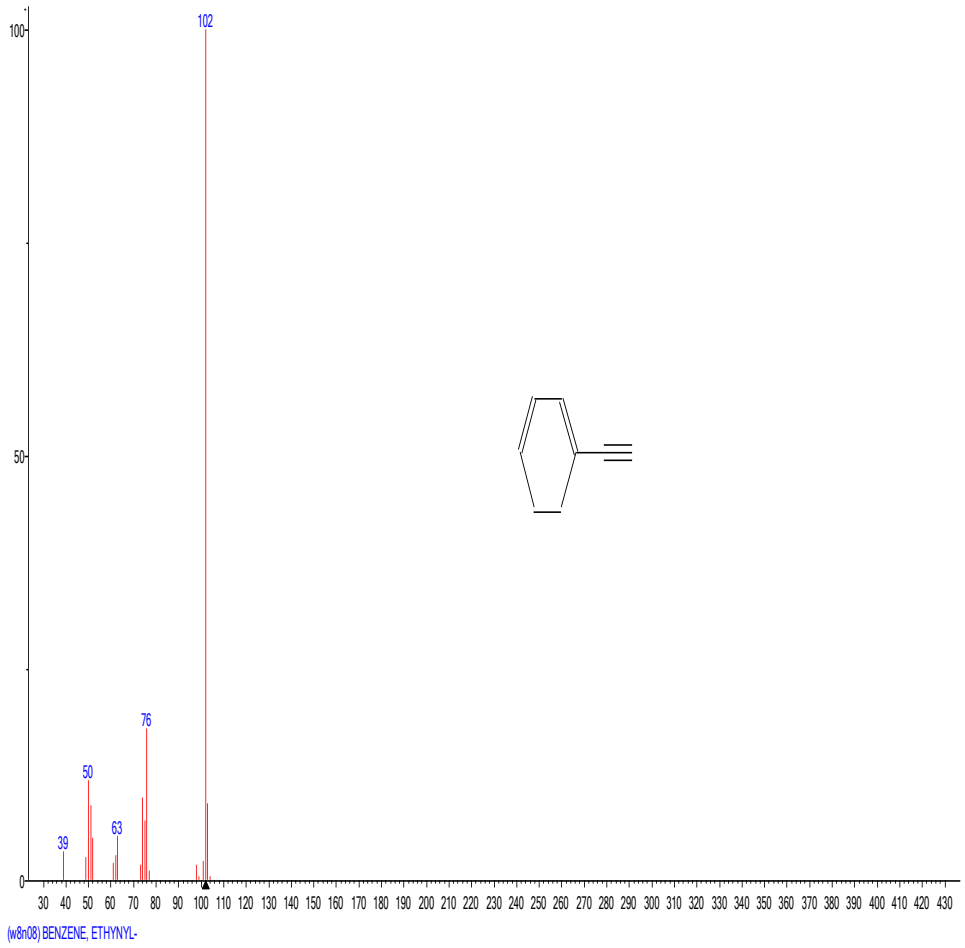

Figure 6.4 NIST mass spectrum of phenylacetylene

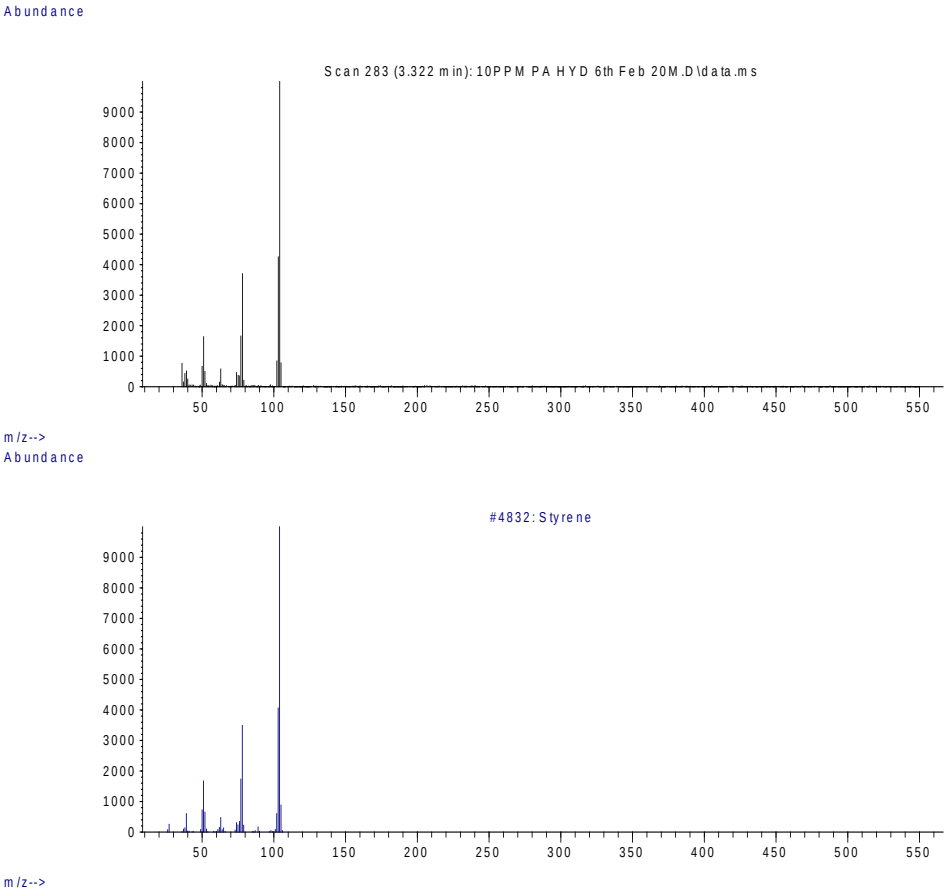

Figure 6.5 Mass spectra of styrene

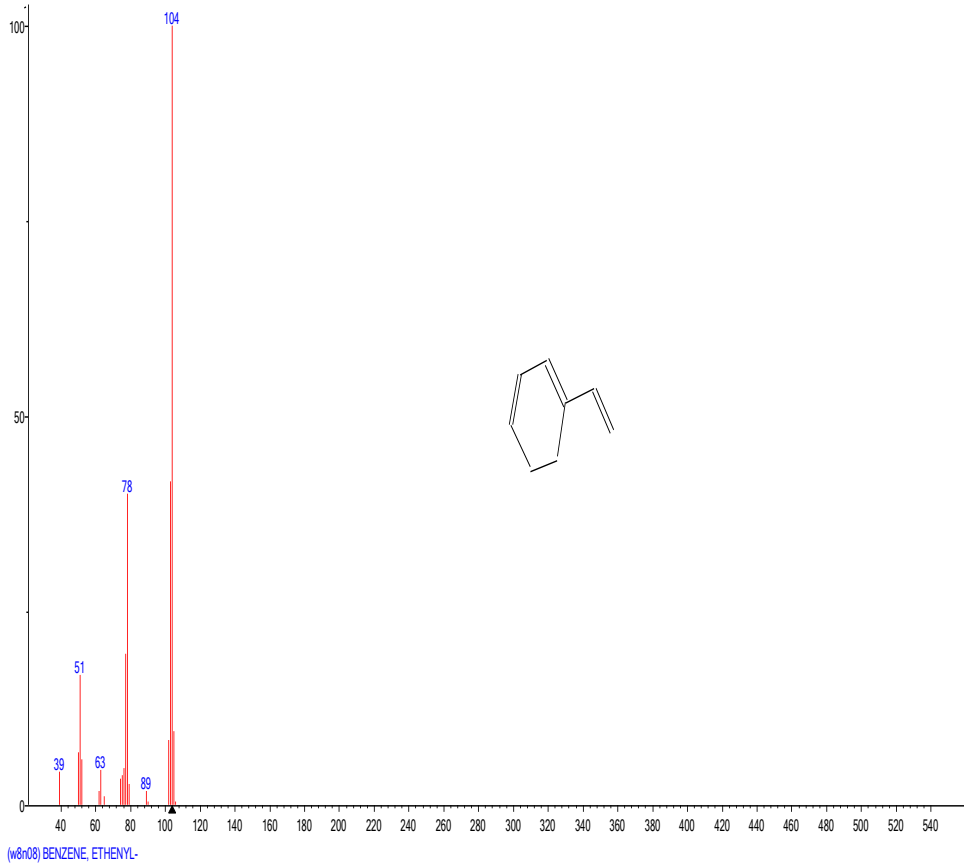

Figure 6.6 NIST mass spectrum of styrene

6.2 External calibration plots

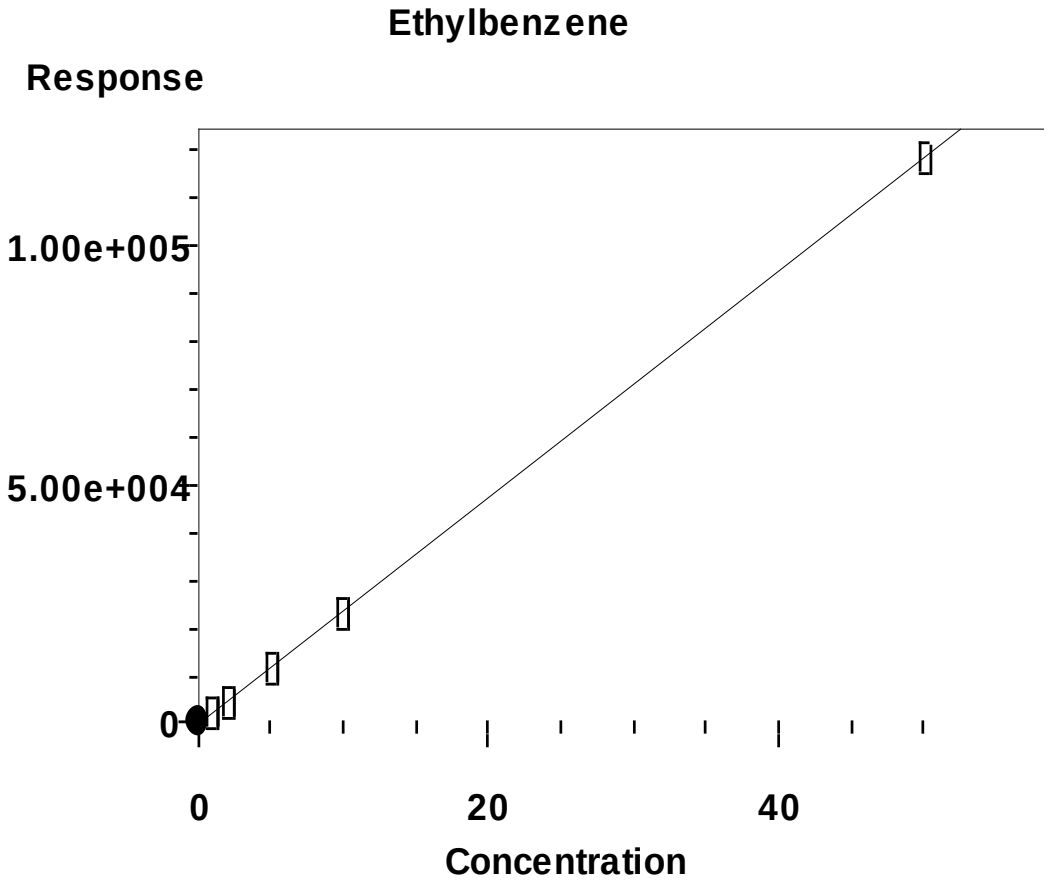

Figure 6.7 Calibration of ethylbenzene with r= 0.99996

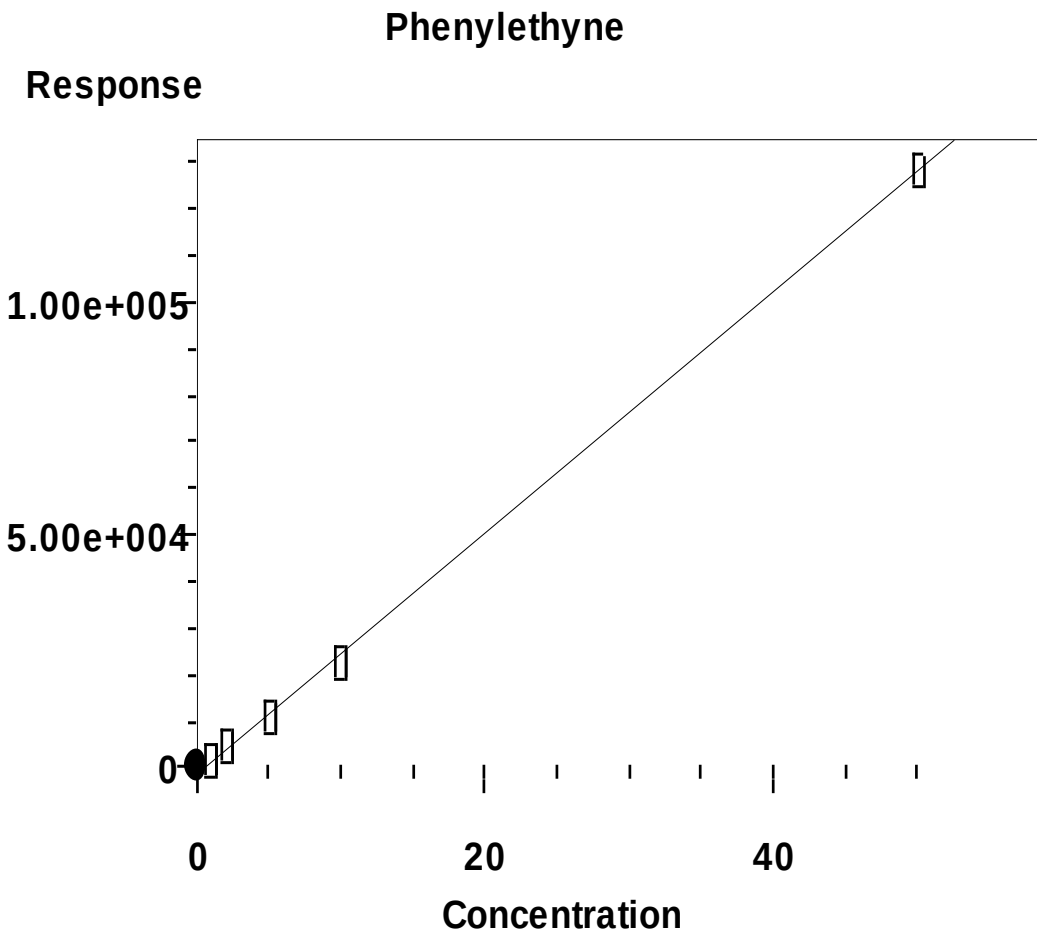

Figure 6.8 Calibration of Phenylacetylene with r= 0.99962

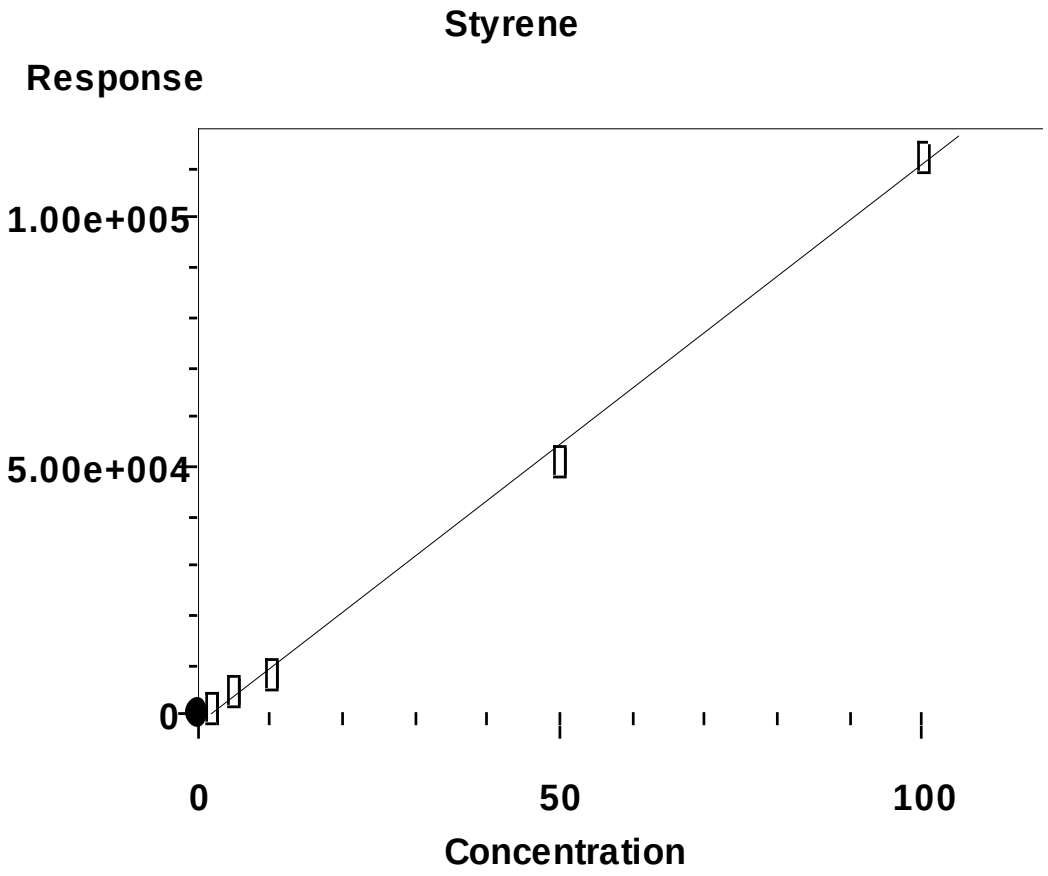

Figure 6.9 Calibration of Styrene with r = 0.9981

6.3 Effect of capillary length at 40 ^{o}C

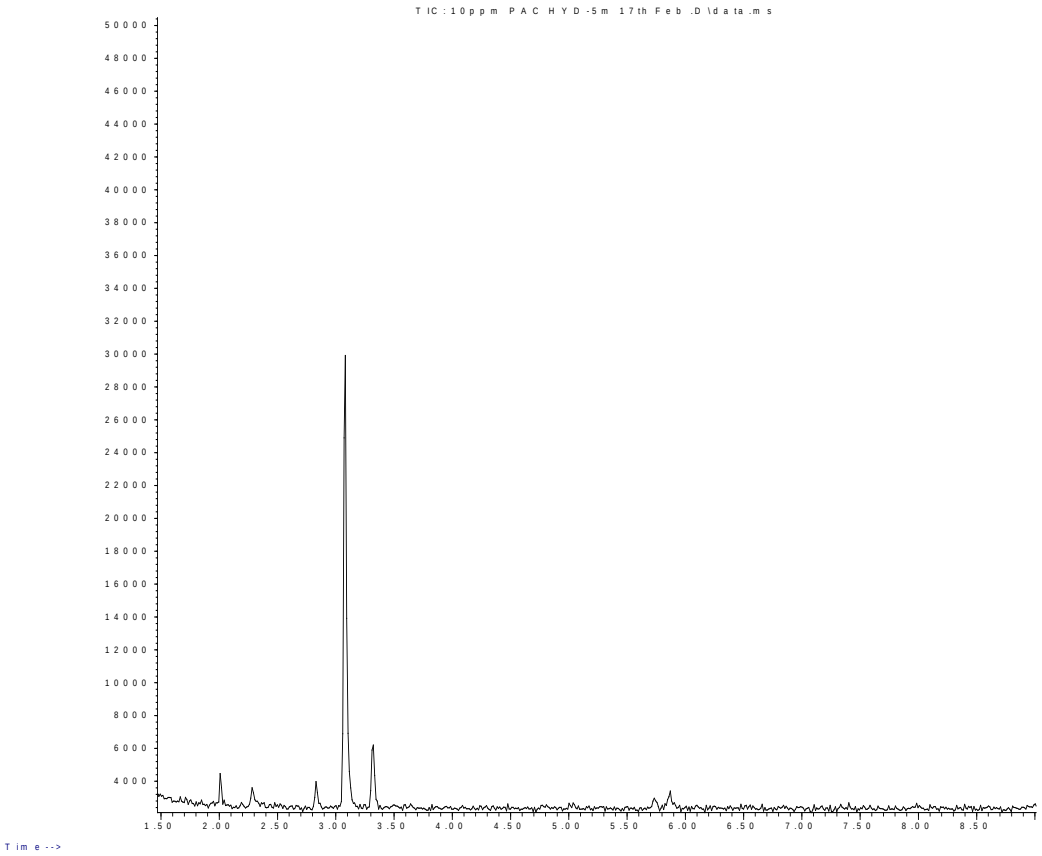

Figure 6.10 GC-MS spectrum of 5 m coated capillary

% Conversion = 24.83

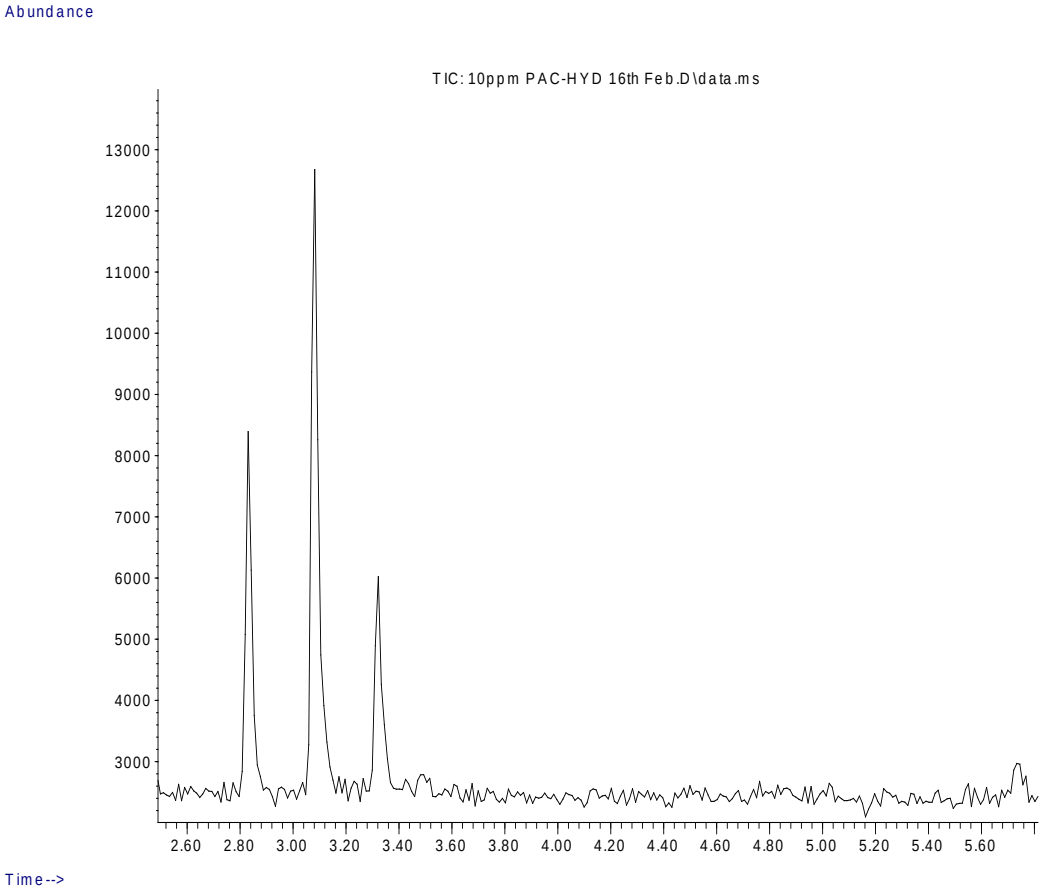

Figure 6.11 GC-MS spectrum of 10 m coated capillary

% Conversion = 27.30

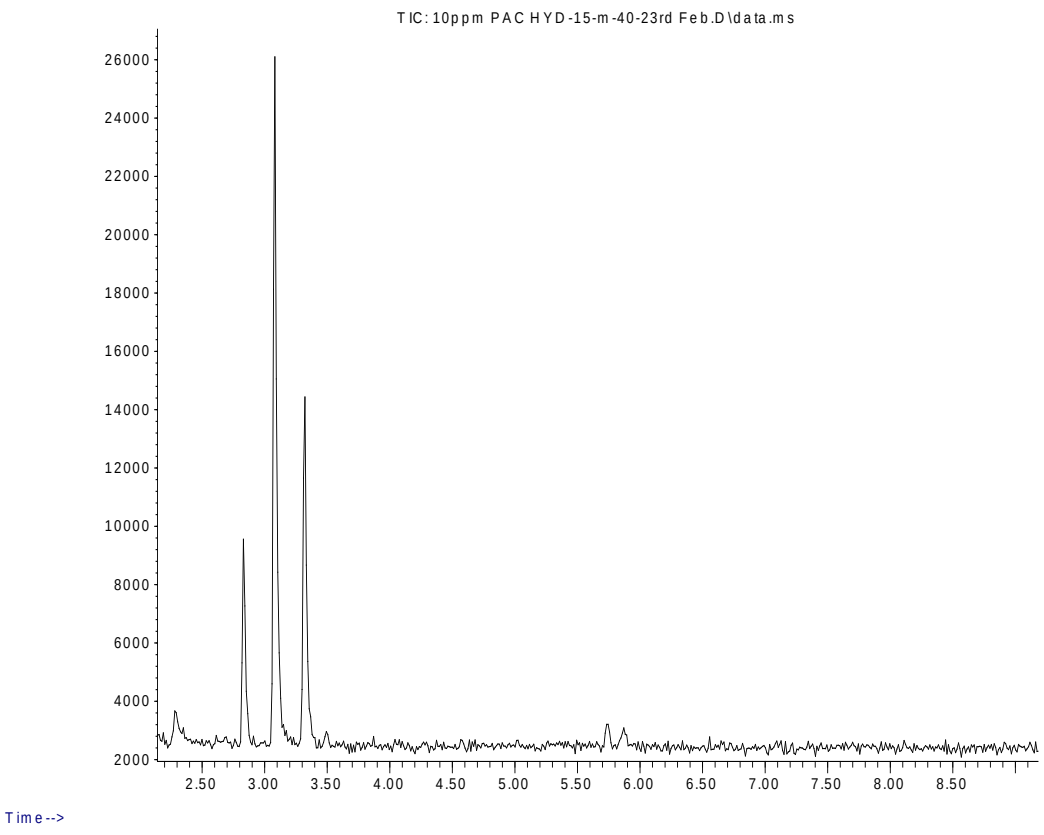

Figure 6.12 GC-MS spectrum of 15 m coated capillary

% Conversion = 42.40

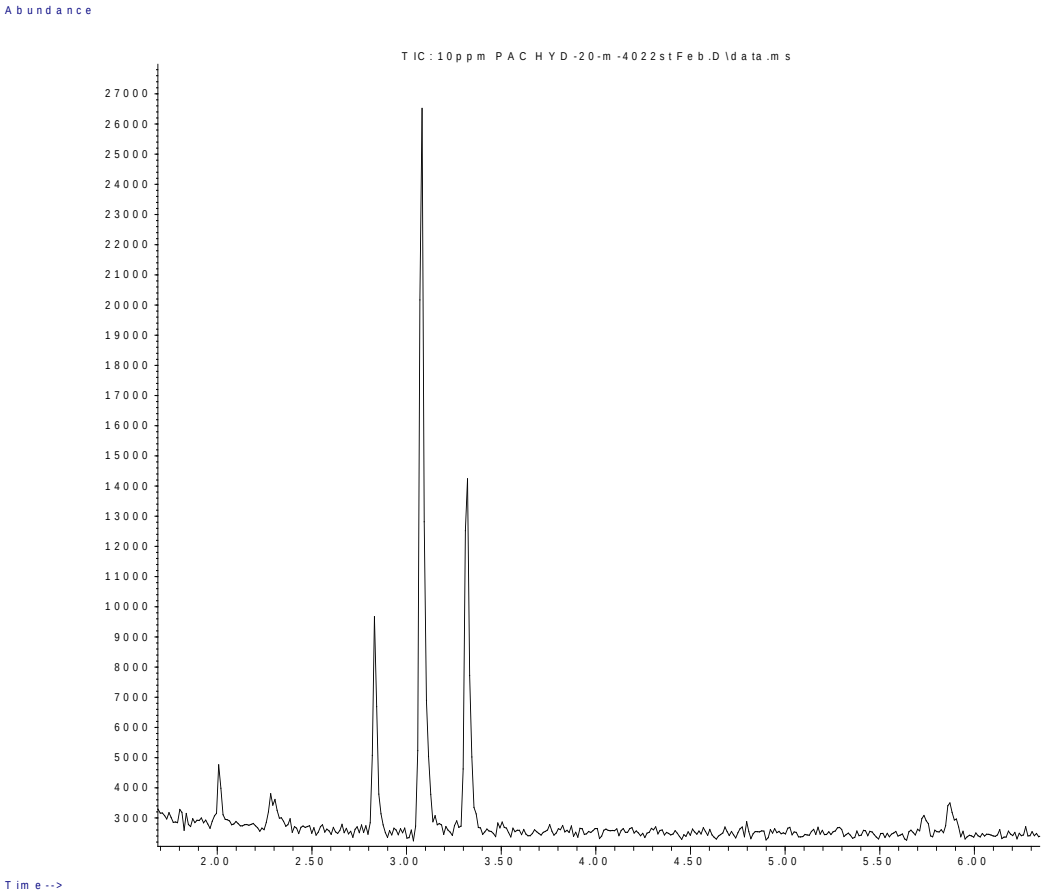

Figure 6.13 GC-MS spectrum of 20 m coated capillary

% Conversion = 34.99

6.4 Effect of temperature for 15 m capillary length

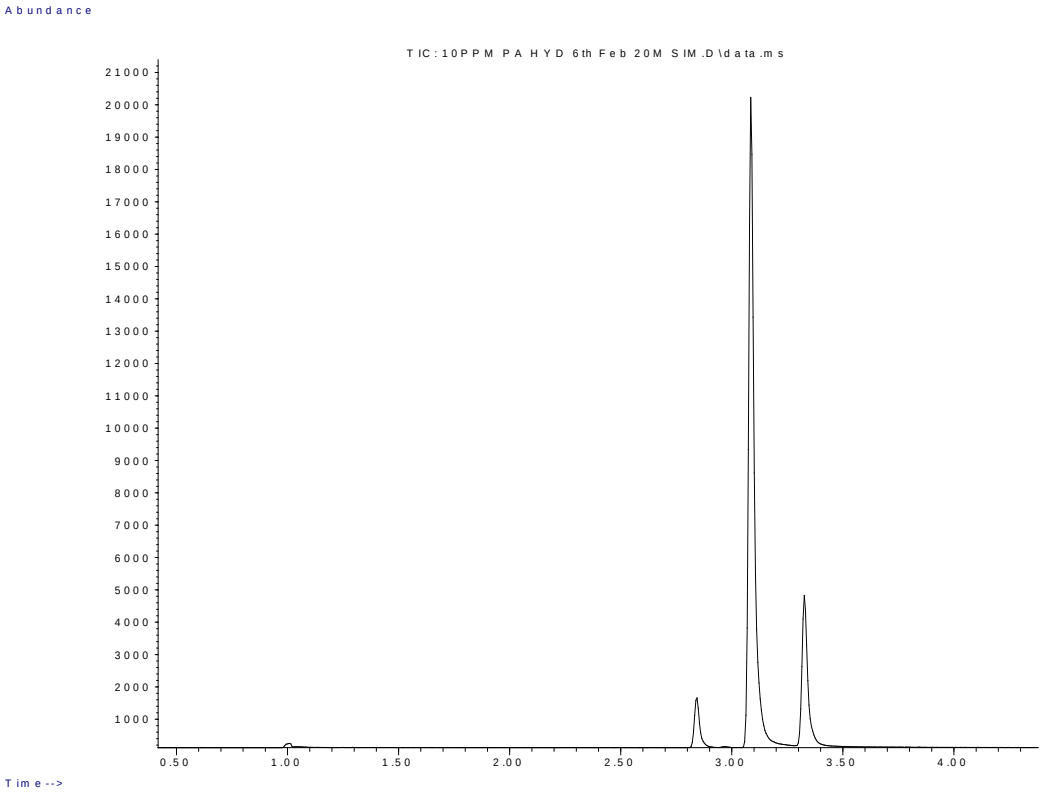

Figure 6.14 GC-MS spectrum of at 30 ^{o}C

% Conversion = 21.10
% Selectivity to ethylbenzene = 9.30
% Selectivity to styrene = 90.80
TOF = 0.021 s^{-1}

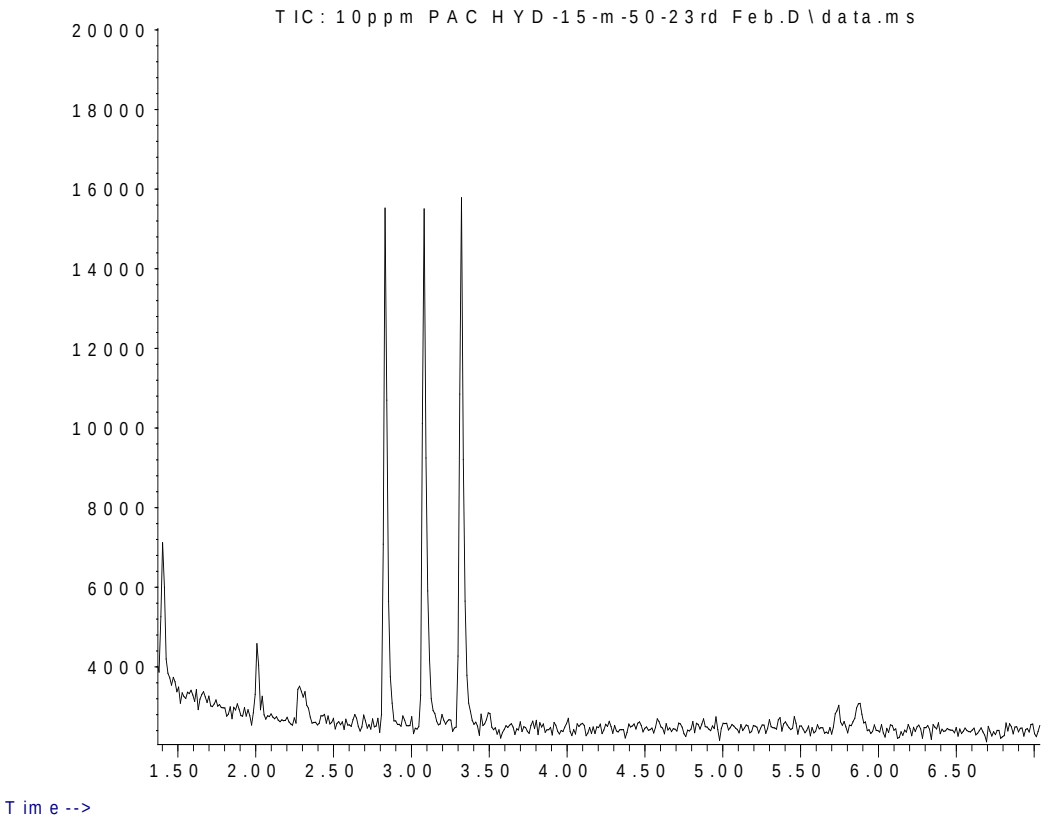

Figure 6.15 GC-MS spectrum of at 50 ^{o}C

% Conversion = 64.14
% Selectivity to ethylbenzene = 41.80
% Selectivity to styrene = 53.30
TOF = 0.10 s^{-1}

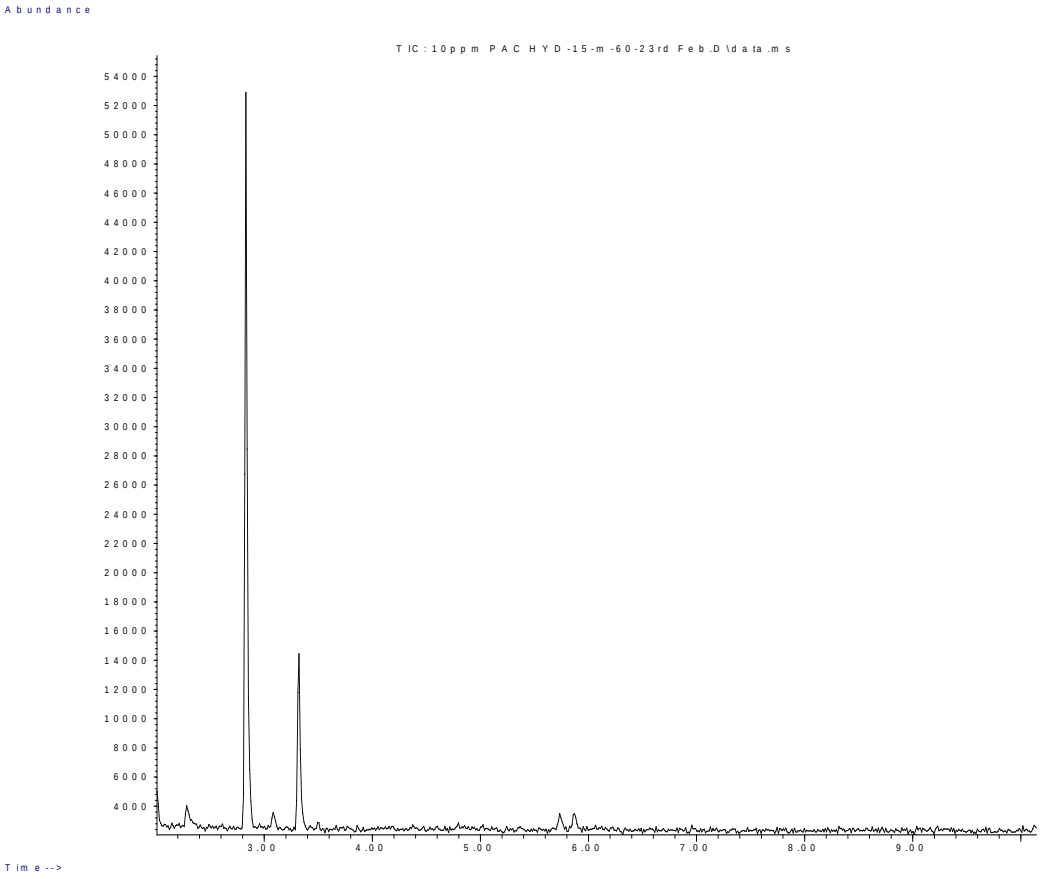

Figure 6.16 GC-MS spectrum of at 60 ^{o}C

% Conversion = 94.94
% Selectivity to ethylbenzene = 81.12
% Selectivity to styrene = 17.60
TOF = 0.185 s^{-1}

6.5 Effect of H_2 flow rate for 15 m capillary and at 60 ^oC

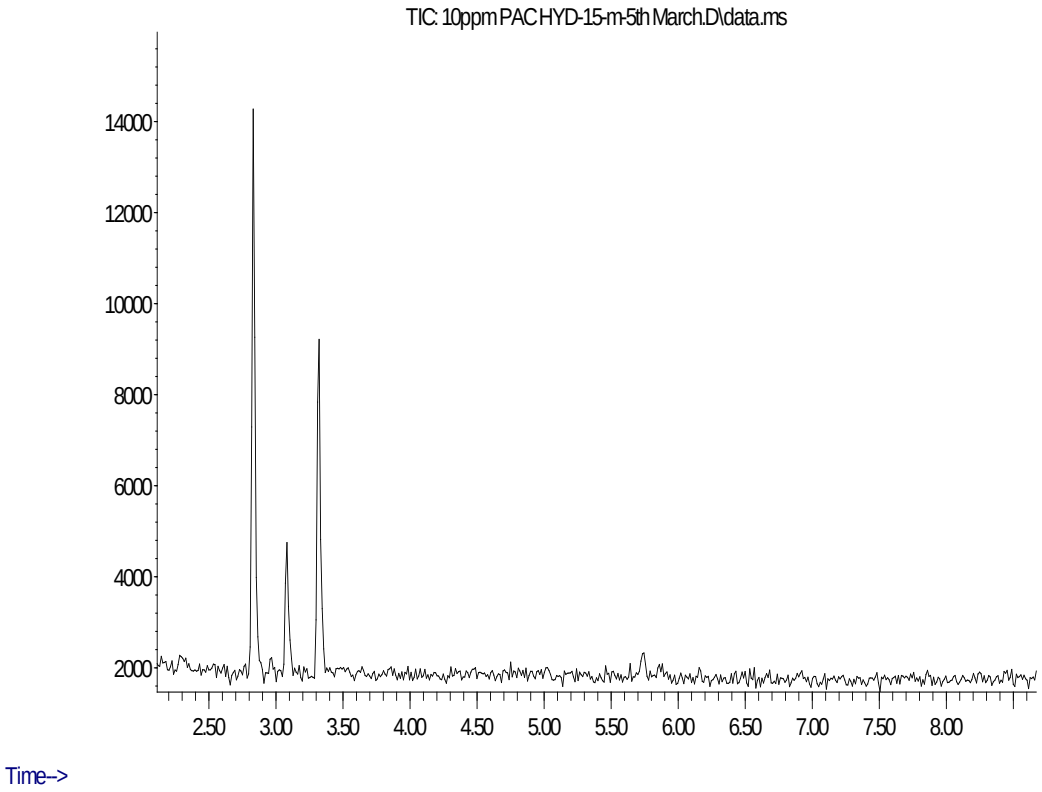

Figure 6.17 GC-MS spectrum at 0.25 ml.min^{-1} flow rate

% Conversion = 83.10
% Selectivity to ethylbenzene = 53.30
% Selectivity to styrene = 44.40

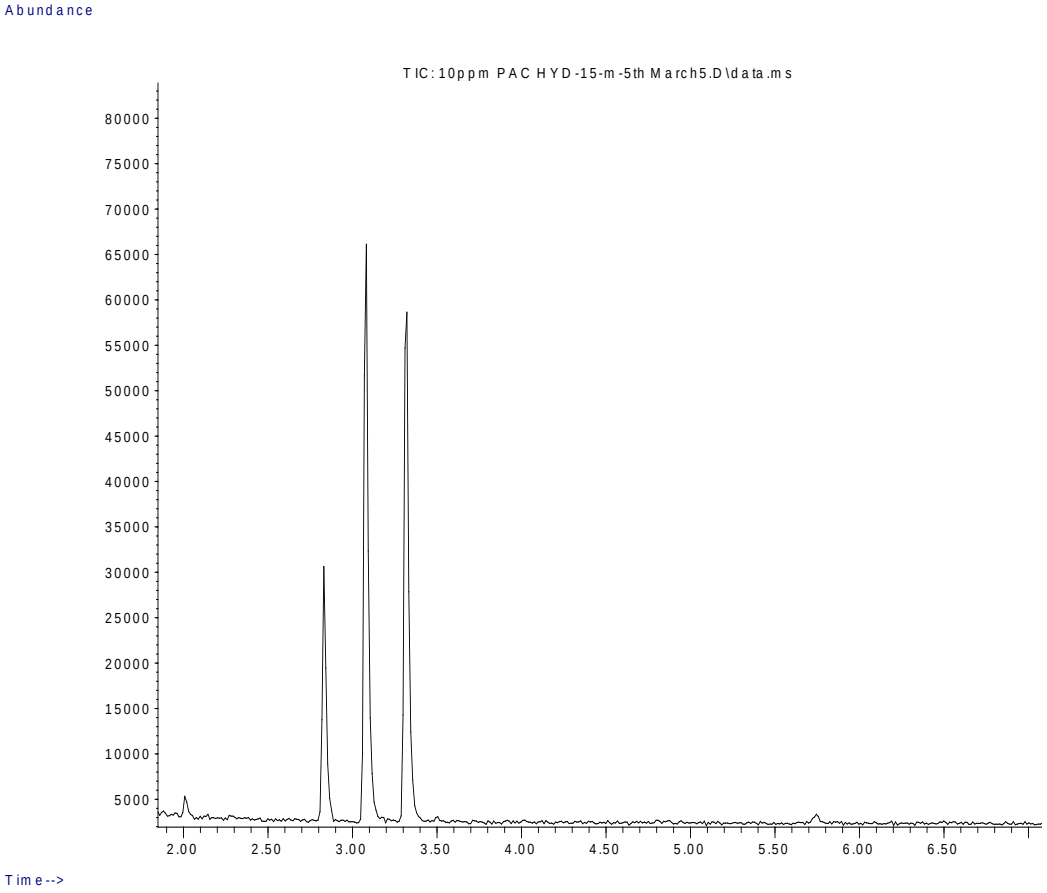

Figure 6.18 GC-MS spectrum at 0.75 ml.min^{-1} flow rate

% Conversion = 60.30
% Selectivity to ethylbenzene = 27.80
% Selectivity to styrene = 69.10

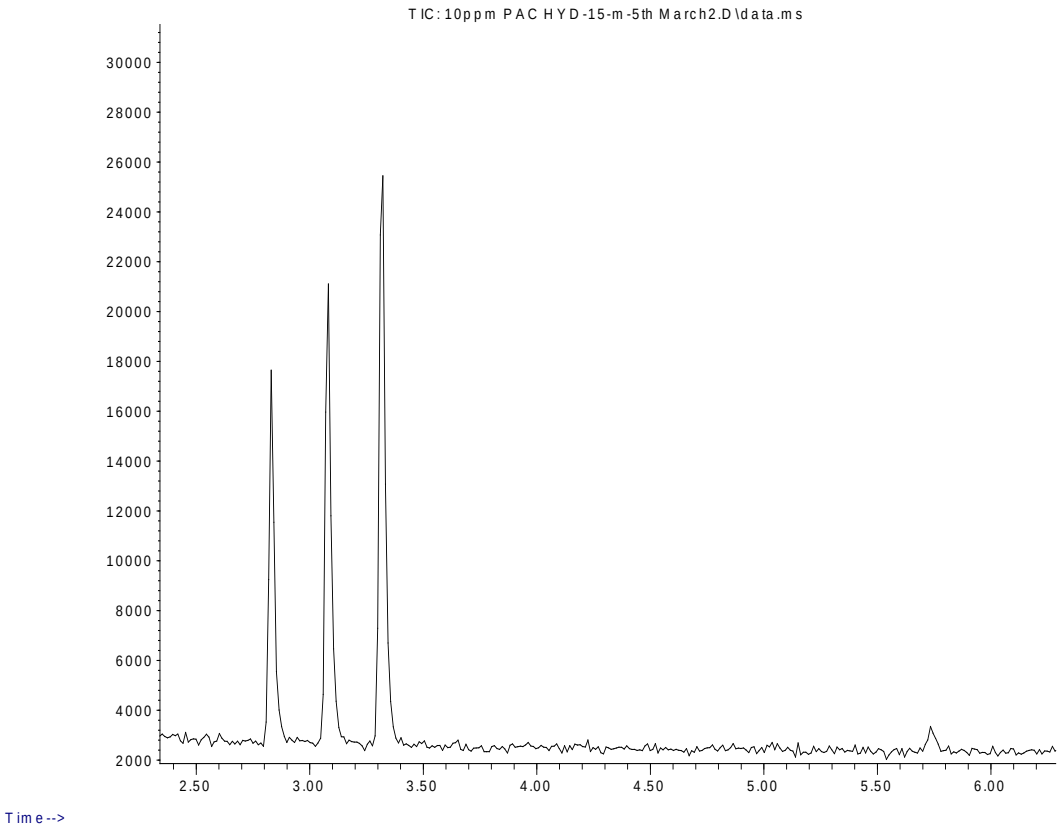

Figure 6.19 GC-MS spectrum at 1.0 ml.min^{-1} flow rate

% Conversion = 63.40
% Selectivity to ethylbenzene = 36.30
% Selectivity to styrene = 61.60

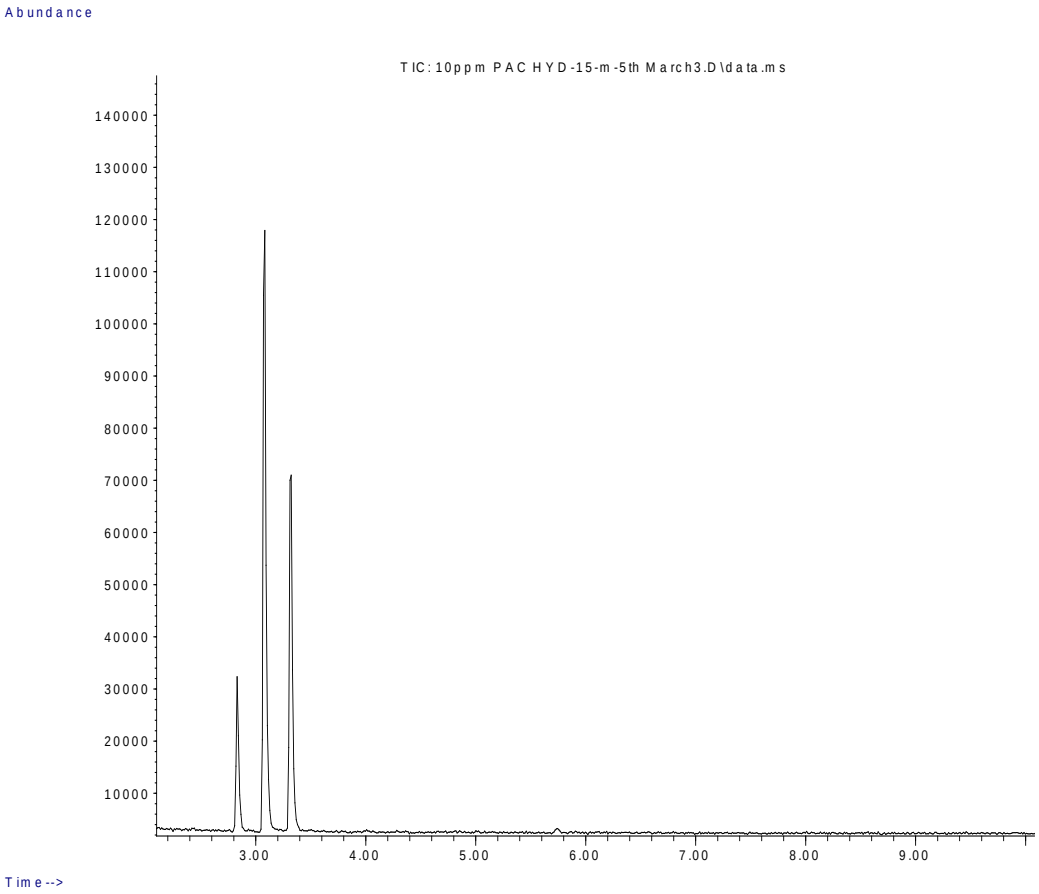

Figure 6.20 GC-MS spectrum at 1.25 ml.min^{-1} flow rate

% Conversion = 43.17
% Selectivity to ethylbenzene = 24.80
% Selectivity to styrene = 76.00

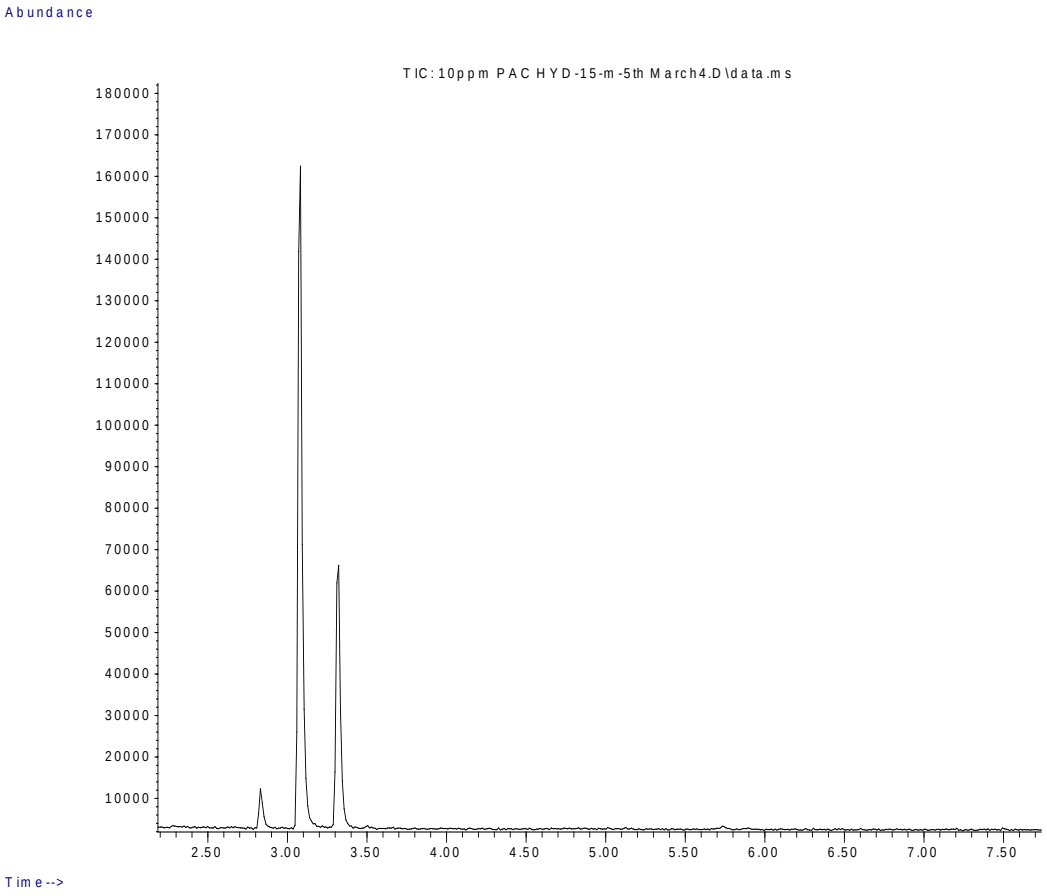

Figure 6.21 GC-MS spectrum at 1.5 ml.min^{-1} flow rate

% Conversion = 35.70
% Selectivity to ethylbenzene = 11.53
% Selectivity to styrene = 86.30

6.6 Effect of phenylacetylene concentration for 15 m capillary and at 60 ^{o}C

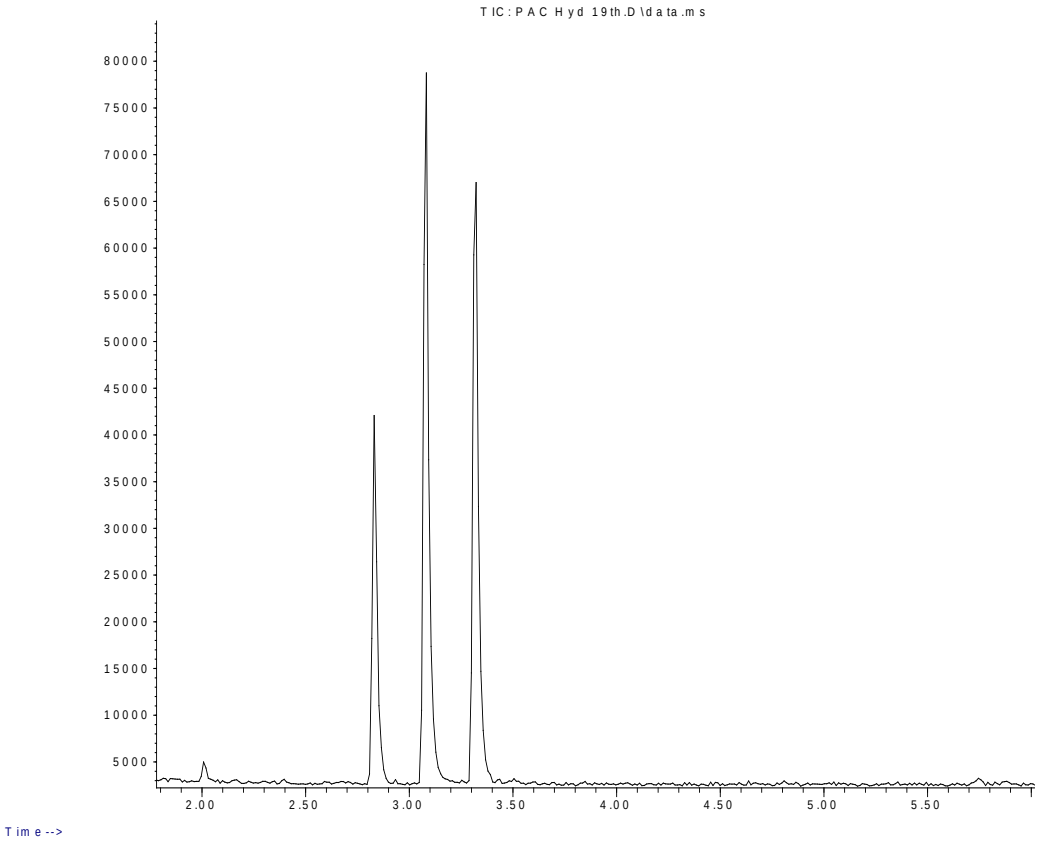

Figure 6.22 GC-MS spectrum for 56 ppm phenylacetylene

% Conversion = 62.50
% Selectivity to ethylbenzene = 33.06
% Selectivity to styrene = 67.30
TOF = 0.384 s^{-1}

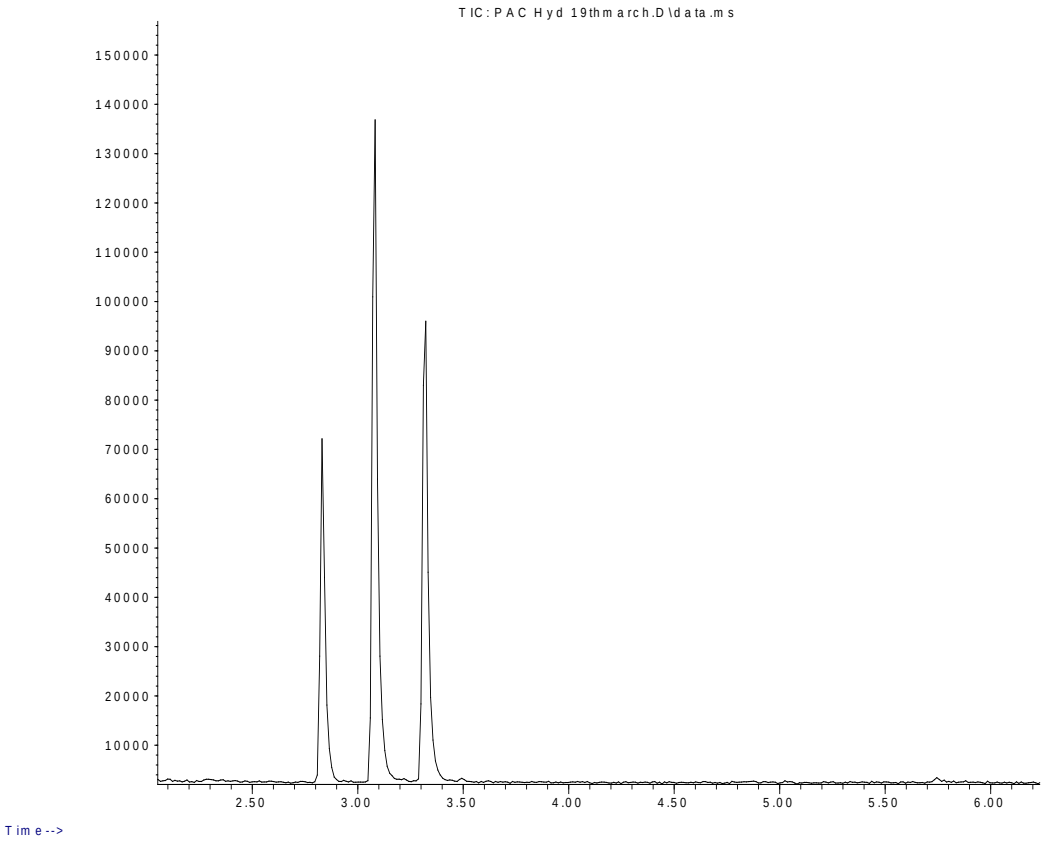

Figure 6.23 GC-MS spectrum for 105 ppm phenylacetylene

% Conversion = 52.4
% Selectivity to ethylbenzene = 35.60
% Selectivity to styrene = 63.35
TOF = 0.609 s^{-1}

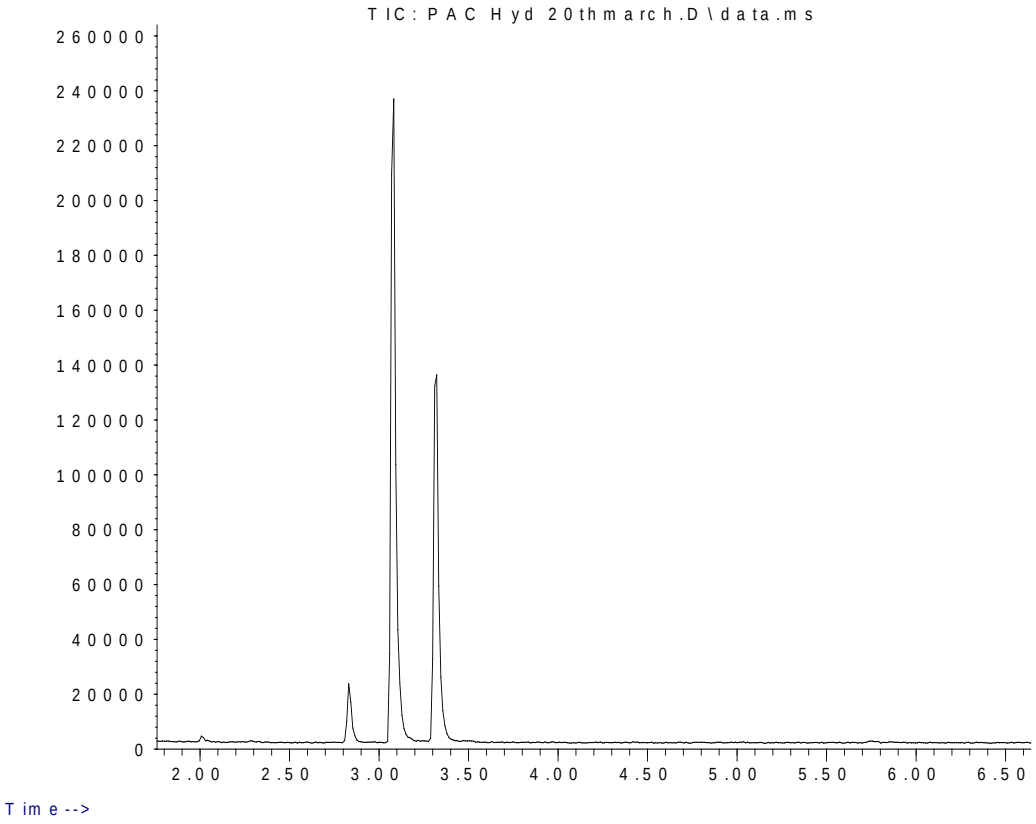

Figure 6.24 GC-MS spectrum for 158 ppm phenylacetylene

Conversion = 42.30
Selectivity to ethylbenzene = 9.52
% Selectivity to styrene = 83.22
TOF = 0.733 s^{-1}

6.7 Catalyst activity for 15 m capillary and at 60 ^{o}C

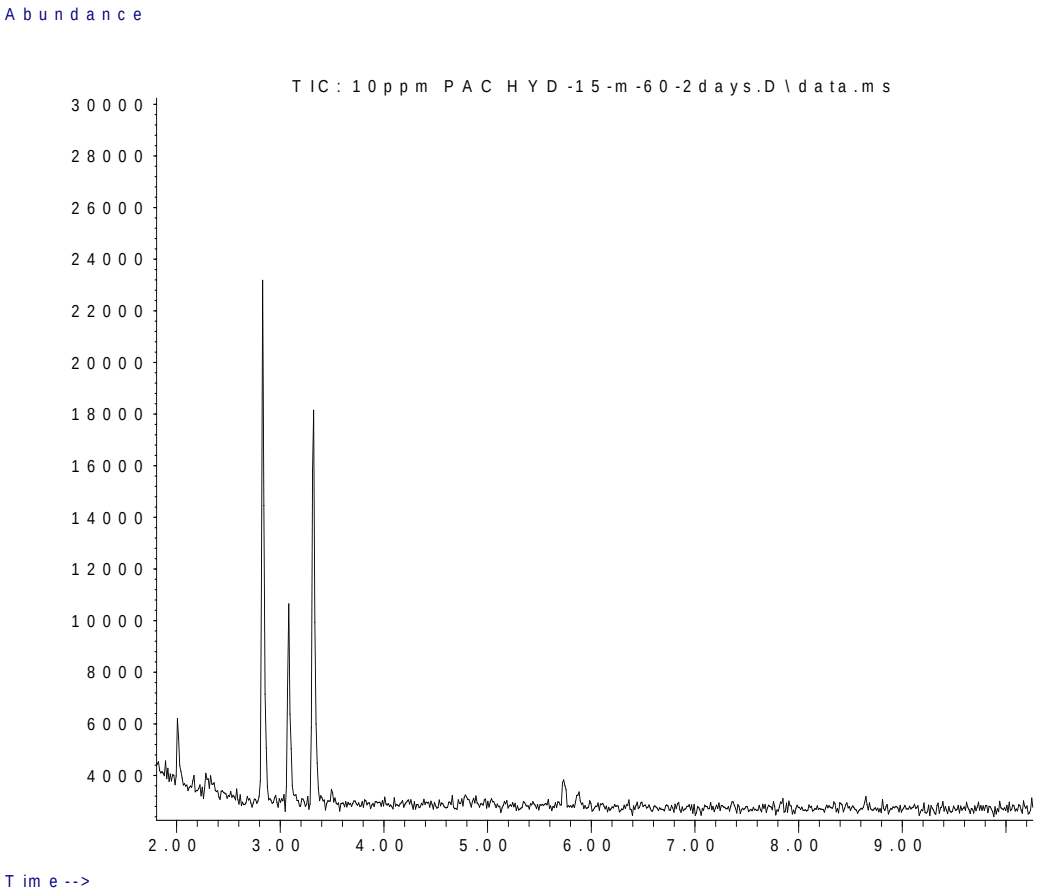

Figure 6.25 GC-MS spectrum after 2days

% Conversion = 79.01

TOF = 0.129 s^{-1}

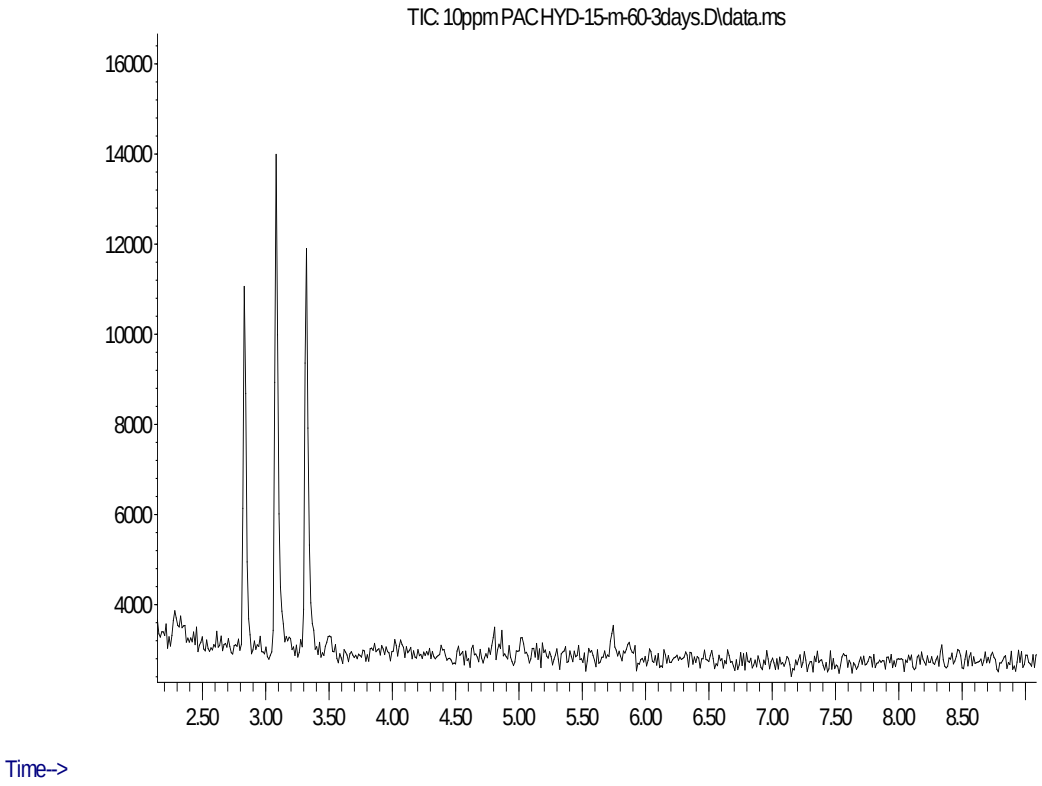

Figure 6.26 GC-MS spectrum after 3 days

% Conversion = 67
TOF = 0.074 s^{-1}

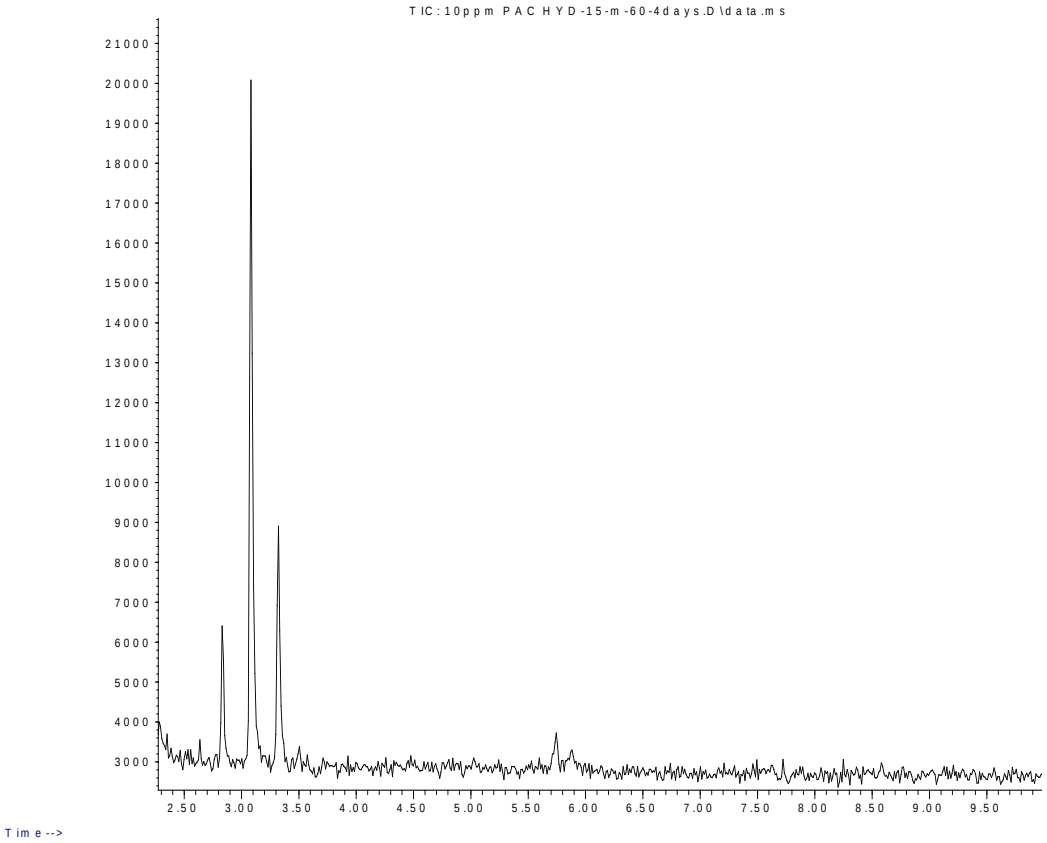

Figure 6.27 GC-MS spectrum after 4 days

% Conversion = 56

TOF = 0.093 s^{-1}

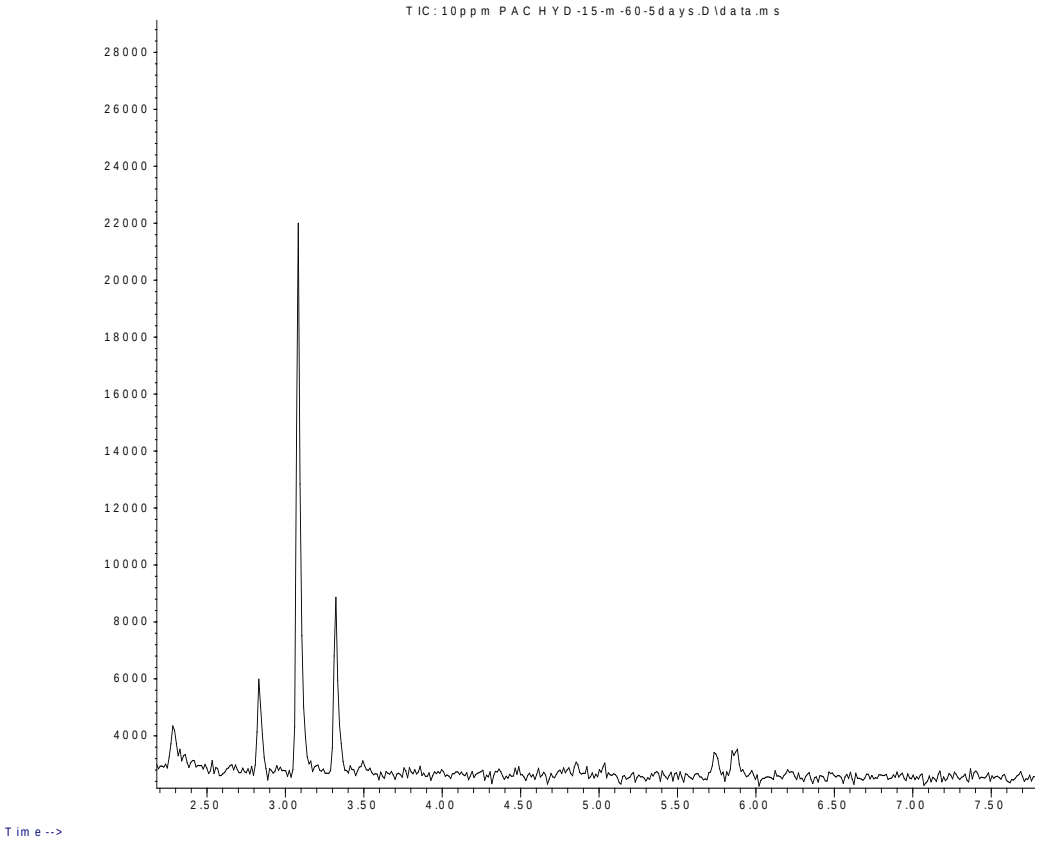

Figure 6.28 GC-MS spectrum after 5 days

% Conversion = 50.1

TOF = 0.083 s^{-1}

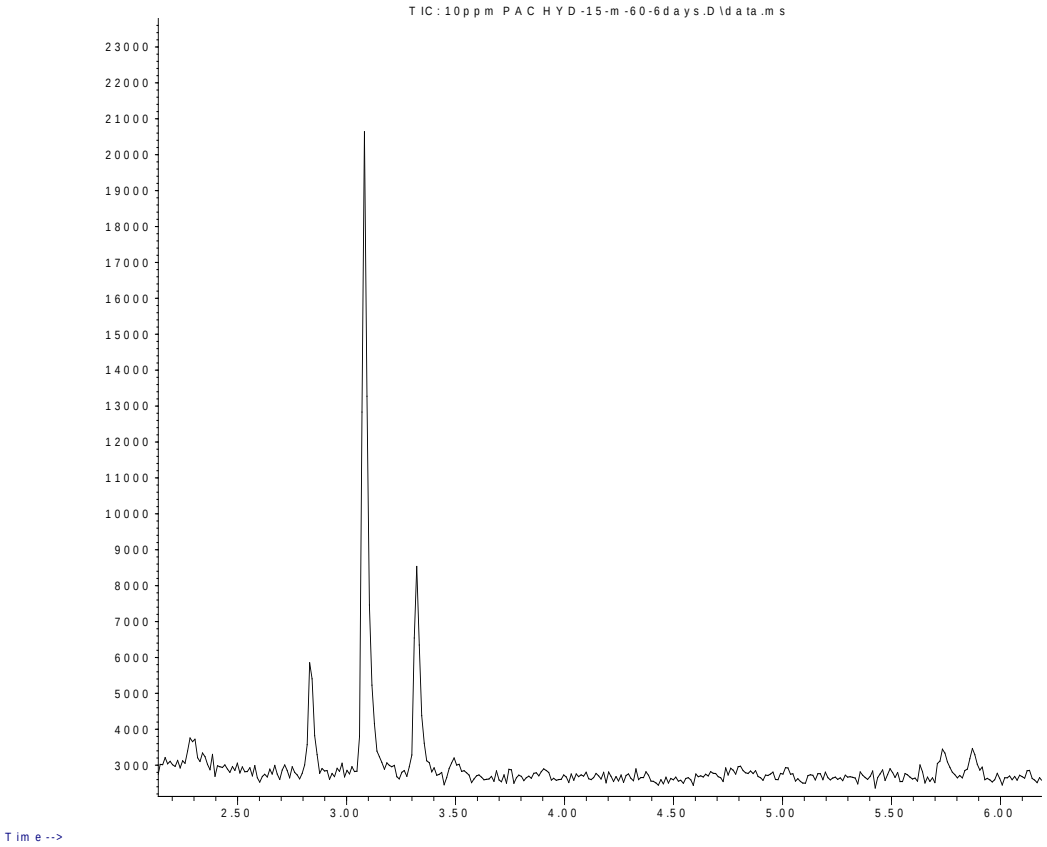

Figure 6.29 GC-MS spectrum after 6 days

% Conversion = 52.61
TOF = 0.086 s^{-1}

6.8 ICP-MS

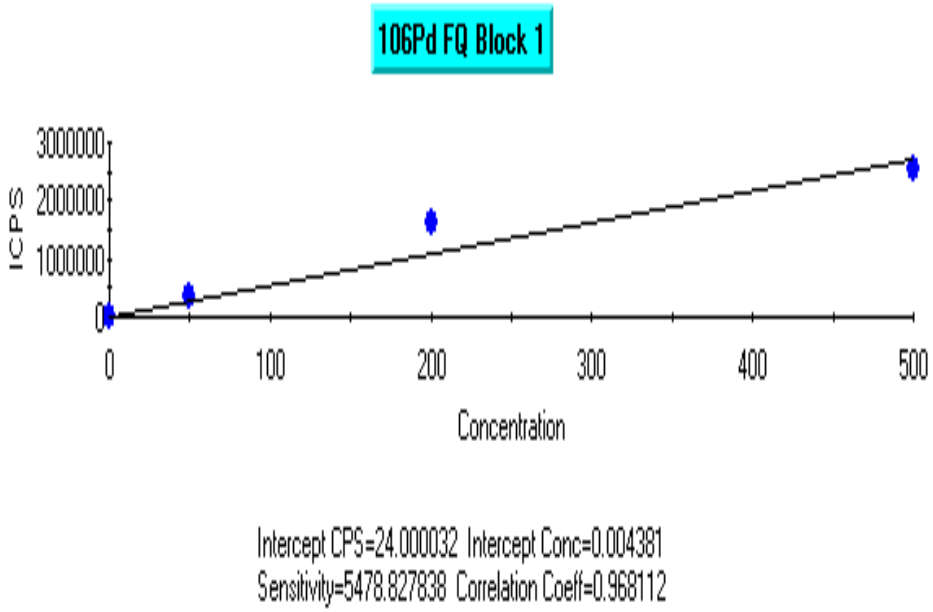

Figure 6.30 ICP-MS calibration curve for palladium

Table 6.1 ICP-MS sample analysis

Sample3/8/2015 2:55:11 PM

User Pre-dilution: 1.000

Run	Time	102Pd	104Pd	105Pd	106Pd	108Pd
		ppb	ppb	ppb	ppb	ppb
1	14:55:18	8.256	6.003	6.414	8.238	8.158
2	14:55:26	6.626	5.471	5.772	7.408	7.286
3	14:55:33	6.431	4.934	5.165	6.581	6.558
x		7.104	5.469	5.784	7.409	7.334
σ		1.002	0.535	0.625	0.829	0.801
%RSD		14.11	9.777	10.8	11.18	10.92

References

1. Ehrfeld, W.; Hessel, V.; Löwe, H., State of the Art of Microreaction Technology. In *Microreactors*, Wiley-VCH Verlag GmbH & Co. KGaA: 2004; pp 1-14.
2. (a) Jähnisch, K.; Hessel, V.; Löwe, H.; Baerns, M., Chemie in Mikrostrukturreaktoren. *Angewandte Chemie* **2004,** *116* (4), 410-451; (b) Rehahn, M., Elektrisch leitfähige Kunststoffe: Der Weg zu einer neuen Materialklasse. *Chemie in unserer Zeit* **2003,** *37* (1), 18-30; (c) Wörz, O.; Jäckel, K. P.; Richter, T.; Wolf, A., Microreactors, a new efficient tool for optimum reactor design. *Chemical Engineering Science* **2001,** *56* (3), 1029-1033; (d) Watts, P.; Wiles, C.; Haswell, S. J.; Pombo-Villar, E., Investigation of racemisation in peptide synthesis within a micro reactor. *Lab on a Chip* **2002,** *2* (3), 141-144.
3. (a) Zhang, X.; Stefanick, S.; Villani, F. J., Application of Microreactor Technology in Process Development. *Organic Process Research & Development* **2004,** *8* (3), 455-460; (b) Jähnisch, K.; Hessel, V.; Löwe, H.; Baerns, M., Chemistry in Microstructured Reactors. *Angewandte Chemie International Edition* **2004,** *43* (4), 406-446.
4. Schwalbe, T.; Autze, V.; Wille, G., Chemical Synthesis in Microreactors. *CHIMIA International Journal for Chemistry* **2002,** *56* (11), 636-646.
5. (a) Agrell, J.; Birgersson, H.; Boutonnet, M., Steam reforming of methanol over a Cu/ZnO/Al2O3 catalyst: a kinetic analysis and strategies for suppression of CO formation. *Journal of Power Sources* **2002,** *106* (1–2), 249-257; (b) Bravo, J.; Karim, A.; Conant, T.; Lopez, G. P.; Datye, A., Wall coating of a CuO/ZnO/Al2O3 methanol steam reforming catalyst for micro-channel reformers. *Chemical Engineering Journal* **2004,** *101* (1–3), 113-121.
6. Watts, P.; Haswell, S. J., The application of micro reactors for organic synthesis. *Chemical Society Reviews* **2005,** *34* (3), 235-246.
7. (a) Rebrov, E. V.; Berenguer-Murcia, A.; Skelton, H. E.; Johnson, B. F. G.; Wheatley, A. E. H.; Schouten, J. C., Capillary microreactors wall-coated with mesoporous titania thin film catalyst supports. *Lab on a Chip* **2009,** *9* (4), 503-506; (b) Kobayashi, J.; Mori, Y.; Okamoto, K.; Akiyama, R.; Ueno, M.; Kitamori, T.; Kobayashi, S., A Microfluidic Device for Conducting Gas-Liquid-Solid Hydrogenation Reactions. *Science* **2004,** *304* (5675), 1305-1308.
8. Kónya, Z.; Puntes, V.; Kiricsi, I.; Zhu, J.; Alivisatos, P.; Somorjai, G., Novel Two-Step Synthesis of Controlled Size and Shape Platinum Nanoparticles Encapsulated in Mesoporous Silica. *Catalysis Letters* **2002,** *81* (3-4), 137-140.
9. Wirnsberger, G.; Scott, B. J.; Stucky, G. D., pH Sensing with mesoporous thin films. *Chemical Communications* **2001,** (1), 119-120.
10. Fattakhova Rohlfing, D.; Rathouský, J.; Rohlfing, Y.; Bartels, O.; Wark, M., Functionalized Mesoporous Silica Films as a Matrix for Anchoring Electrochemically Active Guests. *Langmuir* **2005,** *21* (24), 11320-11329.
11. Hessel, V.; Löwe, H.; Serra, C.; Hadziioannou, G., Polymerisationen in mikrostrukturierten Reaktoren: Ein Überblick. *Chemie Ingenieur Technik* **2005,** *77* (11), 1693-1714.
12. (a) Aljbour, S.; Tagawa, T.; Yamada, H., Ultrasound-assisted capillary microreactor for aqueous–organic multiphase reactions. *Journal of Industrial and Engineering Chemistry* **2009,** *15* (6), 829-834; (b) Aljbour, S.; Yamada, H.; Tagawa, T., Ultrasound-assisted phase transfer catalysis in a capillary microreactor. *Chemical Engineering and Processing: Process Intensification* **2009,** *48* (6), 1167-1172.
13. Shore, G.; Morin, S.; Organ, M. G., Catalysis in Capillaries by Pd Thin Films Using Microwave-Assisted Continuous-Flow Organic Synthesis (MACOS). *Angewandte Chemie* **2006,** *118* (17), 2827-2832.

14. (a) Henglein, A., T. J. Mason, J. P. Lorimer: Sonochemistry (Theory, Applications and Uses of Ultrasound in Chemistry), Ellis Horwood Limited. Chichester, and John Wiley and Sons, New York 1988. 252 Seiten, Preis: £ 38.50. *Berichte der Bunsengesellschaft für physikalische Chemie* **1989,** *93* (10), 1150-1151; (b) Wang, M.-L.; Rajendran, V., Kinetics for dichlorocyclopropanation of 1,7-octadiene under the influence of ultrasound assisted phase-transfer catalysis conditions. *Journal of Molecular Catalysis A: Chemical* **2007,** *273* (1–2), 5-13; (c) Mason, T. J., Ultrasound in synthetic organic chemistry. *Chemical Society Reviews* **1997,** *26* (6), 443-451.
15. (a) Comer, E.; Organ, M. G., A Microreactor for Microwave-Assisted Capillary (Continuous Flow) Organic Synthesis. *Journal of the American Chemical Society* **2005,** *127* (22), 8160-8167; (b) Iida, Y.; Yasui, K.; Tuziuti, T.; Sivakumar, M.; Endo, Y., Ultrasonic cavitation in microspace. *Chemical Communications* **2004,** (20), 2280-2281; (c) Ahmed-Omer, B.; Barrow, D.; Wirth, T., Effect of segmented fluid flow, sonication and phase transfer catalysis on biphasic reactions in capillary microreactors. *Chemical Engineering Journal* **2008,** *135, Supplement 1* (0), S280-S283.
16. Wiles, C.; Watts, P., Continuous flow reactors: a perspective. *Green Chemistry* **2012,** *14* (1), 38-54.
17. Hetsroni, G.; Mosyak, A.; Pogrebnyak, E.; Yarin, L. P., Fluid flow in micro-channels. *International Journal of Heat and Mass Transfer* **2005,** *48* (10), 1982-1998.
18. Wiles, C.; Watts, P., Recent advances in micro reaction technology. *Chemical Communications* **2011,** *47* (23), 6512-6535.
19. Benito-López, F.; Egberink, R. J. M.; Reinhoudt, D. N.; Verboom, W., High pressure in organic chemistry on the way to miniaturization. *Tetrahedron* **2008,** *64* (43), 10023-10040.
20. El-Nahhal, I. M.; El-Ashgar, N. M., A review on polysiloxane-immobilized ligand systems: Synthesis, characterization and applications. *Journal of Organometallic Chemistry* **2007,** *692* (14), 2861-2886.
21. Hair, M. L.; Hertl, W., Reactions of chlorosilanes with silica surfaces. *The Journal of Physical Chemistry* **1969,** *73* (7), 2372-2378.
22. Leyden, D. E.; Luttrell, G. H., Preconcentration of trace metals using chelating groups immobilized via silylation. *Analytical Chemistry* **1975,** *47* (9), 1612-1617.
23. Goodwin, J. W.; Harbron, R. S.; Reynolds, P. A., Functionalization of colloidal silica and silica surfaces via silylation reactions. *Colloid & Polymer Sci* **1990,** *268* (8), 766-777.
24. (a) Silva, C. R.; Jardim, I. C. S. F.; Airoldi, C., New generation of sterically protected C18 stationary phases containing embedded urea groups for use in high-performance liquid chromatography. *Journal of Chromatography A* **2003,** *987* (1–2), 127-138; (b) Wasiak, W.; Urbaniak, W., Chemically bonded chelates as selective complexing sorbents for gas chromatography V. Silica chemically modified by Cu(II) complexes via amino groups. *Journal of Chromatography A* **1997,** *757* (1–2), 137-143.
25. (a) H. Clark, J.; J. Macquarrie, D., Catalysis of liquid phase organic reactions using chemically modified mesoporous inorganic solids. *Chemical Communications* **1998,** (8), 853-860; (b) Ciolino, L. A.; Dorsey, J. G., Synthesis and characterization of silica-based aliphatic ion exchangers. *Journal of Chromatography A* **1994,** *675* (1–2), 29-45.
26. Davis, S. S., Biomédical applications of nanotechnology — implications for drug targeting and gene therapy. *Trends in Biotechnology* **1997,** *15* (6), 217-224.
27. Zha, J.; Roggendorf, H., Sol–gel science, the physics and chemistry of sol–gel processing, Ed. by C. J. Brinker and G. W. Scherer, Academic Press, Boston 1990, xiv, 908 pp., bound—ISBN 0-12-134970-5. *Advanced Materials* **1991,** *3* (10), 522-522.
28. (a) Wang, F.; Jin, G.-Q.; Guo, X.-Y., Sol–gel synthesis of Si3N4 nanowires and nanotubes. *Materials Letters* **2006,** *60* (3), 330-333; (b) Samuel, J.; Strinkovski, A.; Shalom, S.; Lieberman, K.; Ottolenghi, M.; Avnir, D.; Lewis, A., Miniaturization of organically doped sol-gel materials: a microns-size fluorescent pH sensor. *Materials Letters* **1994,** *21* (5–6), 431-434.

29. Buckley, A. M.; Greenblatt, M., The Sol-Gel Preparation of Silica Gels. *Journal of Chemical Education* **1994,** *71* (7), 599.
30. Ai Du; Bin Zhou; Yunong Li; Xiuyan Li; Junjian Ye; Longxiang Li; Zhihua Zhang; Guohua Gao; Jun Shen, Aerogel: a potential three-dimensional nanoporous filler for resins. *Journal of Reinforced Plastics and Composites* **2011,** *30* (11), 912-921.
31. Trueba, M.; Trasatti, S. P., γ-Alumina as a Support for Catalysts: A Review of Fundamental Aspects. *European Journal of Inorganic Chemistry* **2005,** *2005* (17), 3393-3403.
32. Min, B. K.; Friend, C. M., Heterogeneous Gold-Based Catalysis for Green Chemistry: Low-Temperature CO Oxidation and Propene Oxidation. *Chemical Reviews* **2007,** *107* (6), 2709-2724.
33. (a) Davda, R. R.; Shabaker, J. W.; Huber, G. W.; Cortright, R. D.; Dumesic, J. A., Aqueous-phase reforming of ethylene glycol on silica-supported metal catalysts. *Applied Catalysis B: Environmental* **2003,** *43* (1), 13-26; (b) Kataoka, S.; Endo, A.; Oyama, M.; Ohmori, T., Enzymatic reactions inside a microreactor with a mesoporous silica catalyst support layer. *Applied Catalysis A: General* **2009,** *359* (1–2), 108-112.
34. (a) Horiuchi, T.; Chen, L.; Osaki, T.; Sugiyama, T.; Suzuki, K.; Mori, T., A novel alumina catalyst support with high thermal stability derived from silica-modified alumina aerogel. *Catalysis Letters* **1999,** *58* (2-3), 89-92; (b) Enger, B. C.; Fossan, Å.-L.; Borg, Ø.; Rytter, E.; Holmen, A., Modified alumina as catalyst support for cobalt in the Fischer–Tropsch synthesis. *Journal of Catalysis* **2011,** *284* (1), 9-22.
35. Liu, N.; Assink, R. A.; Brinker, C. J., Synthesis and characterization of highly ordered mesoporous thin films with -COOH terminated pore surfaces. *Chemical Communications* **2003,** (3), 370-371.
36. Nakamura, H.; Li, X.; Wang, H.; Uehara, M.; Miyazaki, M.; Shimizu, H.; Maeda, H., A simple method of self assembled nano-particles deposition on the micro-capillary inner walls and the reactor application for photo-catalytic and enzyme reactions. *Chemical Engineering Journal* **2004,** *101* (1–3), 261-268.
37. Kim, N.; Kwon, M. S.; Park, C. M.; Park, J., One-pot synthesis of recyclable palladium catalysts for hydrogenations and carbon–carbon coupling reactions. *Tetrahedron Letters* **2004,** *45* (38), 7057-7059.
38. (a) Gronnow, M. J.; Luque, R.; Macquarrie, D. J.; Clark, J. H., A novel highly active biomaterial supported palladium catalyst. *Green Chemistry* **2005,** *7* (7), 552-557; (b) Bandini, M.; Luque, R.; Budarin, V.; Macquarrie, D. J., Aryl alkynylation versus alkyne homocoupling: unprecedented selectivity switch in Cu, phosphine and solvent-free heterogeneous Pd-catalysed couplings. *Tetrahedron* **2005,** *61* (41), 9860-9868.
39. (a) Bedford, R. B.; Cazin, C. S. J.; Hursthouse, M. B.; Light, M. E.; Pike, K. J.; Wimperis, S., Silica-supported imine palladacycles—recyclable catalysts for the Suzuki reaction? *Journal of Organometallic Chemistry* **2001,** *633* (1–2), 173-181; (b) Yang, Q.; Ma, S.; Li, J.; Xiao, F.; Xiong, H., A water-compatible, highly active and reusable PEG-coated mesoporous silica-supported palladium complex and its application in Suzuki coupling reactions. *Chemical Communications* **2006,** (23), 2495-2497.
40. Jayasree, S.; Seayad, A.; V. Chaudhari, R., Highly active supported palladium catalyst for the regioselective synthesis of 2-arylpropionic acids by carbonylation. *Chemical Communications* **1999,** (12), 1067-1068.
41. Amatore, C.; Jutand, A.; Khalil, F.; M'Barki, M. A.; Mottier, L., Rates and mechanisms of oxidative addition to zerovalent palladium complexes generated in situ from mixtures of Pd0(dba)2 and triphenylphosphine. *Organometallics* **1993,** *12* (8), 3168-3178.
42. Uozumi, Y.; Shibatomi, K., Catalytic Asymmetric Allylic Alkylation in Water with a Recyclable Amphiphilic Resin-Supported P,N-Chelating Palladium Complex. *Journal of the American Chemical Society* **2001,** *123* (12), 2919-2920.

43. Polshettiwar, V.; Len, C.; Fihri, A., Silica-supported palladium: Sustainable catalysts for cross-coupling reactions. *Coordination Chemistry Reviews* **2009,** *253* (21–22), 2599-2626.
44. Lim, M. S.; Kim, M. R.; Noh, J.; Woo, S. I., A plate-type reactor coated with zirconia-sol and catalyst mixture for methanol steam-reforming. *Journal of Power Sources* **2005,** *140* (1), 66-71.
45. Park, G.-G.; Seo, D. J.; Park, S.-H.; Yoon, Y.-G.; Kim, C.-S.; Yoon, W.-L., Development of microchannel methanol steam reformer. *Chemical Engineering Journal* **2004,** *101* (1–3), 87-92.
46. Izquierdo, U.; Wichert, M.; Kolb, G.; Barrio, V. L.; Zapf, R.; Ziogas, A.; Neuberg, S.; Arias, P. L.; Cambra, J. F., Micro reactor hydrogen production from ethylene glycol reforming using Rh catalysts supported on CeO2 and La2O3 promoted α-Al2O3. *International Journal of Hydrogen Energy* **2014,** *39* (10), 5248-5256.
47. Kawamura, Y.; Ogura, N.; Yamamoto, T.; Igarashi, A., A miniaturized methanol reformer with Si-based microreactor for a small PEMFC. *Chemical Engineering Science* **2006,** *61* (4), 1092-1101.
48. Hwang, S.-M.; Kwon, O. J.; Kim, J. J., Method of catalyst coating in micro-reactors for methanol steam reforming. *Applied Catalysis A: General* **2007,** *316* (1), 83-89.
49. Zapf, R.; Becker-Willinger, C.; Berresheim, K.; Bolz, H.; Gnaser, H.; Hessel, V.; Kolb, G.; P.Löb; Pannwitt, A. K.; Ziogas, A., Detailed Characterization of Various Porous Alumina-Based Catalyst Coatings Within Microchannels and Their Testing for Methanol Steam Reforming. *Chemical Engineering Research and Design* **2003,** *81* (7), 721-729.
50. Haas-Santo, K.; Fichtner, M.; Schubert, K., Preparation of microstructure compatible porous supports by sol–gel synthesis for catalyst coatings. *Applied Catalysis A: General* **2001,** *220* (1–2), 79-92.
51. Kundu, A.; Park, J. M.; Ahn, J. E.; Park, S. S.; Shul, Y. G.; Han, H. S., Micro-channel reactor for steam reforming of methanol. *Fuel* **2007,** *86* (9), 1331-1336.
52. Muraza, O.; Rebrov, E. V.; Khimyak, T.; Johnson, B. F. G.; Kooyman, P. J.; Lafont, U.; de Croon, M. H. J. M.; Schouten, J. C., Mesoporous silica films as catalyst support for microstructured reactors: Preparation and characterization. *Chemical Engineering Journal* **2008,** *135, Supplement 1* (0), S99-S103.
53. Li, X.; Zheng, W.; Pan, H.; Yu, Y.; Chen, L.; Wu, P., Pt nanoparticles supported on highly dispersed TiO2 coated on SBA-15 as an efficient and recyclable catalyst for liquid-phase hydrogenation. *Journal of Catalysis* **2013,** *300* (0), 9-19.
54. Bian, Y.; Wang, X.; Zeng, Z.; Hu, Z., Preparation of ordered mesoporous TiO2 thin film and its application in methanol catalytic combustion. *Surface and Interface Analysis* **2013,** *45* (9), 1317-1322.
55. (a) Rebrov, E. V.; Klinger, E. A.; Berenguer-Murcia, A.; Sulman, E. M.; Schouten, J. C., Selective Hydrogenation of 2-Methyl-3-butyne-2-ol in a Wall-Coated Capillary Microreactor with a Pd25Zn75/TiO2 Catalyst. *Organic Process Research & Development* **2009,** *13* (5), 991-998; (b) Protasova, L. N.; Rebrov, E. V.; Skelton, H. E.; Wheatley, A. E. H.; Schouten, J. C., A kinetic study of the liquid-phase hydrogenation of citral on Au/TiO2 and Pt–Sn/TiO2 thin films in capillary microreactors. *Applied Catalysis A: General* **2011,** *399* (1–2), 12-21.
56. Gömann, A.; Deverell, J. A.; Munting, K. F.; Jones, R. C.; Rodemann, T.; Canty, A. J.; Smith, J. A.; Guijt, R. M., Palladium-mediated organic synthesis using porous polymer monolith formed in situ as a continuous catalyst support structure for application in microfluidic devices. *Tetrahedron* **2009,** *65* (7), 1450-1454.
57. Bolton, K. F.; Canty, A. J.; Deverell, J. A.; Guijt, R. M.; Hilder, E. F.; Rodemann, T.; Smith, J. A., Macroporous monolith supports for continuous flow capillary microreactors. *Tetrahedron Letters* **2006,** *47* (52), 9321-9324.
58. Preinerstorfer, B.; Bicker, W.; Lindner, W.; Lämmerhofer, M., Development of reactive thiol-modified monolithic capillaries and in-column surface functionalization by radical addition

of a chromatographic ligand for capillary electrochromatography. *Journal of Chromatography A* **2004,** *1044* (1–2), 187-199.
59. Buchmeiser, M. R., Polymeric monolithic materials: Syntheses, properties, functionalization and applications. *Polymer* **2007,** *48* (8), 2187-2198.
60. Okumura, M.; Akita, T.; Haruta, M., Hydrogenation of 1,3-butadiene and of crotonaldehyde over highly dispersed Au catalysts. *Catalysis Today* **2002,** *74* (3–4), 265-269.
61. Mohr, C.; Hofmeister, H.; Claus, P., The influence of real structure of gold catalysts in the partial hydrogenation of acrolein. *Journal of Catalysis* **2003,** *213* (1), 86-94.
62. Milone, C.; Ingoglia, R.; Schipilliti, L.; Crisafulli, C.; Neri, G.; Galvagno, S., Selective hydrogenation of -unsaturated ketone to -unsaturated alcohol on gold-supported iron oxide catalysts: Role of the support. *Journal of Catalysis* **2005,** *236* (1), 80-90.
63. Gallo, A.; Tiozzo, C.; Psaro, R.; Carniato, F.; Guidotti, M., Niobium metallocenes deposited onto mesoporous silica via dry impregnation as catalysts for selective epoxidation of alkenes. *Journal of Catalysis* **2013,** *298* (0), 77-83.
64. Suzuki, T.; Kosacki, I.; Anderson, H. U.; Colomban, P., Electrical Conductivity and Lattice Defects in Nanocrystalline Cerium Oxide Thin Films. *Journal of the American Ceramic Society* **2001,** *84* (9), 2007-2014.
65. Nikbin, N.; Watts, P., Solid-Supported Continuous Flow Synthesis in Microreactors Using Electroosmotic Flow. *Organic Process Research & Development* **2004,** *8* (6), 942-944.
66. Önal, Y.; Lucas, M.; Claus, P., Application of a Capillary Microreactor for Selective Hydrogenation of α,β-Unsaturated Aldehydes in Aqueous Multiphase Catalysis. *Chemical Engineering & Technology* **2005,** *28* (9), 972-978.
67. Baratto, C.; Sberveglieri, G.; Comini, E.; Faglia, G.; Benussi, G.; La Ferrara, V.; Quercia, L.; Di Francia, G.; Guidi, V.; Vincenzi, D.; Boscarino, D.; Rigato, V., Gold-catalysed porous silicon for NOx sensing. *Sensors and Actuators B: Chemical* **2000,** *68* (1–3), 74-80.
68. Kim, M. C.; Song, D. K.; Shin, H. S.; Baeg, S. H.; Kim, G. S.; Boo, J. H.; Han, J. G.; Yang, S. H., Surface modification for hydrophilic property of stainless steel treated by atmospheric-pressure plasma jet. *Surface and Coatings Technology* **2002,** *171* (1–3), 312-316.
69. Wieβmeier, G.; Hönicke, D., Heterogeneously Catalyzed Gas-Phase Hydrogenation of cis,trans,trans-1,5,9-Cyclododecatriene on Palladium Catalysts Having Regular Pore Systems. *Industrial & Engineering Chemistry Research* **1996,** *35* (12), 4412-4416.
70. (a) Inoue, H.; Sekizawa, K.; Eguchi, K.; Arai, H., Thermal Stability of Hexaaluminate Film Coated on SiC Substrate for High-Temperature Catalytic Application. *Journal of the American Ceramic Society* **1997,** *80* (3), 584-588; (b) Pérez-Cadenas, A. F.; Zieverink, M. M. P.; Kapteijn, F.; Moulijn, J. A., High performance monolithic catalysts for hydrogenation reactions. *Catalysis Today* **2005,** *105* (3–4), 623-628.
71. Burke, L. D.; Hurley, L. M.; Lodge, V. E.; Mooney, M. B., The effect of severe thermal pretreatment on the redox behaviour of gold in aqueous acid solution. *J Solid State Electrochem* **2001,** *5* (4), 250-260.
72. Rohr, T.; Hilder, E. F.; Donovan, J. J.; Svec, F.; Fréchet, J. M. J., Photografting and the Control of Surface Chemistry in Three-Dimensional Porous Polymer Monoliths. *Macromolecules* **2003,** *36* (5), 1677-1684.
73. Greenway, G. M.; Haswell, S. J.; Morgan, D. O.; Skelton, V.; Styring, P., The use of a novel microreactor for high throughput continuous flow organic synthesis. *Sensors and Actuators B: Chemical* **2000,** *63* (3), 153-158.
74. Kato, K.; Uchida, E.; Kang, E.-T.; Uyama, Y.; Ikada, Y., Polymer surface with graft chains. *Progress in Polymer Science* **2003,** *28* (2), 209-259.
75. Muraza, O.; Rebrov, E. V.; Berenguer-Murcia, A.; de Croon, M. H. J. M.; Schouten, J. C., Selectivity control in hydrogenation reactions by nanoconfinement of polymetallic nanoparticles in mesoporous thin films. *Applied Catalysis A: General* **2009,** *368* (1–2), 87-96.

76. Mies, M. J. M.; Rebrov, E. V.; Jansen, J. C.; de Croon, M. H. J. M.; Schouten, J. C., Method for the in situ preparation of a single layer of zeolite Beta crystals on a molybdenum substrate for microreactor applications. *Journal of Catalysis* **2007,** *247* (2), 328-338.
77. Glazneva, T. S.; Rebrov, E. V.; Schouten, J. C.; Paukshtis, E. A.; Ismagilov, Z. R., Synthesis and characterization of mesoporous silica thin films as a catalyst support on a titanium substrate. *Thin Solid Films* **2007,** *515* (16), 6391-6394.
78. Conant, T.; Karim, A.; Datye, A., Coating of steam reforming catalysts in non-porous multi-channeled microreactors. *Catalysis Today* **2007,** *125* (1–2), 11-15.
79. de la Iglesia, O.; Sebastián, V.; Mallada, R.; Nikolaidis, G.; Coronas, J.; Kolb, G.; Zapf, R.; Hessel, V.; Santamaría, J., Preparation of Pt/ZSM-5 films on stainless steel microreactors. *Catalysis Today* **2007,** *125* (1–2), 2-10.
80. Stefanescu, A.; van Veen, A. C.; Mirodatos, C.; Beziat, J. C.; Duval-Brunel, E., Wall coating optimization for microchannel reactors. *Catalysis Today* **2007,** *125* (1–2), 16-23.
81. Zeng, Z.; Qiu, W.; Huang, Z., Solid-Phase Microextraction Using Fused-Silica Fibers Coated with Sol−Gel-Derived Hydroxy-Crown Ether. *Analytical Chemistry* **2001,** *73* (11), 2429-2436.
82. Ng, J. F.; Nie, Y.; Chuah, G. K.; Jaenicke, S., A wall-coated catalytic capillary microreactor for the direct formation of hydrogen peroxide. *Journal of Catalysis* **2010,** *269* (2), 302-308.
83. Perko, D.; Levec, J., Kinetic Study of Methanol Synthesis over CuO/ZnO/Al2O3/V2O3 Catalyst Deposited on a Stainless Steel Surface. *Industrial & Engineering Chemistry Research* **2011,** *51* (2), 710-718.
84. Phan, X. K.; Bakhtiary, H. D.; Myrstad, R.; Thormann, J.; Pfeifer, P.; Venvik, H. J.; Holmen, A., Preparation and Performance of a Catalyst-Coated Stacked Foil Microreactor for the Methanol Synthesis. *Industrial & Engineering Chemistry Research* **2010,** *49* (21), 10934-10941.
85. Zeng, Q., Fabrication of Al2O3-coated carbon fiber-reinforced Al-matrix composites. *Journal of Applied Polymer Science* **1998,** *70* (1), 177-183.
86. Muraza, O.; Rebrov, E. V.; de Croon, M. H. J. M.; Schouten, J. C., Enhancement of the stability of microporous silica films in non-aqueous solvents at elevated temperature. *Microporous and Mesoporous Materials* **2009,** *124* (1–3), 20-29.
87. Mackenzie, J. D., Hybrid Organic?Inorganic Materials. In *Hybrid Organic-Inorganic Composites*, American Chemical Society: 1995; Vol. 585, pp 226-236.
88. Lu, P.; Teranishi, T.; Asakura, K.; Miyake, M.; Toshima, N., Polymer-Protected Ni/Pd Bimetallic Nano-Clusters: Preparation, Characterization and Catalysis for Hydrogenation of Nitrobenzene. *The Journal of Physical Chemistry B* **1999,** *103* (44), 9673-9682.
89. Alberius, P. C. A.; Frindell, K. L.; Hayward, R. C.; Kramer, E. J.; Stucky, G. D.; Chmelka, B. F., General Predictive Syntheses of Cubic, Hexagonal, and Lamellar Silica and Titania Mesostructured Thin Films§. *Chemistry of Materials* **2002,** *14* (8), 3284-3294.
90. Superhydrophilic anatase TiO2 film with the micro- and nanometer-scale hierarchical surface structure. *Materials Letters* **2008,** *62* (20), 3503.
91. Lappalainen, K.; Manninen, M.; Alopaeus, V.; Aittamaa, J.; Dodds, J., An Analytical Model for Capillary Pressure–Saturation Relation for Gas–Liquid System in a Packed-Bed of Spherical Particles. *Transp Porous Med* **2009,** *77* (1), 17-40.
92. Chen, H.; Bednarova, L.; Besser, R. S.; Lee, W. Y., Surface-selective infiltration of thin-film catalyst into microchannel reactors. *Applied Catalysis A: General* **2005,** *286* (2), 186-195.
93. Hayes, J. D.; Malik, A., Sol–gel chemistry-based Ucon-coated columns for capillary electrophoresis. *Journal of Chromatography B: Biomedical Sciences and Applications* **1997,** *695* (1), 3-13.
94. Janicke, M. T.; Kestenbaum, H.; Hagendorf, U.; Schüth, F.; Fichtner, M.; Schubert, K., The Controlled Oxidation of Hydrogen from an Explosive Mixture of Gases Using a

Microstructured Reactor/Heat Exchanger and Pt/Al2O3 Catalyst. *Journal of Catalysis* **2000,** *191* (2), 282-293.
95. Kabir, A.; Furton, K. G.; Malik, A., Innovations in sol-gel microextraction phases for solvent-free sample preparation in analytical chemistry. *TrAC Trends in Analytical Chemistry* **2013,** *45* (0), 197-218.
96. Wawrzyńczak, A.; Dutkiewicz, M.; Guliński, J.; Maciejewski, H.; Marciniec, B.; Fiedorow, R., Hydrosilylation of n-alkenes and allyl chloride over platinum supported on styrene–divinylbenzene copolymer. *Catalysis Today* **2011,** *169* (1), 69-74.
97. Thommes, M.; Smarsly, B.; Groenewolt, M.; Ravikovitch, P. I.; Neimark, A. V., Adsorption Hysteresis of Nitrogen and Argon in Pore Networks and Characterization of Novel Micro- and Mesoporous Silicas. *Langmuir* **2005,** *22* (2), 756-764.
98. (a) Marciniec, B.; Szubert, K.; Potrzebowski, M. J.; Kownacki, I.; Łęszczak, K., Synthesis, Characterization, and Catalytic Activity of a Well-Defined Rhodium Siloxide Complex Immobilized on Silica. *Angewandte Chemie* **2008,** *120* (3), 551-554; (b) Marciniec, B.; Szubert, K.; Potrzebowski, M. J.; Kownacki, I.; Maciejewski, H., Catalysis of Hydrosilylation by Well-Defined Surface Rhodium Siloxide Phosphine Complexes. *ChemCatChem* **2009,** *1* (2), 304-310.
99. Wang, Y.; Song, Z.; Ma, D.; Luo, H.; Liang, D.; Bao, X., Characterization of Rh-based catalysts with EPR, TPR, IR and XPS. *Journal of Molecular Catalysis A: Chemical* **1999,** *149* (1–2), 51-61.
100. Zwijnenburg, A.; Goossens, A.; Sloof, W. G.; Crajé, M. W. J.; van der Kraan, A. M.; Jos de Jongh, L.; Makkee, M.; Moulijn, J. A., XPS and Mössbauer Characterization of Au/TiO2 Propene Epoxidation Catalysts. *The Journal of Physical Chemistry B* **2002,** *106* (38), 9853-9862.
101. Long, J.; Liu, G.; Cheng, T.; Yao, H.; Qian, Q.; Zhuang, J.; Gao, F.; Li, H., Immobilization of rhodium-based transfer hydrogenation catalysts on mesoporous silica materials. *Journal of Catalysis* **2013,** *298* (0), 41-50.
102. Vaartstra, B. A.; Huffman, J. C.; Gradeff, P. S.; Hubert-Pfalzgraf, L. G.; Daran, J. C.; Parraud, S.; Yunlu, K.; Caulton, K. G., Alcohol adducts of alkoxides: intramolecular hydrogen bonding as a general structural feature. *Inorganic Chemistry* **1990,** *29* (17), 3126-3131.
103. Rocio Redon, S. K. R.-L., Ana L. Fernandez-Osorio and V. M. Ugalde-Saldiver, AEROBIC SYNTHESIS OF PALLADIUM NANOPARTICLES. *Rev.Adv.Mater.Sci.* **2011,** *27*, 11.
104. Ribot, F.; Toledano, P.; Sanchez, C., Hydrolysis-condensation process of .beta.-diketonates-modified cerium(IV) isopropoxide. *Chemistry of Materials* **1991,** *3* (4), 759-764.
105. (a) Boudart, M.; Djéga-Mariadassou, G., *Kinetics of heterogeneous catalytic reactions*. Princeton University Press: 2014; (b) Bartholomew, C. H.; Farrauto, R. J., Catalyst Characterization and Selection. In *Fundamentals of Industrial Catalytic Processes*, John Wiley & Sons, Inc.: 2005; pp 118-196.
106. (a) Zhang, Y.; Grass, M. E.; Habas, S. E.; Tao, F.; Zhang, T.; Yang, P.; Somorjai, G. A., One-step Polyol Synthesis and Langmuir−Blodgett Monolayer Formation of Size-tunable Monodisperse Rhodium Nanocrystals with Catalytically Active (111) Surface Structures. *The Journal of Physical Chemistry C* **2007,** *111* (33), 12243-12253; (b) Borodko, Y.; Lee, H. S.; Joo, S. H.; Zhang, Y.; Somorjai, G., Spectroscopic Study of the Thermal Degradation of PVP-Capped Rh and Pt Nanoparticles in H2 and O2 Environments. *The Journal of Physical Chemistry C* **2009,** *114* (2), 1117-1126.
107. Hei, H., Controlled Synthesis and Characterization of Nobel Metal Nanoparticles. *Soft Nanoscience Letters* **2012,** *02* (03), 0-0.
108. Feng, G.; Chen, P.; Lou, H., Palladium catalysts supported on carbon-nitrogen composites for aqueous-phase hydrogenation of phenol. *Catalysis Science & Technology* **2015**.
109. Nakamoto, K., Applications in Inorganic Chemistry. In *Infrared and Raman Spectra of Inorganic and Coordination Compounds*, John Wiley & Sons, Inc.: 2008; pp 149-354.

110. Christophidou, M.; Theocharis, C. R., Preparation And Surface Characterisation Of Novel Ceria-Copper And Ceria-Manganese Mixed Oxides. In *Studies in Surface Science and Catalysis*, F. Rodriguez-Reinoso, B. M. J. R.; Unger, K., Eds. Elsevier: 2002; Vol. Volume 144, pp 75-82.
111. Kosacki, I.; Petrovsky, V.; Anderson, H. U.; Colomban, P., Raman Spectroscopy of Nanocrystalline Ceria and Zirconia Thin Films. *Journal of the American Ceramic Society* **2002,** *85* (11), 2646-2650.
112. Barker, A. S.; Sievers, A. J., Optical studies of the vibrational properties of disordered solids. *Reviews of Modern Physics* **1975,** *47* (S2), S1-S179.
113. Wilhite, B. A.; McCready, M. J.; Varma, A., Kinetics of Phenylacetylene Hydrogenation over Pt/γ-Al2O3 Catalyst. *Industrial & Engineering Chemistry Research* **2002,** *41* (14), 3345-3350.

Vitae

Name	Abdulkadir Tanimu
Nationality	Nigerian
Date of Birth	22 June 1987
Email	atanimu@abu.edu.ng
Address	No. 94 Imamu Road, Tudun Wada, Zaria-Nigeria

Academic Background

2010 – 2011	Federal College of Education, Zaria, Nigeria Professional diploma in education (credit) Project title: The problems of teaching chemistry in secondary school within Zaria zone, Kaduna State, Nigeria.
2004 – 2009	Ahmadu Bello University, Zaria-Nigeria. B.Sc. Chemistry (second class upper) Project title: Kinetics and Mechanisms of the electron-transfer reaction of malachite green with hydroxyl ion in aqueous medium. Supervisor: Dr. S.O. Idris
1999 – 2004	Government Secondary School, Zaria-Nigeria Secondary School Certificate Examination (SSCE)
1994 – 1999	God's Time School, Tudun Wada, Zaria Primary School Certificate

EXPERIENCE

Graduate Assistant:	Ahmadu Bello University-Zaria, Nigeria From June, 2011 – date
Graduate Assistant:	Kaduna State University, Kaduna State, Nigeria From April, 2011 – June, 2011
Assistant Lecturer:	Federal College of Education, Zaria, Nigeria From October, 2010 – April, 2011

AWARD

King Fahd University of Petroleum and Minerals M.Sc. Graduate Scholarship Award
BALCOM Computer Institute Award for best graduating secondary school student

PUBLICATIONS

Kinetics of redox reaction of malachite green and hydroxyl ion. **Tanimu A.**, Idris S.O., Iyun J.F. (2012). *International journal of science and technology*, 2 (3), 112-115.

Kinetics and Mechanism of the Reaction of Malachite Green and Dithionite Ion. Idris, S. O., **Tanimu, A.**, Iyun, J. F., & Mohammed, Y. (2015). *International Research Journal of Pure & Applied Chemistry*, *5*(2), 177-184.

Kinetics and Mechanism of Malachite Green Oxidation by Hypochlorite Ion in Aqueous Acidic Medium. . Idris, S. O., **Tanimu, A.**, Iyun, J. F., & Mohammed, Y. (2015). American Chemical Science Journal, 5(2), 185-193.